

STERIC AND ELECTRONIC EFFECTS ON DIARYLSILYLENE REACTIVITY

---

STUDY OF STERIC AND ELECTRONIC EFFECTS ON THE REACTIVITIES OF  
DIARYLSILYLENE IN SOLUTION BY LASER FLASH PHOTOLYSIS METHODS

By

ADROHA BHATTACHARYA, M.Sc.

A Thesis

Submitted to the School of Graduate Studies

in Partial Fulfillment of the Requirements

---

for the Degree

Master of Science

McMaster University

© Copyright by Adroha Bhattacharya, March, 2011

MASTER OF SCIENCE (2011)

McMASTER UNIVERSITY

(Chemistry)

Hamilton, Ontario

TITLE: Study of Steric and Electronic Effects on the Reactivities of  
Diarylsilylene in Solution by Laser Flash Photolysis  
Methods

AUTHOR: Adroha Bhattacharya, *M. Sc.*  
  
Indian Institute of Technology, Kharagpur, India

SUPERVISOR: Professor William J. Leigh

NUMBER OF PAGES: xv, 116

## ABSTRACT

1,1,1,3,3,3-Hexamethyl-2,2-bis(3,4,5-trimethylphenyl)trisilane (**43**) has been synthesized and its photochemistry studied by steady state and nanosecond laser flash photolysis (NLFP) methods in solution. Photolysis of **43** in the presence of methanol leads to the formation of methoxybis(3,4,5-trimethylphenyl)silane (**53**) as the major product, resulting from the reaction of the alcohol with the reactive intermediate, bis(3,4,5-trimethylphenyl)silylene (**1**, SiTmp<sub>2</sub>).

The reactivity of SiTmp<sub>2</sub> with various substrates such as methanol, acetone, CCl<sub>4</sub>, acetic acid, triethylsilane, cyclohexene, 1,3-dienes, bis(trimethylsilyl)acetylene (BTMSE), and O<sub>2</sub> has been examined by NLFP techniques, and the results are compared to analogous data for diphenylsilylene (**3**). In almost all cases it was found that electronic factors reduce the absolute rate constants by a factor of ca. 2, except for the reactions with triethylsilane and BTMSE where a factor of ca. 5 rate retardation was observed. This indicates that in general the inductive electron-donating effect associated with six methyl groups on the aromatic rings has only a small effect on diarylsilylene reactivity. The reactivity of SiMes<sub>2</sub> (**2**) with some substrates such as alcohols, CCl<sub>4</sub>, acetic acid, isoprene and BTMSE has also been studied. The rate constants for the reactions of SiMes<sub>2</sub> and SiTmp<sub>2</sub> with each substrate were compared to provide a quantitative assessment of steric effects of the *ortho* methyl groups in diarylsilylene reactivity. It has been observed that for substrates like acetone, acetic acid and O<sub>2</sub> there

is almost no sensitivity to steric effects, it is moderate in the cases of triethylsilane,  $\text{CCl}_4$  and methanol and high in the cases of alkenes, dienes and alkynes. This study is the first quantitative assessment of the individual effects of steric hindrance and electronics on the reactivities of diarylsilylenes.

## ACKNOWLEDGEMENTS

This dissertation would not have been possible without the guidance and the help of several individuals who in one way or another contributed and extended their valuable assistance in the preparation and completion of this study.

First and foremost, my utmost gratitude to my supervisor, Dr. Willie Leigh, whose sincerity and encouragement I will never forget. Willie has been my inspiration as I hurdle all the obstacles in the completion of this research work. Thanks also to my committee members, Drs. Brook and Emslie, who provided invaluable input at my committee meetings.

To the WJL group members, past and present: I have been extremely lucky to have worked with an amazing group of chemists and wonderful human beings. I have learnt so much from all of you whether it was about chemistry or life in general.

I would like to thank my friends for all the fun times we have had here in Hamilton.

I would like to thank my family. Mom, Dad and Dia you will never know how much your support has meant to me over the years.

Finally, I want to thank my girlfriend, Shaon, for being there whenever needed. I look forward to our future together.

## TABLE OF CONTENTS

<b>List of Figures</b>	ix
<b>List of Tables</b>	xiv
<b>Chapter 1 - Introduction</b>	1
<b>1.1. Thesis Overview</b>	1
<b>1.2. Nomenclature</b>	2
<b>1.3. Electronic Structure and Thermochemistry</b>	3
1.3.1. Electronic Structure	3
1.3.2. Divalent State Stabilization Energy (DSSE)	5
<b>1.4. Generation of Silylenes</b>	7
1.4.1. Thermal Generation of Silylenes	7
1.4.2. Generation of Silylenes under Strong Reducing Conditions	8
1.4.3. Photolytic Generation of Silylenes	8
<b>1.5. Electronic Spectra of Silylenes</b>	10
<b>1.6. Reactivity of Silylenes</b>	11
1.6.1. Addition of Silylenes to Alkenes and Alkynes	13
1.6.2. Reaction of Silylenes with halocarbons	16
1.6.3. Complexation of Silylenes with Lewis bases	20
1.6.4. Insertion of Silylenes into Single Bonds (O – H, Si – H)	21
1.6.5. Ene-type Addition Reactions of Silylenes with Acetic acid and Acetone	23

<b>1.7.</b>	<b>Application of Silylene Chemistry</b>	25
<b>1.8.</b>	<b>Steric vs. Electronic Effects on Silylene Reactivity</b>	25
<b>1.9.</b>	<b>Goals of this work</b>	30
<b>1.10.</b>	<b>Experimental Techniques used for the Study of Transient Silylenes</b>	31
1.10.1.	Steady state Photolysis Experiments	31
1.10.2.	Nanosecond Laser Flash Photolysis (LFP) Experiments: <sup>1</sup>	
	Determination of Rate Constants	31
<b>1.11.</b>	<b>Kinetic Isotope Effect (KIE)</b>	35
<b>1.11.</b>	<b>Note</b>	36
<b>Chapter 2 – Reactions of Dimesitylsilylene</b>		
<b>2.1.</b>	<b>Synthesis of 2,2 – dimesityl - 1,1,1,3,3,3 – hexamethyltrisilane (20)</b>	44
<b>2.2.</b>	<b>Laser Flash Photolysis Experiments of 2,2 – dimesityl - 1,1,1,3,3,3 – hexamethyltrisilane (20)</b>	44
2.2.1.	Reactions of SiMes <sub>2</sub> with alkenes and alkynes	47
2.2.2.	Reactions of SiMes <sub>2</sub> with CCl <sub>4</sub>	53
2.2.3.	Reactions of SiMes <sub>2</sub> with AcOH	55
2.2.4.	Reactions of SiMes <sub>2</sub> with alcohols	57
<b>Chapter 3 – Photochemistry of 1,1,1,3,3,3 – Hexamethyl - 2,2-bis(3,4,5–trimethylphenyl)trisilane and reactions of bis(3,4,5–trimethylphenyl)silylene (SiTmp<sub>2</sub>)</b>		
<b>3.1.</b>	<b>Overview</b>	66
<b>3.2.</b>	<b>Choice of Aryl Substituents</b>	66
<b>3.3.</b>	<b>Choice of Precursor to New Silylene (1)</b>	70



<b>3.4.</b>	<b>Synthesis of 1,1,1,3,3,3– hexamethyl-2,2–bis(3,4,5-trimethylphenyl) trisilane (43)</b>	<b>70</b>
<b>3.5.</b>	<b>Steady State Photolysis of 43</b>	<b>73</b>
<b>3.6.</b>	<b>Laser Flash Photolysis of 1,1,1,3,3,3 – hexamethyl - 2,2 – bis(3,4,5-trimethylphenyl)trisilane (43)</b>	<b>77</b>
3.6.1.	Reactions of SiTmp <sub>2</sub> with Alkenes, Dienes and Alkynes	83
3.6.2.	Reactions of SiTmp <sub>2</sub> with CCl <sub>4</sub>	87
3.6.3.	Reactions of SiTmp <sub>2</sub> with Oxygenated Substrates	89
3.6.4.	Reactions of SiTmp <sub>2</sub> with Et <sub>3</sub> SiH	96
<b>Chapter 4 – Summary and Conclusion</b>		
<b>4.1.</b>	<b>Contributions of the study</b>	<b>100</b>
<b>4.2.</b>	<b>Future directions</b>	<b>102</b>
<b>Chapter 5 – Experimental</b>		
<b>5.1.</b>	<b>General</b>	<b>106</b>
<b>5.2.</b>	<b>Solvents</b>	<b>107</b>
<b>5.3.</b>	<b>Commercial Reagents</b>	<b>107</b>
<b>5.4.</b>	<b>Synthesis</b>	<b>108</b>
<b>5.5.</b>	<b>Steady-State Photolysis Experiments</b>	<b>115</b>
<b>5.6.</b>	<b>Laser Flash Photolysis Experiments</b>	<b>115</b>

## LIST OF FIGURES

<b>Figure 1.1.</b> Singlet and triplet electronic structures of Group 14 divalent species.....	3
<b>Figure 1.2.</b> Examples of triplet silylenes.....	5
<b>Figure 1.3.</b> Electronic absorptions of singlet silylenes.....	11
<b>Figure 1.4.</b> Configuration of a LFP system.....	32
<b>Fig. 2.1.</b> (a) Transient absorption spectra recorded at 0.640-1.28 $\mu\text{s}$ (o), 155.20-157.44 $\mu\text{s}$ ( $\square$ ) after the laser pulse, by laser flash photolysis of a deoxygenated hexanes solution of <b>20</b> (ca. $6 \times 10^{-5}$ M). (b) Transient growth/decay profiles recorded at 420 and 580 nm.....	46
<b>Figure 2.2.</b> Plots of the pseudo-first-order rate constants ( $k_{\text{decay}}$ ) for the decay of $\text{SiMes}_2$ vs. [isoprene] in hexanes solution at 25 $^\circ\text{C}$ .....	50
<b>Figure 2.3.</b> Plots of the pseudo-first-order rate constants ( $k_{\text{decay}}$ ) for the decay of $\text{SiMes}_2$ vs. [BTMSE] in hexanes solution at 25 $^\circ\text{C}$ .....	50
<b>Figure 2.4.</b> (a) Transient absorption spectra recorded at 0.096 - 0.122 $\mu\text{s}$ ( $-\Delta-$ ) and 2.144 - 2.170 $\mu\text{s}$ ( $-\circ-$ ) after laser pulse, by laser flash photolysis of a 0.05 mM solution of <b>20</b> in deoxygenated hexanes containing 23 mM of BTMSE; the inset shows transient decay profiles at 280 and 580 nm. (b) Transient decay profile recorded at 280 nm for the laser photolysis of ca. 0.05 mM of <b>20</b> in the presence of ca. 27 mM of BTMSE.....	52
<b>Figure 2.5.</b> (a) Transient absorption spectra recorded at 0.16 - 0.19 $\mu\text{s}$ ( $-\diamond-$ ) and 0.54 - 0.59 $\mu\text{s}$ ( $-\circ-$ ) after laser pulse, by laser flash photolysis of a 0.05 mM solution of <b>20</b> in	

deoxygenated hexanes containing 29 mM of CCl<sub>4</sub>; the inset shows transient decay profiles at 290, 330 and 580 nm. (b) Plots of the pseudo – first – order decay rate coefficients ( $k_{\text{decay}}$ ) vs [CCl<sub>4</sub>] of free SiMes<sub>2</sub> (570 nm, (○)) and of SiMes<sub>2</sub>Cl (330 nm, (●)).....54

**Figure 2.6.** (a) Plots of the pseudo-first-order rate constants ( $k_{\text{decay}}$ ) for the decay of SiMes<sub>2</sub> vs. bulk AcOH concentrations in hexanes solution at 25 °C. (b) Plots of the pseudo-first-order rate constants ( $k_{\text{decay}}$ ) for the decay of SiMes<sub>2</sub> vs. monomeric AcOH concentrations in hexanes solution at 25 °C.....57

**Figure 2.7.** Plots of the pseudo-first order rate constants for decay of SiMes<sub>2</sub> vs. [MeOL] (L = H, (●) or D (○)) in hexane at 25° C. (b) Plots of the pseudo-first order rate constants for decay of SiMes<sub>2</sub> vs. [*t*-BuOL] (L = H, (●) or D (○)) in hexane at 25° C. The solid lines are the non-linear least squares fits of the data to equation 2.13.....63

**Figure 3.1.** Diagram showing new silylene SiTmp<sub>2</sub> (1) in the middle which is expected to allow separation of the steric and electronic effects from SiMes<sub>2</sub>.....68

**Figure 3.2.** Plausible precursors to SiTmp<sub>2</sub>.....70

**Figure 3.3.** Concentration vs. time plots for (a) **43** (slope: - 0.00001527 ± 0.0000007). (b) **53**, and Si<sub>2</sub>Me<sub>6</sub> (slopes: **53**, 0.00001010 ± 0.0000002 from OMe, 0.0001048 ± 0.0000002 from Ar-H; Si<sub>2</sub>Me<sub>6</sub>, 0.00001030 ± 0.0000003) from photolysis of **43** (0.03956 M) in C<sub>6</sub>D<sub>12</sub> containing 0.10 M MeOH.....74

**Figure 3.4.** (i) <sup>1</sup>H NMR spectrum **43** in C<sub>6</sub>D<sub>12</sub> in the presence of MeOH (0.4 M). (ii) <sup>1</sup>H NMR spectra **43** after photolysis for 15 min in C<sub>6</sub>D<sub>12</sub> in the presence of 0.4 M MeOH. (iii) Expansion of <sup>1</sup>H NMR spectra **43** after photolysis for 15 min in C<sub>6</sub>D<sub>12</sub> in the presence of 0.4 M MeOH showing array resonances in the δ 3.5 – 6.5 and δ 0.8 –

1.8 ranges.....	75
<b>Figure 3.5.</b> (a) Transient absorption spectra recorded at 160-224 ns (o), 9.12-9.18 $\mu$ s (□) after the laser pulse, by laser flash photolysis of a deoxygenated hexanes solution of <b>43</b> (ca. $6 \times 10^{-5}$ M). (b) Transient growth/decay profiles recorded at 380, 460 and 540 nm.....	79
<b>Figure 3.6.</b> (a) Transient absorption spectra recorded at 160 – 224 ns (o), 1.44 – 1.50 $\mu$ s (□) after the laser pulse, by laser flash photolysis of a deoxygenated hexanes solution of <b>43</b> (ca. $6 \times 10^{-5}$ M) containing 5 mM Et <sub>3</sub> SiH. The dashed line is the difference spectrum resulting from subtracting the 1.44 – 1.50 $\mu$ s spectrum from the 160 – 224 ns spectrum. (b) Transient decay profiles recorded at 380, 460 and 540 nm.....	81
<b>Figure 3.7.</b> Plots of the pseudo-first-order rate constants ( $k_{\text{decay}}$ ) for the decay of SiTmp <sub>2</sub> vs. [cyclohexene] in hexanes solution at 25 °C.....	83
<b>Figure 3.8.</b> Plots of the pseudo-first-order rate constants ( $k_{\text{decay}}$ ) for the decay of SiTmp <sub>2</sub> vs. (a) [DMB] and (b) [isoprene], in hexanes solution at 25 °C.....	84
<b>Figure 3.9.</b> Plots of the pseudo-first-order rate constants ( $k_{\text{decay}}$ ) for the decay of SiTmp <sub>2</sub> vs. [BTMSE] in hexanes solution at 25 °C.....	85
<b>Figure 3.10.</b> (a) Transient absorption spectra recorded by laser flash photolysis of deoxygenated hexanes solution of <b>43</b> (ca. $6 \times 10^{-5}$ M) containing (a) 0.70 mM DMB, 3.20 – 9.60 $\mu$ s (-o-) and 1552.00 – 1574.40 $\mu$ s (-Δ-) after the laser pulse, (b) 0.69 mM isoprene, 3.20 – 9.60 $\mu$ s (-o-) and 1552.00 – 1574.40 $\mu$ s (-Δ-) after the laser pulse, (c) 0.71 mM cyclohexene, 6.40 – 19.20 $\mu$ s (-o-) and 1552.00 – 1571.20 $\mu$ s (-Δ-) after the laser pulse, and (d) 0.92 mM BTMSE, 6.40 – 19.20 $\mu$ s (-o-) and 1552.00 – 1574.40 $\mu$ s (-Δ-) after the laser pulse. The insets show transient decay recorded at 280 and 460 nm. .....	86

**Figure 3.11.** Plots of the pseudo-first-order rate constants ( $k_{\text{decay}}$ ) for (a) the decay of SiTmp<sub>2</sub> vs. [CCl<sub>4</sub>] and (b) the decay of silene **54** vs. [CCl<sub>4</sub>], in hexanes solution at 25 °C.....88

**Figure 3.12.** Plots of the pseudo-first-order rate constants ( $k_{\text{decay}}$ ) for the decay of SiTmp<sub>2</sub> vs. (a) [THF] and (b) [MeOH], in hexanes solution at 25 °C.....91

**Figure 3.13.** (a) Transient absorption spectra recorded 128 – 141 ns (-□-) and 864 – 877 ns (-○-) after the laser pulse, from laser flash photolysis of **43** (ca.  $6 \times 10^{-5}$  M) in deoxygenated hexanes containing 0.26 mM THF; the inset shows transient growth/decay profiles recorded at 380 nm, 460 nm, and 540 nm. (b) Transient absorption spectra recorded 77 – 90 ns (-○-), 224 – 250 ns (-Δ-), and 1.50 – 1.53 μs (-□-) after the pulse, from laser flash photolysis of **43** in deoxygenated hexanes containing 0.56 mM MeOH; the inset shows transient decay profiles recorded at 380 nm, 460 nm, and 540 nm.....91

**Figure 3.14.** (a) Transient absorption spectra recorded 96 – 109 ns (-□-), 352 – 378 ns (-○-) and 2.78 – 2.81 μs (-Δ-) after the laser pulse, from laser flash photolysis of **43** (ca.  $6 \times 10^{-5}$  M) in deoxygenated hexanes containing 0.30 mM acetone; the inset shows transient growth/decay profiles recorded at 380 nm, 460 nm, and 540 nm. (b) Transient absorption spectra recorded 205 – 218 ns (-○-), 352 – 378 ns (-□-), and 2.16 – 2.20 μs (-Δ-) after the pulse, from laser flash photolysis of **43** in deoxygenated hexanes containing 0.30 mM AcOH; the inset shows transient decay profiles recorded at 380 nm, 460 nm, and 540 nm.....93

**Figure 3.15.** Plots of the pseudo-first-order rate constants ( $k_{\text{decay}}$ ) for the decay of SiTmp<sub>2</sub> vs. (a) [acetone] and (b) [acetic acid], in hexanes solution at 25 °C.....93

**Figure 3.16.** Plots of the pseudo-first-order rate constants ( $k_{\text{decay}}$ ) for (a) the decay of

SiTmp<sub>2</sub> vs. [O<sub>2</sub>] and (b) the decay of silene **54** vs. [O<sub>2</sub>], in hexanes solution at 25 °C...96

**Figure 3.17.** Transient absorption spectra recorded at 480 – 554 ns (o), 1.28 – 1.36 μs (Δ), and 2.72 – 2.82 μs (□) after the laser pulse, by laser flash photolysis of a O<sub>2</sub> saturated hexanes solution of **43** (ca. 6 × 10<sup>-5</sup> M).....96

**Figure 3.18.** Plots of the pseudo-first-order rate constants (*k*<sub>decay</sub>) for the decay of SiTmp<sub>2</sub> vs. [Et<sub>3</sub>SiH] in hexanes solution at 25 °C.....97

**Figure 4.1.** (a) Transient absorption spectra recorded at 1.44 – 1.76 μs (o), 9.12 – 9.76 μs (□) after the laser pulse, by laser flash photolysis of a deoxygenated hexanes solution of **44**. (b) Transient growth/decay profiles at 460 and 540 nm.....104

## LIST OF TABLES

<b>Table 1.1.</b> Nomenclature for some Group 14 species.....	2
<b>Table 1.2.</b> Calculated $\Delta E_{ST}$ and the <i>DSSE</i> for CH <sub>2</sub> , SiH <sub>2</sub> , GeH <sub>2</sub> and SnH <sub>2</sub> . Units in kcal/mol.....	6
<b>Table 1.3.</b> Absolute rate constants (in units of 10 <sup>9</sup> M <sup>-1</sup> s <sup>-1</sup> ) for quenching of transient silylenes by various substrates in hexanes or cyclohexane solution at room temperature.....	19
<b>Table 1.4.</b> Absorption maxima for SiMe <sub>2</sub> and SiMes <sub>2</sub> complexes in 3 – MP matrix at 77 K.....	21
<b>Table 1.5.</b> Relative rate constants for Si – H insertion reactions of SiH <sub>2</sub> compared with other silylenes in the gas phase at 298 K.....	26
<b>Table 1.6.</b> Ratio of Absolute Rate Constants for the Reaction of Diphenyl- and Dimesitylsilylene with Various Silylene Scavengers in hydrocarbon solution at 298 K.....	29
<b>Table 2.1.</b> Absolute rate constants for quenching of SiMes <sub>2</sub> by various substrates studied in this work in hexanes solution at room temperature.....	46
<b>Table 2.2.</b> Kinetic data for the quenching of free SiMes <sub>2</sub> by alcohols in deoxygenated hexanes at 25 °C.....	62
<b>Table 3.1.</b> Ratios of Absolute Rate Constants for the Reaction of Diphenyl – and Dimesitylsilylene with Various Silylene Scavengers in Hexanes or Cyclohexane solution at 25 °C (including present work).....	69

**Table 3.2.** Absolute rate constants (in units of  $10^9 \text{ M}^{-1} \text{ s}^{-1}$ ) for quenching of  $\text{SiPh}_2$ ,  $\text{SiMes}_2$  and  $\text{SiTmp}_2$  by various substrates in hexanes or cyclohexane solution at  $25^\circ \text{C}$ .....82



## Chapter 1 – Introduction

### 1.1. Thesis Overview

Silylenes are silicon analogues of carbenes having the general formula  $\text{SiR}_2$  (R = alkyl group, aryl group, hydrogen, halide, alkoxy etc.) which in the absence of any substrate undergo dimerization to form disilenes of general formula  $\text{R}_2\text{Si}=\text{SiR}_2$ , provided the substituents are sterically unencumbered or electronically not highly stabilized (*e.g.* –Me, –Ph, –Mes). The disilenes undergo further oligomerization depending on the nature of the substituents. The lifetimes of the transient silylenes studied in this thesis are on the order of microseconds and the absolute rate constants of their reactions with various substrates range from ca.  $10^7$  to  $10^{10} \text{ M}^{-1} \text{ s}^{-1}$ ; hence fast time-resolved spectroscopy is employed to detect these highly reactive intermediates and study their reactivities in solution. This thesis presents the results of fast kinetic studies of a new diarylsilylene, bis(3,4,5-trimethylphenyl)silylene (**1**, SiTmp<sub>2</sub>) and dimesitylsilylene (**2**, SiMes<sub>2</sub>) with various substrates. These results along with the corresponding data for the parent diarylsilylene, diphenylsilylene (**3**, SiPh<sub>2</sub>), provide the first quantitative assessment of the individual effects of steric hindrance and electronics on the reactivities of diarylsilylenes.

## 1.2. Nomenclature<sup>1</sup>

Group 14 elements are known as *tetrels*, and Group 14 divalent species are known as *tetrellylenes*.<sup>2</sup> More commonly, the heavy carbene analogues are known as *metallylenes* and the alkene analogues are known as *metallenes* ( $R_2M=CR_2$ ) and *dimetallenes* ( $R_2M=MR_2$ ), where M = Si, Ge, Sn. The latter terms are misleading because the bonding situation is very different from the carbon analogues.<sup>3</sup> Table 1.1 lists some Group 14 species and their common nomenclature.

**Table 1.1.** Nomenclature for some Group 14 species.

	<i>Metallylene</i>	<i>Dimetallene</i>	<i>Metallene</i>
<b>M</b>	<b>MR<sub>2</sub></b>	<b>R<sub>2</sub>M=MR<sub>2</sub></b>	<b>R<sub>2</sub>M=CR<sub>2</sub></b>
<b>Si</b>	Silylene	Disilene	Silene
<b>Ge</b>	Germylene	Digermene	Germene
<b>Sn</b>	Stannylene	Distannene	Stannene

### 1.3. Electronic Structure and Thermochemistry

#### 1.3.1. Electronic Structure

In divalent Group 14 species the central atom is connected to two substituents and possesses two non-bonding electrons. Thus, there are two possible ground state electronic configurations for these species, the closed shell *singlet* and open shell *triplet*. In the singlet state the two non-bonded electrons are paired in an orbital of  $\sigma$  symmetry, leaving a vacant p – orbital, whilst in the triplet state these electrons are not paired and one electron is in an orbital of  $\pi$  symmetry and the other remains in the orbital of  $\sigma$  symmetry (Fig. 1.1). The energy difference between the singlet state and the triplet state ( $\Delta E_{ST}$ , Eq. 1.1) determines whether these species should be a ground state triplet or singlet. A positive  $\Delta E_{ST}$  indicates that the singlet state is more stable than the triplet state.

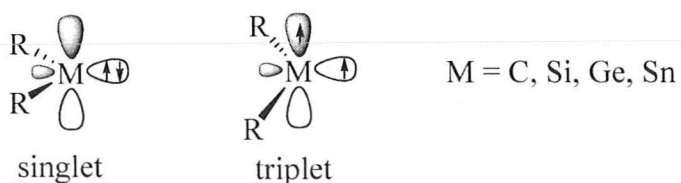


**Figure 1.1.** Singlet and triplet electronic structures of Group 14 divalent species.

$$\Delta E_{ST} = E_{\text{triplet}} - E_{\text{singlet}} \quad (1.1)$$

The  $\Delta E_{ST}$  is dependent on both the steric and electronic effects exerted by the substituents.<sup>4-9</sup> Sterically encumbered substituents force a wider angle between the substituents, hence stabilizing the triplet state relative to the singlet state.<sup>4-5</sup> The singlet state is stabilized by  $\sigma$  acceptors or  $\pi$  donors as substituents;  $\sigma$  acceptors stabilize the singlet state by stabilizing the non-bonding  $\sigma$  orbital by increasing its  $s$ -character whereas  $\pi$  donors stabilize the singlet by bonding with the empty  $p$  – orbital.<sup>4-7,10-11</sup> For diaryl and dialkyl carbenes,  $\Delta E_{ST}$  is only a few kcal/mol, and hence the ground state multiplicity is strongly dependent on the nature of the substituents. For example, the parent carbene  $\text{CH}_2$  is a ground state triplet while dichlorocarbene is a ground state singlet.<sup>4</sup> The situation is much different with the heavier carbene analogues, the singlet ground state being favoured progressively as one goes down the Group 14.<sup>12-13</sup> A theoretical study by Apeloig *et al.* suggests that about 60% of the difference in  $\Delta E_{ST}$  between  $\text{CH}_2$  and  $\text{SiH}_2$  may be attributed to reduced repulsion of the two frontier electrons in the case of the latter due to the increased size of the  $\sigma$  orbital in the heavier analogue.<sup>13</sup> Only four ground state triplet silylenes are known (Fig. 1.2),<sup>14-16</sup> and all other heavy carbene analogues that have been reported have singlet ground states. The triplet silylenes **4**, **6**, **7** were characterized by EPR studies by Sekiguchi *et al.*<sup>14-15</sup> while **5** is speculated to have a triplet ground state based on its unusually high reactivity toward intramolecular C-H bond insertion.<sup>16</sup> Calculated values of  $\Delta E_{ST}$  for the series of Group 14 dihydrides ( $\text{MH}_2$ ,  $M = \text{C, Si, Ge, Sn}$ ) are listed in Table 1.2.<sup>12</sup>

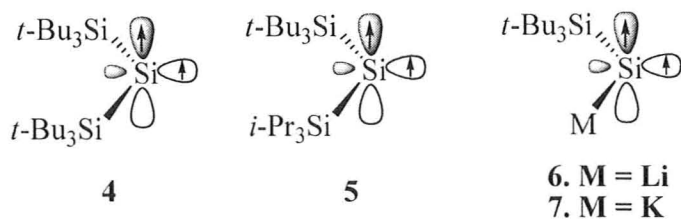
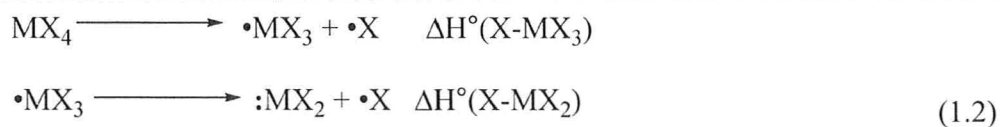


**Figure 1.2.** Examples of triplet silylenes

### 1.3.2. Divalent State Stabilization Energy (DSSE)

The Divalent State Stabilization Energy or DSSE is defined as the difference between the M – X bond dissociation enthalpies ( $\Delta H^\circ$ ) of  $\text{MX}_4$  and  $\text{MX}_3$  (Eqs. 1.2 – 1.3).<sup>17-18</sup> The lower the  $\Delta H^\circ$  value for the second step, the more stable the divalent species and the larger its DSSE. Table 1.2 lists the DSSE values for the Group 14 dihydrides ( $\text{MH}_2$ , M = C, Si, Ge, Sn).<sup>19-23</sup> The DSSE increases as Group 14 is descended because the valence shell  $s$  electrons (HOMO) of the heavier elements are successively lower lying.<sup>17</sup>



$$\text{DSSE} = \Delta H^\circ(\text{X-MX}_3) - \Delta H^\circ(\text{X-MX}_2)
 \tag{1.3}$$

**Table 1.2.** Calculated  $\Delta E_{ST}$  and the  $DSSE$  for  $\text{CH}_2$ ,  $\text{SiH}_2$ ,  $\text{GeH}_2$  and  $\text{SnH}_2$ . Units in kcal/mol.

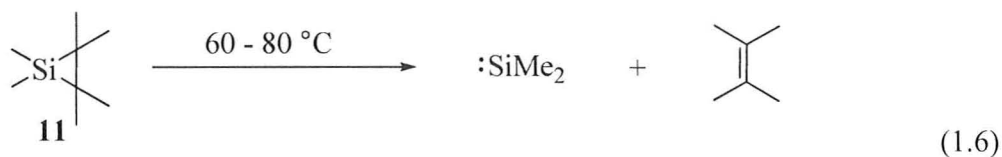
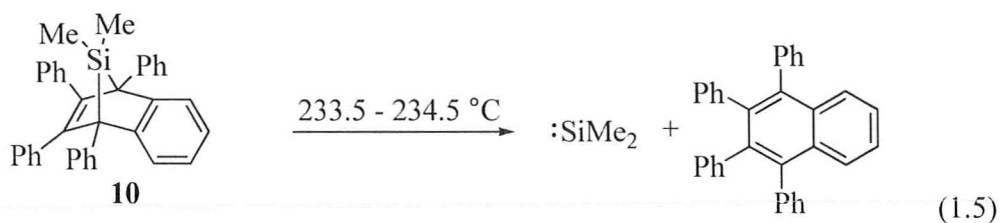
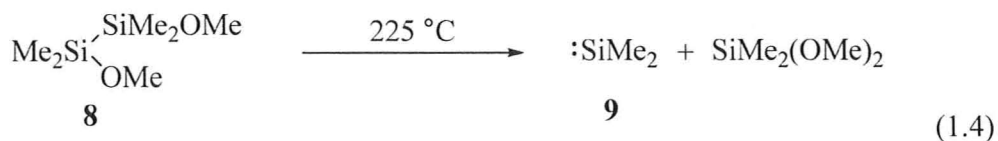
	$\Delta E_{ST}^a$	$DSSE$
<b><math>\text{CH}_2</math></b>	-10.4	-6 ( $^3\text{B}_1$ ) <sup>b</sup>
<b><math>\text{SiH}_2</math></b>	+20.0	+22 <sup>c</sup>
<b><math>\text{GeH}_2</math></b>	+22.0	+28 <sup>d</sup>
<b><math>\text{SnH}_2</math></b>	+23.4	+26 <sup>e</sup>

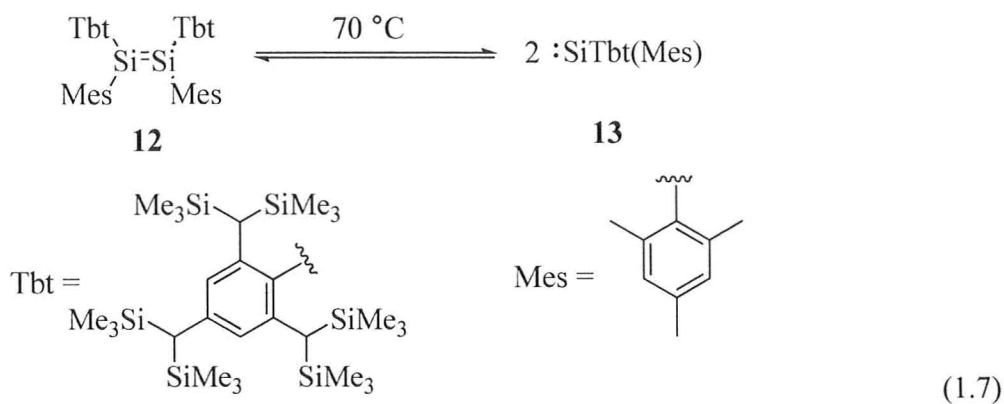
<sup>a</sup> CCSD(T)/EC; ref. 12. <sup>b</sup> MP4SDTQ/6-311G\*\*; ref. 19. <sup>c</sup> Experimental; ref 20. <sup>d</sup> Experimental; ref. 21. <sup>e</sup> BAC-MP4 (298 K); ref. 22.

## 1.4. Generation of Silylenes

### 1.4.1. Thermal Generation of Silylenes

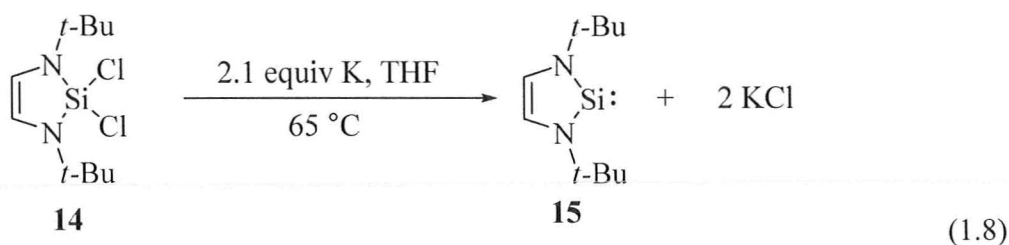
Silylenes can be generated by pyrolysis of polysilanes (*e. g.* Eq. 1.4),<sup>24</sup> 7-silanorbornadienes (*e. g.* Eq. 1.5),<sup>25</sup> siliranes (*e. g.* Eq. 1.6),<sup>26</sup> and from extremely hindered disilenes (*e. g.* Eq. 1.7)<sup>27</sup>. In all these cases, the precursors were pyrolysed in the presence of substrates considered as silylene traps and products obtained were consistent with the respective silylene intermediacy.





#### 1.4.2. Generation of Silylenes under Strong Reducing Conditions

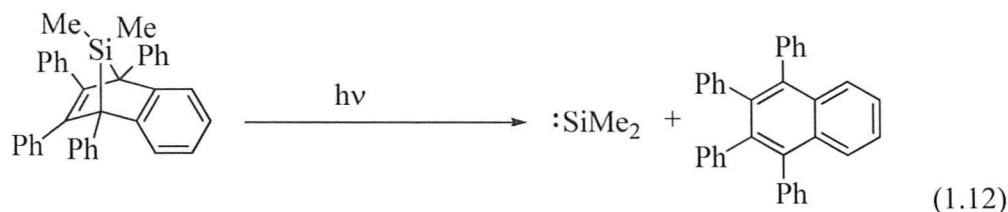
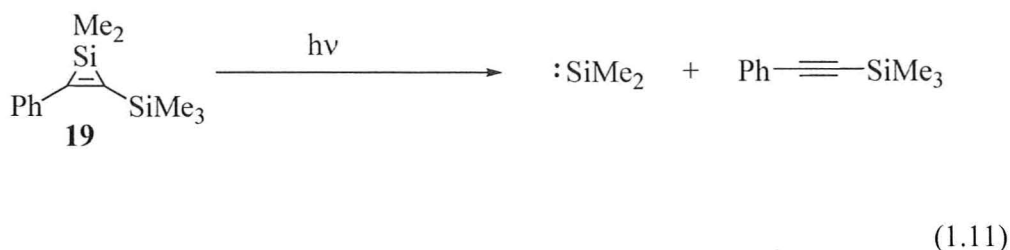
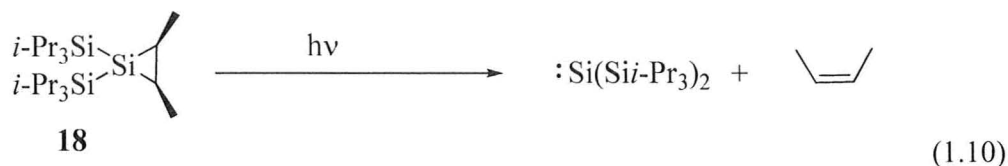
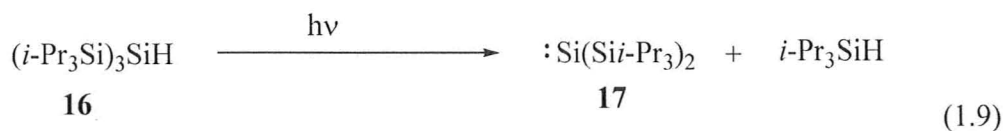
Silylenes can also be synthesized by the reduction of dihalosilanes using alkali metals, the method being used extensively for the synthesis of kinetically<sup>28</sup> or thermodynamically<sup>29-30</sup> stable silylenes (*e. g.* Eq. 1.8)<sup>29</sup>.



#### 1.4.3. Photolytic Generation of Silylenes

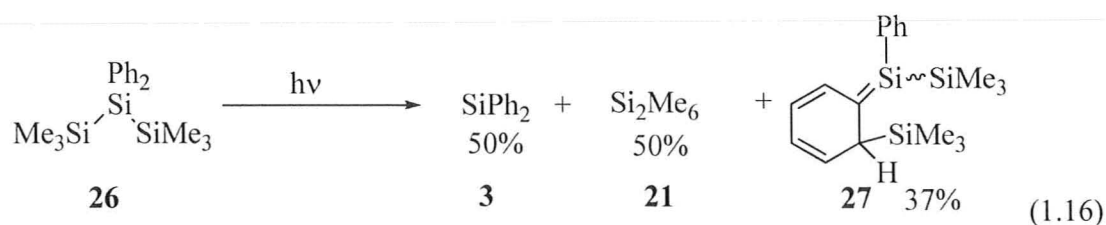
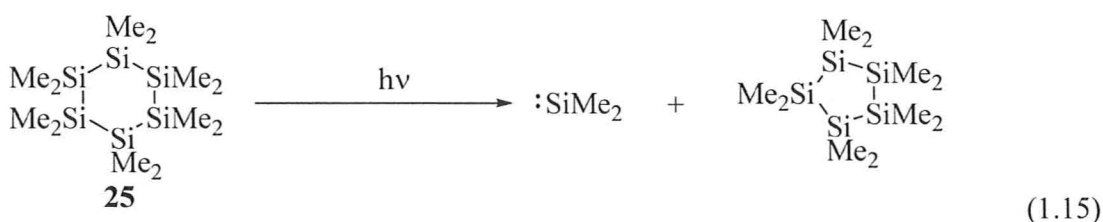
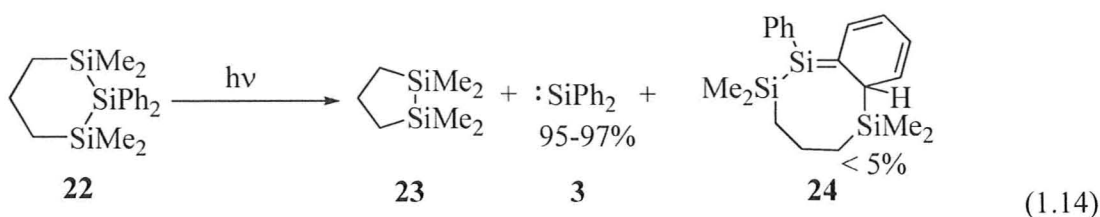
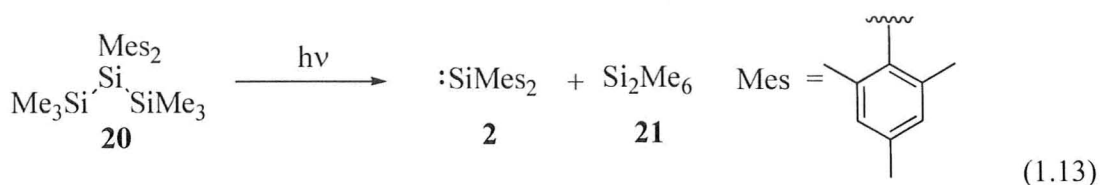
Photochemical irradiation of oligosilanes (*e. g.* Eq. 1.9),<sup>31</sup> siliranes (*e. g.* Eq. 1.10),<sup>5</sup> silirenes (*e. g.* Eq. 1.11)<sup>32</sup> and 7-silanorbornadienes (*e. g.* Eq. 1.12)<sup>33</sup> is known to generate silylenes.





Commonly used photochemical precursors are acyclic (*e. g.* Eq. 1.13)<sup>34-36</sup> or cyclic (*e. g.* Eq. 1.14)<sup>37</sup> trisilanes and cyclic oligosilanes (*e. g.* Eq. 1.15).<sup>38</sup> In solution at room temperature, phenylated trisilanes undergo competitive 1,3 – silyl migration reactions to form strongly absorbing silatrienes (*e. g.* Eq. 1.16).<sup>37,39-44</sup> In early time – resolved studies, the strong absorptions of these silatrienes were assigned to those for  $\text{SiMePh}^{45-46}$  and  $\text{SiPh}_2^{47}$  and in these studies the rate constants reported for the mentioned silylenes were significantly different from those obtained later for  $\text{SiMe}_2^{48-51}$

and  $\text{SiMe}_2$ <sup>36</sup> with the same substrates. Recently, our group has used cyclic trisilanes to suppress this side reaction and facilitate direct detection of these silylenes.<sup>37,39,41</sup>



### 1.5. Electronic Spectra of Silylenes

The lowest energy electronic absorption of silylenes can be represented as a transition from the ground state singlet ( $S^0$ ) in which both electrons are localized in a  $3s$

orbital on Si, to an excited state singlet ( $S^1$ ) which has one electron in a  $3p$  orbital perpendicular to the molecular plane and the other in the  $3s$  orbital (Fig. 1.3).<sup>5</sup> The electronic spectra of several organosilylenes have been reported in low temperature matrixes<sup>34,52-55</sup> and also in solution.<sup>36-37,39,41,48,50</sup> The transition occurs in the spectral range of 390 – 600 nm (*e.g.*  $\lambda_{\text{max}}$  SiMes(*t*-BuO) = 396;<sup>34</sup> SiMe<sub>2</sub> = 465;<sup>48</sup> SiPh<sub>2</sub> = 515 nm;<sup>37</sup> SiMePh = 520 nm;<sup>41</sup> SiMes<sub>2</sub> = 580 nm<sup>36</sup>). The electronic transition of the ground state singlet silylenes as shown in figure 1.3 is formally allowed;<sup>56</sup> however, the movement of an electron from one orbital to another is associated with small migration of charge and hence the dipole-moment operator ( $\mu$ ) is small and this leads to a low extinction coefficient for this transition.

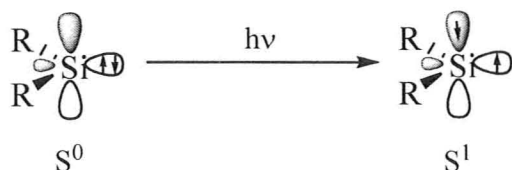
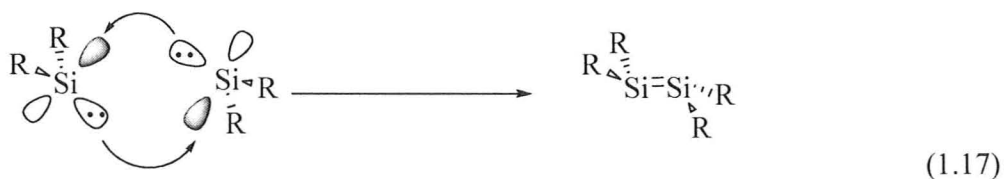


**Figure 1.3.** Electronic absorption of Silylenes

## 1.6. Reactivity of Silylenes

Ground state singlet silylenes possess a lone pair of electrons and an empty  $p$  – orbital ( $3p_z$ ) on silicon, and thus the silicon center can potentially behave both as an electrophile and a nucleophile. Dimerization, the most typical reaction of silylenes, exhibits both of these properties. All but the most severely protected silylenes dimerize along the path in which the lone pair of one molecule overlaps with the empty  $3p_z$

orbital of the other to form a slightly trans – bent disilene (Eq. 1.17).<sup>6,57-59</sup> The electrophilic and nucleophilic character of silylenes can be tuned by changing the substituents. Increasing the  $\pi$  – donating capabilities of the substituents decreases the electrophilicity of the silylenes.<sup>6</sup>



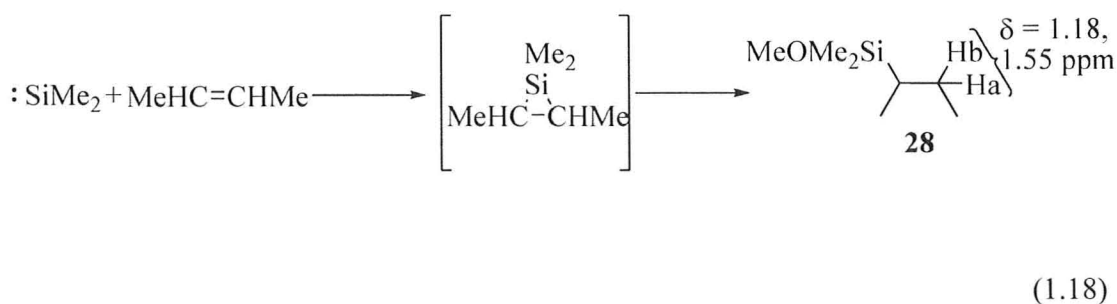
The reactions of silylenes have been discussed in several early reviews.<sup>5,20,23,35,46,60-64</sup> Most of the silylene reactivity was inferred from product analyses of the reactions of silylenes with various trapping agents. Initially the direct detection of transient silylenes was restricted to low temperature glasses where the reactivity was studied by UV/Vis and IR spectroscopy.<sup>34,38,65-72</sup> Inoue *et al.* reported the first time resolved spectroscopic study of  $\text{SiH}_2$  in the gas phase using Laser Induced Fluorescence and reported several rate constants for its reactions.<sup>73</sup> Since then several time resolved gas phase kinetic studies have been carried out on  $\text{SiH}_2$  and several simple substituted derivatives  $\text{SiXY}$  (X, Y = H, Me or halogen).<sup>20,23,74-80</sup> In solution though kinetic data is limited to the reactions of  $\text{SiMe}_2$ ,<sup>48-51,81-82</sup>  $\text{SiMe}_2$ ,<sup>36-37,82</sup>  $\text{SiPh}_2$ <sup>37,81-82</sup> and  $\text{SiMePh}$ ,<sup>41</sup> the bulk of which were reported by our group in recent years. All the reactions indicate an electrophilic character of the silylenes although nucleophilic silylenes are known.<sup>83</sup> This section introduces the reactions of silylenes studied in this

thesis. These fall into the following general classes: (i) addition to alkenes and alkynes, (ii) halogen atom abstraction, (iii) complexation reactions, (iv) insertion into  $\sigma$  bonds and (v) ene – type addition.

### 1.6.1. Addition of Silylenes to Alkenes and Alkynes

Silylenes are known to react with alkenes and alkynes to form three membered ring compounds – siliranes from alkenes and silirenes from alkynes.<sup>84-91</sup> The addition to alkenes is stereospecific, which was first established by studies of the reactions of  $\text{SiMe}_2$  and  $\text{SiPh}_2$  with *cis* – and *trans*-2- butene, where the obtained siliranes were trapped as the methanolysis products.<sup>84-85</sup> The siliranes in these cases were difficult to distinguish from the side products by NMR studies and hence their methanolysis was adopted as an indirect approach to determine the stereospecificity of the reactions.<sup>84</sup> When the  $\text{SiMe}_2$  adducts of *cis* and *trans*-2- butene were treated with methanol the methylene protons of the resulting 2 – butylmethoxydimethyl (**28**) appeared in the  $^1\text{H}$  NMR spectrum as diastereotopic hydrogens with chemical shifts  $\delta$  1.18 and 1.55 ppm (Eq 1.18).<sup>85</sup> When  $\text{CH}_3\text{OD}$  is added to the silirane one of these hydrogens disappears from the  $^1\text{H}$  NMR spectrum and appears in the  $^2\text{H}$  NMR spectrum: for *cis*-2-butene it is the proton at  $\delta$  1.18 ppm and for *trans*-2-butene it is the hydrogen at  $\delta$  1.55 ppm.<sup>85</sup> This experiment did not establish whether the addition was stereospecifically *cis* or *trans*. Ishikawa *et al.* showed that  $\text{Si}(\text{SiMe}_3)\text{Ph}$  in the presence of *trans*-2-butene led to the formation of only a single silirane, while two stereoisomeric siliranes were formed from addition to *cis*-2-

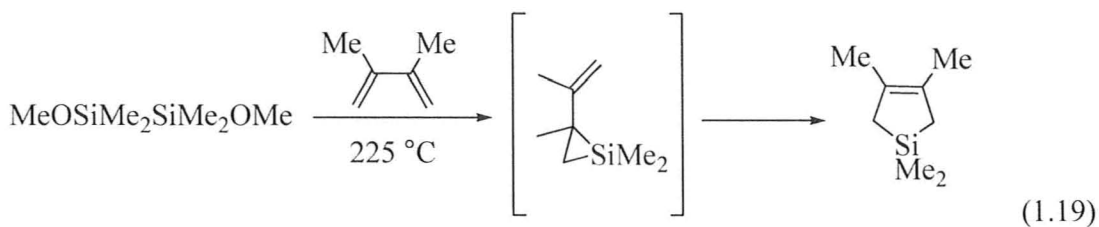
butene and this observation is consistent with a *cis* – addition mechanism.<sup>92</sup> Stereospecific *cis* – addition to olefins has also been reported for Si(Si<sup>i</sup>Pr<sub>3</sub>)<sub>2</sub>,<sup>31</sup> SiMe<sub>2</sub>,<sup>90</sup> and diadamantylsilylene (SiAd<sub>2</sub>).<sup>88</sup> The type of stereospecificity is also common to the reactions of singlet carbenes, where the intermediacy of a  $\pi$  complex has been proposed.<sup>93-95</sup> Siliranes are thermally less stable than the corresponding cyclopropanes and this is attributed to the higher *DSSE* of the silylenes involved compared to the carbenes and also due to greater ring strain relative to the corresponding cyclopropanes.<sup>96</sup>

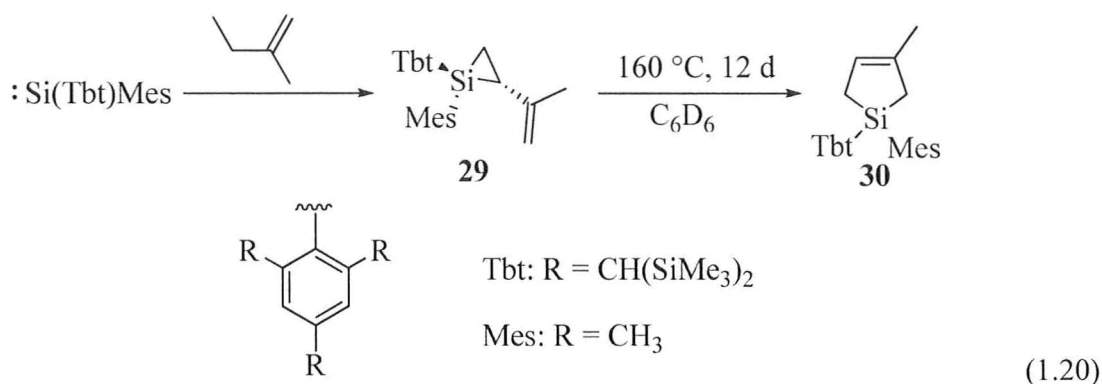


The absolute rate constants of the reactions of SiMe<sub>2</sub>,<sup>49,81</sup> SiPh<sub>2</sub>,<sup>81</sup> SiMes<sub>2</sub>,<sup>36</sup> SiMePh<sup>41</sup> with various alkenes and alkynes like 1 – hexene (only for SiMe<sub>2</sub>), 4,4 – dimethyl – 1 – pentene (DMP) (for SiMe<sub>2</sub>, SiPh<sub>2</sub>, SiMePh), trimethylsilylethylene (only for SiMe<sub>2</sub>), cyclohexene (for SiMe<sub>2</sub>, SiPh<sub>2</sub>, SiMes<sub>2</sub>), 3,3 – dimethyl – 1 – butyne (TBE) (for SiMe<sub>2</sub>, SiPh<sub>2</sub>, SiMePh), bis(trimethylsilyl)acetylene (BTMSE) (for SiMe<sub>2</sub>, SiPh<sub>2</sub>) have already been reported in cyclohexane or hexanes (Table 1.3). It has been observed that SiMe<sub>2</sub>, SiPh<sub>2</sub> and SiMePh react within a factor of 3 of the diffusional rate constant

( $k_{\text{diffusion}} = 2.3 \times 10^{10} \text{ M}^{-1} \text{ s}^{-1}$ )<sup>97</sup> with these alkenes and alkynes while the absolute rate constant for the reaction of cyclohexene with  $\text{SiMe}_2$  was found to be  $2.8 \times 10^6 \text{ M}^{-1} \text{ s}^{-1}$ .<sup>36</sup>

Atwell and Weyenberg were the first to report the reaction of silylenes with 1,3 – dienes in which 1 – silacyclopent – 3 – ene was observed as the product (Eq. 1.19).<sup>98</sup> The intermediacy of 2 – vinyl – 1 – silirane was proposed for this reaction. Since then, several reactions of silylenes with 1,3 – dienes were reported in which 1 – silacyclopent – 3 – enes were observed.<sup>60,99-101</sup> Ishikawa *et al.* were the first to establish the intermediacy of 2 – vinyl – 1 – silirane by methanol trapping of the intermediate.<sup>102</sup> Zhang and Conlin's successful isolation of several vinylsiliranes from the reaction of  $\text{SiMe}_2$  with aliphatic dienes verified this proposal.<sup>89</sup> Takeda *et al.* found that the vinylsilirane (**29**) generated from the reaction of isoprene with  $\text{Si}(\text{Tbt})\text{Me}_2$  upon heating at  $160 \text{ }^\circ\text{C}$  for 12 days gives the corresponding silacyclopentene (**30**) in high yield (Eq. 1.20).<sup>103</sup> The last observation and a similar one in our group,<sup>81</sup> where vinylsilirane from  $\text{SiPh}_2$  and 2,3 – dimethyl – 1,3 – butadiene (DMB) isomerized to the silacyclopentene derivative at  $25 \text{ }^\circ\text{C}$  over 48 h, put the vinylsilirane formation as a primary step for the reaction on a firm footing.





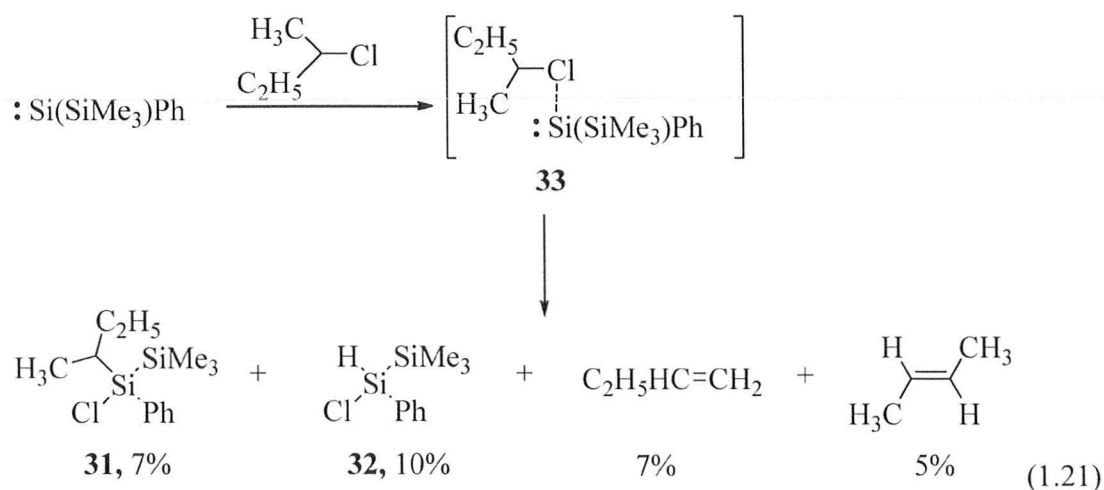
The absolute rate constants for the reaction of  $\text{SiMe}_2$ ,  $\text{SiPh}_2$ ,  $\text{SiMes}_2$  and  $\text{SiMePh}$  with dienes such as DMB and isoprene are roughly 2 – 3 times larger than those for the reactions with alkenes and the rate constant obtained for the reaction of DMB with  $\text{SiMes}_2$  was found to be substantially smaller than those obtained for  $\text{SiMe}_2$ ,  $\text{SiPh}_2$  and  $\text{SiMePh}$  (Table 1.3).<sup>36,41,81</sup>

### 1.6.2. Reaction of Silylenes with halocarbons

Silylenes react with halocarbons to give different types of chlorinated silanes depending on the nature of the silylene and the halocarbon.<sup>104-108</sup> They undergo C – Cl insertion and/or HCl abstraction with monochloroalkanes<sup>107,109</sup> and halogen atom abstraction with  $\text{CCl}_4$  which leads to dichlorosilanes and other radical derived products.<sup>105-106,110-111</sup> Ishikawa *et al.* observed that the reaction of  $\text{Si}(\text{SiMe}_3)\text{Ph}$  with *sec* – butyl chloride yields a C – Cl insertion product, 1 - (*sec* – butyl) – 1 – chloro – 1 – phenyltrimethyldisilane (31), and an HCl insertion product, 1 – chloro – 1 – phenyl – 2,2,2 – trimethyldisilane (32), along with 1 – butane and *trans* – 2 – butene (Eq. 1.21).<sup>107</sup>



The authors proposed the intermediacy of silylene – halocarbon Lewis acid – base complex (**33**, Eq. 1.21) for the reaction.<sup>107</sup> Oka and Nakao supported this notion by their product studies of a more comprehensive set of halocarbons with the same silylene.<sup>108</sup> Taraban *et al.* studied the reaction of SiMe<sub>2</sub> with CCl<sub>4</sub> by laser flash photolysis and chemically induced dynamic nuclear polarization (CIDNP) methods and assigned a relatively long – lived transient observed at λ<sub>max</sub> = 334 nm to the SiMe<sub>2</sub> – CCl<sub>4</sub> complex.<sup>111</sup> The partition of the silylene - halocarbon Lewis acid – base complex between halogen atom abstraction and other pathways is dependent on the nature of the halocarbon and Cl atom abstraction is favoured in the case of CCl<sub>4</sub>.<sup>105,108,112</sup> Theoretical studies by Becerra *et al.* indicate that the insertion products observed might well be the result of Cl atom abstraction followed by radical recombination within the solvent cage.<sup>113</sup>



The absolute rate constants for the reaction of  $\text{CCl}_4$  with  $\text{SiMe}_2$  and  $\text{SiPh}_2$  in hexanes solution are on the order of  $10^9 \text{ M}^{-1} \text{ s}^{-1}$  and are approximately 40 and 100 times faster than the reactions of their respective germylene analogues with  $\text{CCl}_4$  (Table 1.3).<sup>81,114-115</sup> The reasons for such large differences are not yet clear.

**Table 1.3.** Absolute rate constants (in units of  $10^9 \text{ M}^{-1} \text{ s}^{-1}$ ) for quenching of transient silylenes by various substrates in hexanes or cyclohexane solution at room temperature.

Substrate	SiMe <sub>2</sub>	SiMePh <sup>c</sup>	SiPh <sub>2</sub>	SiMes <sub>2</sub>
THF	$17.3 \pm 1.5^a$		$15.2 \pm 1.3^a$	-
MeOH	$21 \pm 3^b$	$16.3 \pm 0.8$	$18 \pm 2^b$	$1.01 \pm 0.09^b$
<i>t</i> -BuOH	$14 \pm 2^b$		$14 \pm 1^b$	$0.136 \pm 0.005^b$
Et <sub>3</sub> SiH	$3.6 \pm 0.3^a$	$2.96 \pm 0.05$	$3.3 \pm 0.2^d$	$0.079 \pm 0.004^f$
O <sub>2</sub>	$0.47 \pm 0.04^a$		$0.12 \pm 0.02^a$	$0.032 \pm 0.004^f$
Acetone	$14.1 \pm 1.2^d$		$14.4 \pm 2.0^d$	$8.3 \pm 0.4^d$
AcOH	$15.9 \pm 1.0^a$		$10.1 \pm 1.0^a$	
DMP	$11.7 \pm 0.5^a$	$7.0 \pm 0.3$	$7.9 \pm 1.6^e$	
Cyclohexene	$7.8 \pm 1.0^a$		$7.9 \pm 0.7^a$	$0.0028 \pm 0.0003^f$
DMB	$15.9 \pm 0.7^a$	$12.9 \pm 0.8$	$14.5 \pm 1.3^a$	$0.0088 \pm 0.0007^f$
Isoprene	$19.8 \pm 0.7^a$	$19.5 \pm 0.6$	$13.6 \pm 1.4^a$	
TBE	$17.8 \pm 0.6^a$	$9.5 \pm 0.2$	$8.3 \pm 0.7^e$	
BTMSE	$13.8 \pm 0.5^a$		$7.6 \pm 0.6^a$	
CCl <sub>4</sub>	$3.4 \pm 0.2^a$		$1.37 \pm 0.09^a$	

<sup>a</sup> In hexanes, data from ref. 81. <sup>b</sup> In hexanes, data from ref. 82. <sup>c</sup> In hexanes, data from ref. 41. <sup>d</sup> In hexanes, data from ref. 37. <sup>e</sup> In hexanes, data from ref. 39. <sup>f</sup> In cyclohexane, data from ref. 36.

### 1.6.3. Complexation of Silylenes with Lewis bases

The Lewis acid – base complexation of silylenes with different heteroatom containing nucleophiles has generated enormous interest over the past several decades.<sup>49,51,65,68,72,81,116-126</sup> A large number of complexes of this kind were detected in low – temperature matrices.<sup>65,68,72,116,125</sup> In a typical experiment of this kind a silylene precursor is frozen at 77 K in a hydrocarbon matrix containing a Lewis base. Irradiation of the matrix yields the silylene which upon annealing gives the silylene – nucleophile complex. Both the silylene and the complex can be detected by UV spectroscopy. In all cases the Lewis acid – base complexes were blue shifted relative to the silylene absorption. Table 1.4 lists the absorption maxima of some Lewis acid – base complexes of SiMe<sub>2</sub> and SiMes<sub>2</sub> with various Lewis bases in low temperature matrices.

In solution the complexation with ethers, although unproductive except for strained ethers,<sup>127</sup> moderates the reactivity of silylenes towards other substrates.<sup>49,128-129</sup> Kinetic studies of SiMe<sub>2</sub> with various nucleophilic substrates have been carried out in hexanes and cyclohexane solutions where effectively irreversible (*i.e.* reaction proceeds with a very high equilibrium constant,  $K_{eq} > 25\ 000\ M^{-1}$ ) complexation have been observed with absolute rate constants very close to the diffusion limit (Table 1.3).<sup>37,49,51,81-82</sup> The complexation reactions of SiPh<sub>2</sub> with THF and MeOSiMe<sub>3</sub> were found to be irreversible with rate constants similar to those for SiMe<sub>2</sub> (Table 1.3).<sup>81</sup> It is interesting to note that the reaction of SiMes<sub>2</sub> with THF was found to be reversible with

a small equilibrium constant of  $3 \text{ M}^{-1}$  and the reaction of  $\text{SiMe}_2$  with  $\text{MeOSiMe}_3$  was too slow to be measured; the upper limit is  $< 10^6 \text{ M}^{-1} \text{ s}^{-1}$ .<sup>36,130</sup>

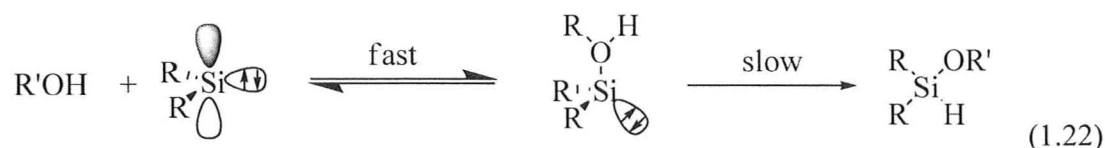
**Table 1.4.** Absorption maxima for  $\text{SiMe}_2$  and  $\text{SiMe}_2$  complexes in 3 – MP matrix at 77 K<sup>65</sup>

Base	$\text{SiMe}_2$	$\text{SiMe}_2$
None	450	580
$\text{Et}_2\text{O}$	299	320
THF	280	328
$\text{Et}_3\text{N}$	287	350
<i>t</i> – $\text{Bu}_2\text{S}$	322	316
<i>n</i> – $\text{Bu}_3\text{P}$	290	345

#### 1.6.4. Insertion of Silylenes into Single Bonds (O – H, Si – H)

Insertion of silylenes into the O – H bonds of alcohols is one of the best known reactions of silylenes.<sup>5,35,62,131</sup> The insertion of  $\text{SiMe}_2$  into the O – H and O – D bonds of water and alcohol were the first such reaction studied, where ca. 90% yield was observed for the insertion products.<sup>132</sup> The fact that the intermediate Lewis acid – base complexes of alcohols with several silylenes were detected directly in low temperature

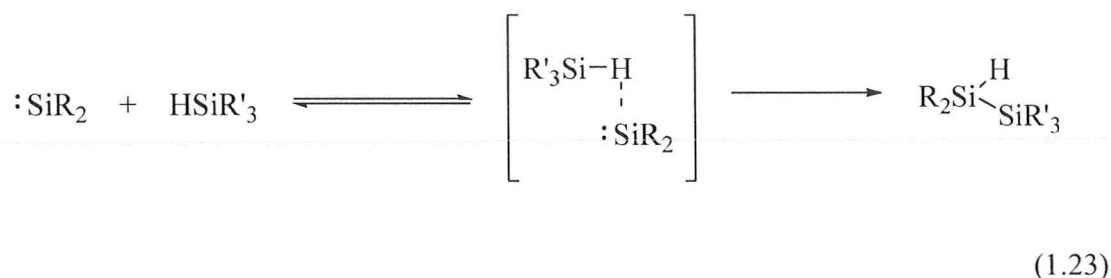
glasses<sup>65</sup> and in solution,<sup>37,49,82</sup> was interpreted as the reaction proceeds through the formation of the corresponding Lewis acid – base complex followed by H – transfer from oxygen to the silicon center (Eq. 1.22). This is supported by theoretical calculations, which predict the initial complexation step to be barrierless, and the overall barrier arises in the second step.<sup>117-118,133-135</sup>



A detailed mechanistic study in our group aimed at elucidating the reactivity of SiMe<sub>2</sub>, SiPh<sub>2</sub> and SiMes<sub>2</sub> with MeOH/D and *t*-BuOH/D in hexanes suggests that the reaction proceeds by an effectively irreversible complexation as the first step in the cases of SiPh<sub>2</sub> and SiMe<sub>2</sub>, the catalytic proton transfer by another molecule of alcohol being unambiguously the major pathway for converting the intermediate complexes to the respective alcohol insertion products.<sup>82</sup> The major difference of the reactivity of SiMes<sub>2</sub> with the other two silylenes is that the complexation step was found to be reversible in the case of SiMes<sub>2</sub> with the same alcohols.<sup>82</sup> While the intermediate complexes of alcohols with SiMe<sub>2</sub> ( $\lambda_{\text{max}} \sim 300\text{nm}$ ) and SiPh<sub>2</sub> ( $\lambda_{\text{max}} \sim 360\text{ nm}$ ) have been detected at low concentrations of the alcohol, the SiMes<sub>2</sub> – alcohol complex could not be detected under any of the conditions studied. The measured rate constants for the reactions of SiMe<sub>2</sub> and SiPh<sub>2</sub> with MeOH and *t*-BuOH are all within a factor of two of

the diffusion control limit and do not vary with alcohol structure. For  $\text{SiMe}_2$ , the initial complexation step in the reaction with MeOH is more than an order of magnitude slower than  $\text{SiPh}_2$ . The complexation rate constant is further reduced by a factor of 7 in the case of *t*-BuOH relative to MeOH (Table 1.3).<sup>82</sup>

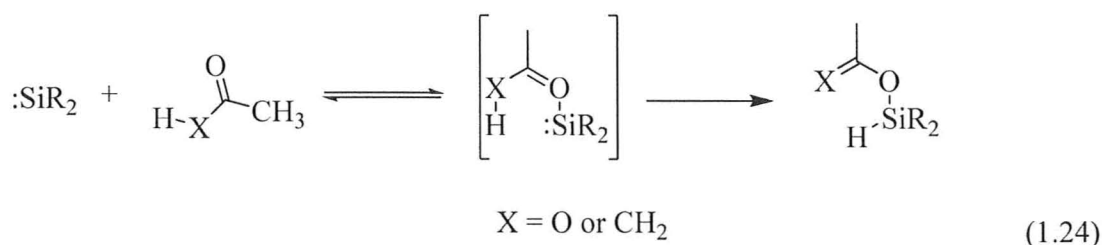
The insertion of silylenes into the Si – H bond is among the most extensively studied reaction in silylene chemistry.<sup>20,60,136</sup> The reaction is believed to proceed by the initial formation of a weak H – bonded silylene – hydridosilane complex, followed by a rearrangement to yield the final insertion product. (Eq. 1.23).<sup>5,20,80,136</sup> The absolute rate constants for the reactions of  $\text{SiMe}_2$  and  $\text{SiPh}_2$  with  $\text{Et}_3\text{SiH}$  in hexanes are both ca.  $3 \times 10 \text{ M}^{-1} \text{ s}^{-1}$  which is about 40 times faster than the rate constant obtained for the reaction of the same silane with  $\text{SiMe}_2$  (Table 1.3).<sup>36,81</sup>



### 1.6.5. Ene type Addition Reactions of Silylenes with Acetic acid and Acetone

Silylenes react with acetic acid or acetone to give formal ene type addition products.<sup>37,81,137-138</sup> These reactions also have been proposed to occur via a stepwise mechanism (Eq 1.24), involving initial complexation followed by rearrangement to yield

the final products. Although the silylene – carbonyl Lewis acid – base complexes with acetone or acetic acid were not observed in any of the time resolved spectroscopic studies in solution, the mechanism in equation 1.24 is supported by the spectroscopic detection of the complex of SiMes<sub>2</sub> with a nonenolizable ketone at cryogenic temperatures.<sup>70</sup>



The absolute rate constants for the reaction of SiMe<sub>2</sub>, SiMePh and SiPh<sub>2</sub> with acetone and acetic acid are within a factor of 3 of the diffusional rate constant ( $k_{\text{diff}} = 2.3 \times 10^{10} \text{ M}^{-1}\text{s}^{-1}$  in hexane at 25 °C)<sup>97</sup> while the rate constant for SiMes<sub>2</sub> with acetone was found to be slower by only a factor of 2 relative to those for the other two silylenes (Table 1.3).<sup>37,41,81</sup>



### 1.7. Application of Silylene Chemistry

Silylenes, specially  $\text{SiH}_2$ , act as intermediates in the chemical vapour deposition of thin silicon films.<sup>139</sup> The last decade has also witnessed ingenious applications of silylenes in the field of organic synthesis.<sup>140-148</sup> The latter work have been mainly developed by Woerpel and co-workers in which the silylene was generated as metal-silylenoid species.<sup>142</sup> The application of silylene chemistry to organic synthesis is particularly important because several organosilicon compounds show appreciable biological activity.<sup>149</sup> Stable silylenes have been used as catalysts for alkene polymerization<sup>150</sup> and Pd (0) complexes of stable silylenes catalyze the Suzuki reaction.<sup>151</sup> Recently the stable silylene **15** was used to mediate C-H activation of various alkanes, ethers and amines and is expected to have a huge impact in future organic synthesis of organosilicon compounds.<sup>152</sup>

### 1.8. Steric vs. Electronic Effects on Silylene Reactivity

Substituents on the silicon center of silylenes play a major role in modifying their reactivity. Walsh *et al.* have extensively studied the Si-H insertion reaction of silylenes with hydridosilanes in the gas phase with several silylene derivatives such as  $\text{SiH}_2$ ,<sup>136,153</sup>  $\text{SiMeH}$ ,<sup>154</sup>  $\text{SiPhH}$ ,<sup>155</sup>  $\text{SiClH}$ ,<sup>156</sup> and  $\text{SiMe}_2$ <sup>157</sup> as a function of methyl substitution in the silane ( $\text{Me}_n\text{SiH}_{4-n}$ ;  $n = 0 - 3$ ). The ratio of rate constants of  $\text{SiH}_2$  compared with those of  $\text{SiMeH}$ ,  $\text{SiPhH}$ ,  $\text{SiClH}$ , and  $\text{SiMe}_2$  (Table 1.5) for the insertion reactions in the Si-H bonds of hydridosilanes revealed that: (i) substituents tend to

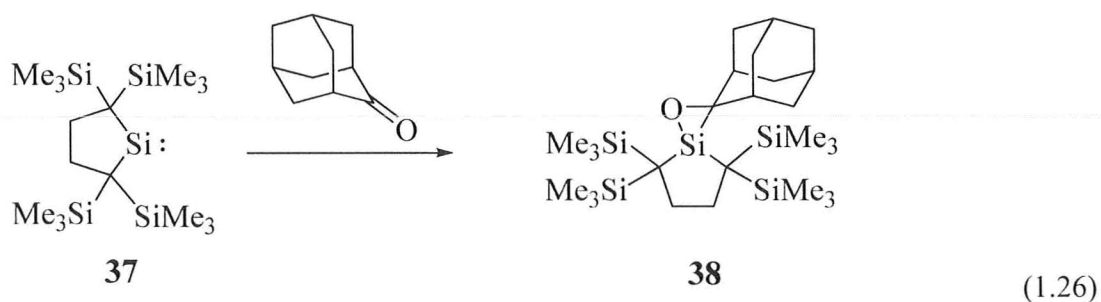
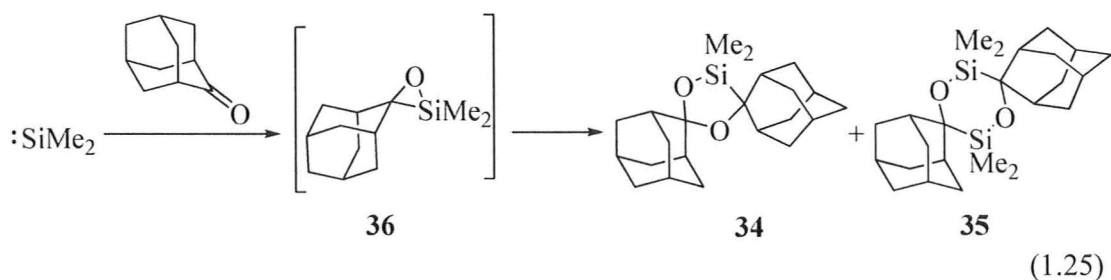
reduce the reactivity of silylenes in a non – systematic fashion (the second methyl substitution has a much larger effect than the first); and (ii) for a given silylene the relative rate constants diminish with increasing methyl substitution in the substrate.<sup>23</sup> The effect has been rationalized by an increase in the barrier for the second step (see Sec. 1.6.4, Eq. 1.23) in the substituted silylenes, due to the electron withdrawing nature of alkyl, aryl and chloro substituents.<sup>20,23</sup> In addition to this, the back donation of a chlorine atom lone pair of electrons into the empty  $3p_z$  orbital of silylene will reduce its electrophilicity and deactivate it towards the insertion reaction.<sup>20,23</sup> The comparative study explains how electronic effects control the gas phase silylene reactivities.<sup>23,136</sup>

**Table 1.5.** Relative rate constants for Si – H insertion reactions of  $\text{SiH}_2$  compared with other silylenes in the gas phase at 298 K.

Substrate	$k_{\text{SiH}_2}/k_{\text{SiMeH}}^b$	$k_{\text{SiH}_2}/k_{\text{SiPhH}}^c$	$k_{\text{SiH}_2}/k_{\text{SiMe}_2}^d$	$k_{\text{SiH}_2}/k_{\text{SiClH}}^e$
<b>SiH<sub>4</sub></b>	5.6	7.8	2300	87 000
<b>MeSiH<sub>3</sub></b>	2.0	1.05	215	1290
<b>Me<sub>2</sub>SiH<sub>2</sub></b>	2.1	1.7	64	245
<b>Me<sub>3</sub>SiH</b>	0.90	0.65	57	144

<sup>a</sup> Based on  $k_{\text{SiH}_2}$  data from ref. 136 and ref. 153 (high pressure limit). <sup>b</sup> Based on  $k_{\text{SiMeH}}$  data from ref. 154. <sup>c</sup> Based on  $k_{\text{SiPhH}}$  data from ref. 155. <sup>d</sup> Based on  $k_{\text{SiMe}_2}$  data from ref. 157. <sup>e</sup> Based on  $k_{\text{SiClH}}$  data from ref. 156.

Ando and co – workers have reported that the reaction of photochemically generated  $\text{SiMe}_2$  with adamantane affords a mixture of 1:2- and 2:2 – cycloadducts (**34** and **35**, respectively) *via* the intermediate formation of siloxirane **36** (Eq. 1.25).<sup>158</sup> In contrast, the reaction of the sterically congested stable dialkylsilylene **37** (which is electronically similar to  $\text{SiMe}_2$ ) with adamantane afforded the very stable siloxirane **38** (Eq. 1.26).<sup>159</sup> These two reactions provide an extreme example of the role of steric factors, where the nature of the products are changed.



Kinetic studies of dimethylsilylene ( $\text{SiMe}_2$ , **2**) by laser flash photolysis methods were first carried out by Conlin *et al.*, and rate constants for its reaction with substrates such as silanes, ketones, molecular  $\text{O}_2$ , alkenes, and alkoxy silanes in cyclohexane were reported.<sup>36</sup> Recently, our group have employed cyclotrisilane

derivative **22** for the photoextrusion of SiPh<sub>2</sub> and studied its reactivity against a more comprehensive set of substrates.<sup>37,81</sup> The ratio of the rate constants for reaction of SiMes<sub>2</sub> and SiPh<sub>2</sub> with a common substrate was proposed to provide the first quantitative measure of the effects of steric hindrance on specific reaction types in silylene chemistry.<sup>81</sup> At that point the seven substrates for which the rate constants were measured for both SiPh<sub>2</sub> and SiMes<sub>2</sub> could be divided into three groups: (i) little apparent sensitivity to steric effects (O<sub>2</sub>, acetone); (ii) moderate sensitivity (MeOH, Et<sub>3</sub>SiH) and (iii) high sensitivity (cyclohexene, DMB, MeOTMS) (Table 1.6).<sup>36-37,81</sup> It was also observed that the mechanism for alcohol addition to diarylsilylene undergoes a shift in mechanism from SiPh<sub>2</sub> to SiMes<sub>2</sub>.<sup>82</sup>

**Table 1.6.** Ratio of Absolute Rate Constants for the Reaction of Diphenyl- and Dimesitylsilylene with Various Silylene Scavengers in hydrocarbon solution at 298 K:<sup>36-37,81</sup>

Scavenger	$k_{(\text{SiPh}_2)}/k_{(\text{SiMes}_2)}$
$\text{O}_2^a$	3.8
Acetone <sup>b</sup>	1.7
$\text{Et}_3\text{SiH}^a$	41.8
MeOH <sup>b</sup>	16.3
Cyclohexene <sup>a</sup>	2800
DMB <sup>a</sup>	1600
MeOTMS <sup>a</sup>	> 4200

<sup>a</sup> Based on  $k_{(\text{SiPh}_2)}$  data in hexane solution from ref. 81 and  $k_{(\text{SiMes}_2)}$  data in cyclohexane solution from ref. 36 at 298 K. <sup>b</sup> Based on data in hexane at 298 K from ref. 37.

### 1.9. Goals of this work

In this work attempts were made to answer some of the following questions:

- What are rate constants for  $\text{SiMes}_2$  with other common silylene scavengers?
- What are the mechanistic differences in the reaction of  $\text{SiMes}_2$  compared to that for  $\text{SiPh}_2$ ?
- How much of the reactivity differences are due to the electronic effects of the six methyl groups present in  $\text{SiMes}_2$ ? Due to the inductive effects of three methyl groups, a mesityl group will be less electron withdrawing than a phenyl group. Thus, the electrophilicity of  $\text{SiMes}_2$  should be less than that of  $\text{SiPh}_2$  and this might play a role in the slower reactivity of  $\text{SiMes}_2$ . Now, is it possible to design a silylene which would better separate the electronic and steric effects of  $\text{SiMes}_2$ ? If yes, what could be the photochemical precursor to this silylene?

Attempts to answer these questions will rely mainly on fast kinetic studies by laser flash photolysis while product studies are the other important part. The following sections describe these techniques in brief.

## 1.10. Experimental Techniques used for the Study of Transient Silylenes

### 1.10.1 Steady state Photolysis Experiments

Product studies were carried out as steady state experiments in which the silylene precursor, as a deoxygenated solution in cyclohexane -  $d_{12}$ , was photolyzed in presence of the suitable silylene scavenger. If the products are not reported previously, preliminary identification of it is done by  $^1\text{H}$  NMR and GC/MS. The confirmation of the product is dependent on isolation followed by characterization or by  $^1\text{H}$  NMR analysis of the crude photolysis mixture after that was spiked with independently prepared expected product. The product yields were determined from the relative slopes of concentration versus time plots over the range of a considerable amount of precursor consumption.

### 1.10.2. Nanosecond Laser Flash Photolysis (LFP) Experiments:<sup>160</sup> Determination of Rate Constants

The kinetic studies in this work have been carried out using the laser flash photolysis methods. Figure 1.5 depicts the component parts of the laser flash photolysis spectrometer. The laser used is a Kr/F<sub>2</sub>/Ne 248 nm excimer laser with a 20 ns pulse width, the energy per pulse being tuned to 95-110 mJ. The monitoring beam from a Xe – lamp and the detection unit are aligned orthogonal to the laser excitation source. The detection unit consists of a monochromator and photomultiplier (MC/PMT)

combination. The PMT changes the light intensity to an electrical signal and amplifies it. Using proper lenses the monitoring beam is concentrated into the sample cell which is made of optical quartz tubing. Digital oscilloscopes are used to convert the PMT output to digital format and to transfer this data to the computer for further processing. The triggering of the laser and the data acquisition can be controlled from the computer. Silylenes are quenched by oxygen,<sup>36,70-71,81,161</sup> hence the precursor solution is deoxygenated prior passing through the sample cell, by bubbling Argon through the reservoir frit. The solution is flowed through the sample cell in order to replenish the contents of the sample cell and to wash away the photoproducts.

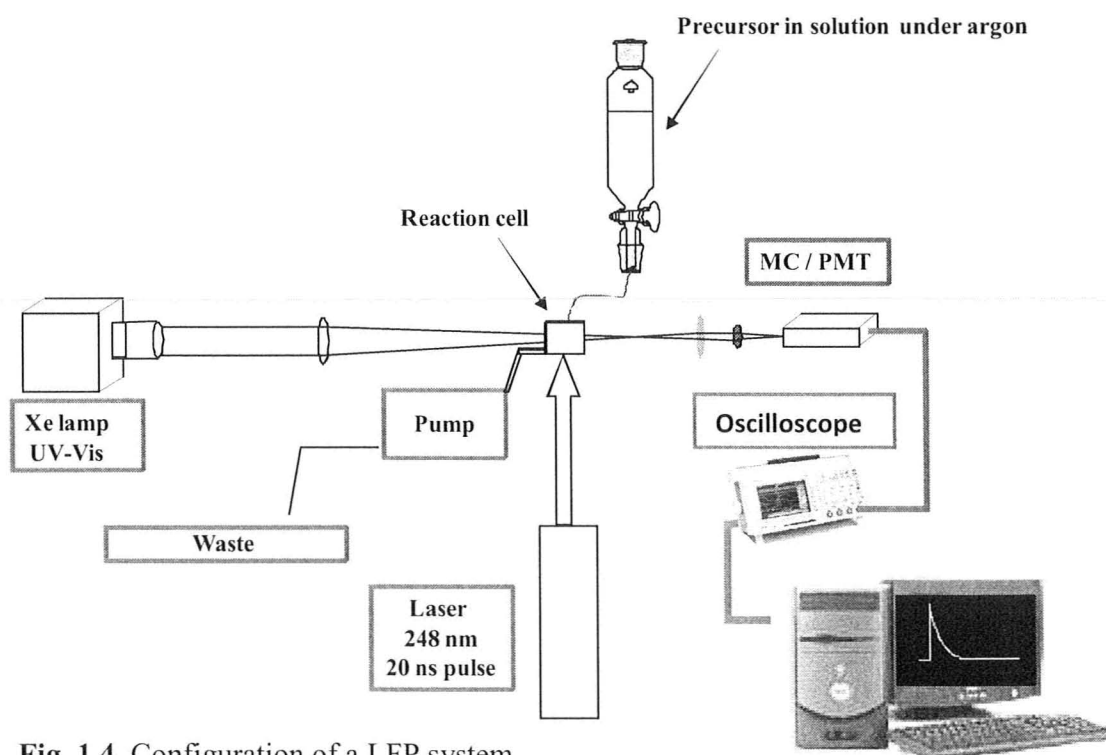


Fig. 1.4. Configuration of a LFP system



When the laser fires, silylenes are generated and this causes an increase in absorbance in the sample. As a result, the light reaching the detector is decreased. The reference signal ( $I_0$ ) is acquired before flashing the laser which is then subtracted from the sample beam ( $I_t$ ) (Eq. 1.27). Thus, the absorbance observed is in reality the change in optical density ( $\Delta OD$ ) or absorbance ( $\Delta A$ ) after the laser irradiates the sample.

$$\Delta OD = \Delta A = -\log\left(\frac{I_t}{I_0}\right) = -\log\left(1 - \frac{\text{signal}}{I_0}\right) \quad (1.27)$$

The Beer – Lambert law states that the absorbance ( $\Delta A$ ) is directly proportional to the extinction coefficient ( $\epsilon$ ), concentration ( $c$ ) of the transient and the path length ( $l$ ) that the monitoring beam travels through the solution (Eq. 1.28).

$$\Delta A = \epsilon cl \quad (1.28)$$

Transient spectroscopy relates to point by point construction of absorbance vs. wavelength plots at a fixed time window. The time windows can be selected according to the wish of the user or can be changed during final data processing. The transient spectra at different time windows allow the user to study the time evolution of the transient spectra.

In the absence of a silylene scavenger (Q) the silylene ( $\text{SiR}_2$ ) dimerizes to form the disilene. The rate of disappearance of the silylene under the conditions would then be given by equation 1.29, where  $k_{\text{dim}}$  is the dimerization rate constant. When a

scavenger is added there is a competition between the dimerization and reaction of the silylene with Q. The overall rate expression is then given by equation 1.30. At low concentration of the Q, dimerization is the major process, but at higher concentration of Q the other pathway takes over. Furthermore, in all the experiments in our group, the amount of silylene generated at each flash of the laser are always much lower than the concentration of Q. Thus, Q practically remains unchanged throughout the reaction and thus reduces the kinetics to pseudo – first order to give pseudo – first order rate constant  $k_Q'$  (Eq. 1.31) which also happens to be rate coefficient for decay ( $k_{\text{decay}}$ ). Integrating equation 1.31 and substituting for the absorbances, gives equation 1.32 from which  $k_Q'$  can be directly measured.

$$- \frac{d[\text{R}_2\text{Si}]}{dt} = 2k_{\text{dim}}[\text{R}_2\text{Si}]^2 \quad (1.29)$$

$$- \frac{d[\text{R}_2\text{Si}]}{dt} = 2k_{\text{dim}}[\text{R}_2\text{Si}]^2 + k_Q[\text{Q}][\text{R}_2\text{Si}] \quad (1.30)$$

$$- \frac{d[\text{R}_2\text{Si}]}{dt} = k_Q'[\text{R}_2\text{Si}] \quad (1.31)$$

$$\Delta A = \Delta A_0 \exp(-k_Q't) \quad (1.32)$$

Now since  $k_Q' = k_Q[\text{Q}]$ , from the slope of a plot of  $k_Q'$  vs.  $[\text{Q}]$ ,  $k_Q$  can be obtained.

Ideally the y – intercept of the plot should be zero but this is never the case as silylene

dimerization and impurity quenching occurs in the absence of a scavenger. The intercept is referred to as a “hypothetical pseudo first – order rate constant” ( $k_0$ ). Thus,  $k_{\text{decay}}$  is given by equation 1.33.

$$k_{\text{decay}} = k_0 + k_{\text{Q}}[\text{Q}] \quad (1.33)$$

### 1.11. Kinetic Isotope Effect (*KIE*)<sup>162</sup>

The situation in which isotopic substitution changes the rate of a reaction is known as kinetic isotope effect (*KIE*). It is in general defined as the ratio of the rate constant for the “light” isotopomer to the rate constant of the “heavy” isotopomer (Eq. 1.34).

$$KIE = \frac{k_{\text{light}}}{k_{\text{heavy}}} \quad (1.34)$$

The effect originates from the zero point energy (ZPE) differences of the two reactant isotopomers and the respective transition states. ZPE, which is the lowest vibrational state of a molecule, is dependent mainly on the reduced mass of the bond of interest as the force constant remains almost unaffected due to isotopic distribution. Largest *KIE* is observed when the difference of ZPE at the transition states ( $\Delta ZPE^\ddagger$ ) for the two isotopomers is least, a situation encountered in thermoneutral reactions. The transition state ZPE vibration in this case is independent of the isotope as it is linear and symmetrical due to equal amounts of bond breaking and bond making which does not

incorporate any bending motions. For, endothermic and exothermic reactions, the transition states behave more like the products and reactants respectively, generating the same effect as in ground state reactants. In these scenarios,  $KIE \approx 1$ .

The magnitude of  $KIE$  holds important mechanistic information if it deviates from 1.

### 1.12. Note

- All the laser flash photolysis experiments in this work were carried out in dry hexanes.
- Until otherwise mentioned all solvents were deoxygenated by bubbling Argon during and at least for 30 min before the start of the experiment.
- All the rate constants reported are obtained from linear least squares fits of the data to appropriate equations.
- Errors are reported as twice the standard error ( $\pm 2\sigma$ ).

## References

- (1) Huck, L. A., McMaster University, 2010.
- (2) Wiberg, N.; Jutzi, P.; Schubert, U. In *Silicon Chemistry. From the Atom to Extended Systems.*; Wiley - VCH: Darmstadt, 2003, p 85.
- (3) Power, P. P. *J. Chem. Soc., Dalton Trans.* **1998**, 1998, 2939.
- (4) Jones, M., Jr.; Moss, R. A.; Moss, R. A.; Platz, M. S.; Jones, M., Jr. In *Reactive Intermediate Chemistry*; John Wiley & Sons: New York, 2004, p 273.
- (5) Tokitoh, N.; Ando, W.; Moss, R. A.; Platz, M. S.; Jones, M., Jr. In *Reactive Intermediate Chemistry*; John Wiley & Sons: New York, 2004, p 651.
- (6) Oláh, J.; Veszprémi, T.; DeProft, F.; Geerlings, P. *J. Phys. Chem. A* **2007**, *111*, 10815.
- (7) Oláh, J.; De Proft, F.; Veszprémi, T.; Geerlings, P. *J. Phys. Chem. A* **2004**, *108*, 490.
- (8) Bauschlicher, C. W.; Schaefer, H. F.; Bagus, P. S. *J. Am. Chem. Soc.* **1977**, *99*, 7106.
- (9) Tomioka, H. *Acc. Chem. Res.* **1997**, *30*, 315.
- (10) Harrison, J. F.; Liedtke, R. C.; Liebman, J. F. *J. Am. Chem. Soc.* **1979**, *101*, 7162.
- (11) Su, M. D.; Chu, S. Y. *J. Am. Chem. Soc.* **1999**, *121*, 4229.
- (12) Szabados, A.; Hargittai, M. *J. Phys. Chem. A* **2003**, *107*, 4314.
- (13) Apeloig, Y.; Pauncz, R.; Karni, M.; West, R.; Steiner, W.; Chapman, D. *Organometallics* **2003**, *22*, 3250.
- (14) Sekiguchi, A.; Tanaka, T.; Ichinohe, M.; Akiyama, K.; Tero-Kubota, S. *J. Am. Chem. Soc.* **2003**, *125*, 4962.
- (15) Sekiguchi, A.; Tanaka, T.; Ichinohe, M.; Akiyama, K.; Gaspar, P. P. *J. Am. Chem. Soc.* **2008**, *130*, 426.
- (16) Jiang, P.; Gaspar, P. P. *J. Am. Chem. Soc.* **2001**, *123*, 8622.
- (17) Walsh, R. *Acc. Chem. Res.* **1981**, *14*, 246.
- (18) Grev, R. S. *Adv. Organomet. Chem.* **1991**, *33*, 125.
- (19) Pople, J. A.; Head-Gordon, M.; Fox, D. J.; Raghavachari, K.; Curtiss, L. A. *J. Chem. Phys.* **1989**, *90*, 5622.
- (20) Becerra, R.; Walsh, R. *Res. Chem. Kinetics* **1995**, *3*, 263.
- (21) Becerra, R.; Boganov, S. E.; Egorov, M. P.; Faustov, V. I.; Nefedov, O. M.; Walsh, R. *J. Am. Chem. Soc.* **1998**, *120*, 12657.
- (22) Allendorf, M. D.; Melius, C. F. *J. Phys. Chem. A* **2005**, *109*, 4939.
- (23) Becerra, R.; Walsh, R. *Phys. Chem. Chem. Phys.* **2007**, *9*, 2817.
- (24) Atwell, W. H.; Weyenberg, D. R. *J. Organomet. Chem.* **1966**, *5*, 594.

- (25) Gilman, H.; Cottis, S. G.; Atwell, W. H. *J. Am. Chem. Soc.* **1964**, *86*, 1596.
- (26) Seyferth, D.; Annarelli, D. C. *J. Am. Chem. Soc.* **1975**, *97*, 7162.
- (27) Tokitoh, N.; Suzuki, H.; Okazaki, R.; Ogawa, K. *J. Am. Chem. Soc.* **1993**, *115*, 10428.
- (28) Kira, M.; Ishida, S.; Iwamoto, T.; Kabuto, C. *J. Am. Chem. Soc.* **1999**, *121*, 9722.
- (29) Denk, M.; Lennon, R.; Hayashi, R.; West, R.; Belyakov, A. V.; Verne, H. P.; Haaland, A.; Wagner, M.; Metzler, N. *J. Am. Chem. Soc.* **1994**, *116*, 2691.
- (30) Haaf, M.; Schmiedl, A.; Schmedake, T. A.; Powell, D. R.; Millevolte, A. J.; Denk, M.; West, R. *J. Am. Chem. Soc.* **1998**, *120*, 12714.
- (31) Gaspar, P. P.; Beatty, A. M.; Chen, T.; Haile, T.; Lei, D.; Winchester, W. R.; Braddock-Wilking, J.; Rath, N. P.; Klooster, W. T.; Koetzle, T. F.; Mason, S. A.; Albinati, A. *Organometallics* **1999**, *18*, 3921.
- (32) Sakurai, H.; Kamiyama, Y.; Nakadaira, Y. *J. Am. Chem. Soc.* **1977**, *99*, 3879.
- (33) Hawari, J. A.; Griller, D. *Organometallics* **1984**, *3*, 1123.
- (34) Michalczyk, M. J.; Fink, M. J.; De Young, D. J.; Carlson, C. W.; Welsh, K. M.; West, R.; Michl, J. *Sil. Germ. Tin Lead Cpds.* **1986**, *9*, 75.
- (35) Gaspar, P. P.; West, R. In *The chemistry of organic silicon compounds, Vol. 2*; Rappoport, Z., Apeloig, Y., Eds.; John Wiley and Sons: New York, 1998, p 2463.
- (36) Conlin, R. T.; Netto-Ferreira, J. C.; Zhang, S.; Scaiano, J. C. *Organometallics* **1990**, *9*, 1332.
- (37) Moiseev, A. G.; Leigh, W. J. *Organometallics* **2007**, *26*, 6268.
- (38) Drahnak, T. J.; Michl, J.; West, R. *J. Am. Chem. Soc.* **1979**, *101*, 5427.
- (39) Moiseev, A. G.; Leigh, W. J. *J. Am. Chem. Soc.* **2006**, *128*, 14442.
- (40) Leigh, W. J.; Moiseev, A. G.; Coulais, E.; Lollmahomed, F.; Askari, M. S. *Can. J. Chem.* **2008**, *86*, 1105.
- (41) Moiseev, A. G.; Coulais, E.; Leigh, W. J. *Chem. Eur. J.* **2009**, *15*, 8485.
- (42) Ishikawa, M.; Nakagawa, K. I.; Ishiguro, M.; Ohi, F.; Kumada, M. *J. Organomet. Chem.* **1978**, *152*, 155.
- (43) Ishikawa, M.; Nakagawa, K. I.; Enokida, R.; Kumada, M. *J. Organomet. Chem.* **1980**, *201*, 151.
- (44) Miyazawa, T.; Koshihara, S. Y.; Liu, C.; Sakurai, H.; Kira, M. *J. Am. Chem. Soc.* **1999**, *121*, 3651.
- (45) Gaspar, P. P.; Boo, B. H.; Chari, S.; Ghosh, A. K.; Holten, D.; Kirmaier, C.; Konieczny, S. *Chem. Phys. Lett.* **1984**, *105*, 153.
- (46) Gaspar, P. P.; Holten, D.; Konieczny, S.; Corey, J. Y. *Acc. Chem. Res.* **1987**, *20*, 329.
- (47) Konieczny, S.; Jacobs, S. J.; Braddock Wilking, J. K.; Gaspar, P. P. *J. Organomet. Chem.* **1988**, *341*, C17.
- (48) Levin, G.; Das, P. K.; Lee, C. L. *Organometallics* **1988**, *7*, 1231.
- (49) Levin, G.; Das, P. K.; Bilgrien, C.; Lee, C. L. *Organometallics* **1989**, *8*, 1206.

- (50) Shizuka, H.; Tanaka, H.; Tonokura, K.; Murata, K.; Hiratsuka, H.; Ohshita, J.; Ishikawa, M. *Chem. Phys. Lett.* **1988**, *143*, 225.
- (51) Yamaji, M.; Hamanishi, K.; Takahashi, T.; Shizuka, H. *J. Photochem. Photobiol. A: Chem.* **1994**, *81*, 1.
- (52) Maier, G.; Reisenauer, H. P.; Schttler, K.; Wessolek-Kraus, U. *J. Organomet. Chem.* **1989**, *366*, 25.
- (53) Maier, G.; Mihm, G.; Reisenauer, H. P. *Chem. Ber.* **1984**, *117*, 2351.
- (54) Bott, S. G.; Marshall, P.; Wagenseller, P. E.; Wang, Y.; Conlin, R. T. *J. Organomet. Chem.* **1995**, *499*, 11.
- (55) Kira, M.; Maruyama, T.; Sakurai, H. *Chem. Lett.* **1993**, 1345.
- (56) Orchin, M.; Jaffe, H. H. *Symmetry, Orbitals, and Spectra (S. O. S.)*; John Wiley & Sons: New York, 1971.
- (57) West, R. *Science* **1984**, *225*, 1109.
- (58) Malcolm, N. O. J.; Gillespie, R. J.; Popelier, P. L. A. *J. Chem. Soc., Dalton Trans.* **2002**, *2002*, 3333.
- (59) Oláh, J.; Veszprémi, T. *J. Organomet. Chem.* **2003**, *686*, 112.
- (60) Gaspar, P. P.; Jones, M., Jr.; Moss, R. A. In *Reactive Intermediates, Vol. 1*; John Wiley & Sons: New York, 1978, p 229.
- (61) Gaspar, P. P.; Jones, M., Jr.; Moss, R. A. In *Reactive Intermediates, Vol. 2*; John Wiley & Sons: New York, 1981, p 335.
- (62) Gaspar, P. P.; Jones, M., Jr.; Moss, R. A. In *Reactive Intermediates, Vol. 3*; John Wiley & Sons: New York, 1985, p 333.
- (63) West, R.; Patai, S.; Rappoport, Z. In *The Chemistry of organic silicon compounds*; John Wiley & Sons: New York, 1989, p 1207.
- (64) Hill, N. J.; West, R. *J. Organomet. Chem.* **2004**, *689*, 4165.
- (65) Gillette, G. R.; Noren, G. H.; West, R. *Organometallics* **1989**, *8*, 487.
- (66) Arrington, C. A.; West, R.; Michl, J. *J. Am. Chem. Soc.* **1983**, *105*, 6176.
- (67) Vancik, H.; Raabe, G.; Michalczyk, M. J.; West, R.; Michl, J. *J. Am. Chem. Soc.* **1985**, *107*, 4097.
- (68) Gillette, G. R.; Noren, G. H.; West, R. *Organometallics* **1987**, *6*, 2617.
- (69) Raabe, G.; Vancik, H.; West, R.; Michl, J. *J. Am. Chem. Soc.* **1986**, *108*, 671.
- (70) Ando, W.; Hagiwara, K.; Sekiguchi, A. *Organometallics* **1987**, *6*, 2270.
- (71) Akasaka, T.; Nagase, S.; Yabe, A.; Ando, W. *J. Am. Chem. Soc.* **1988**, *110*, 6270.
- (72) Belzner, J.; Ihmels, H. *Adv. Organomet. Chem.* **1998**, *43*, 1.
- (73) Inoue, G.; Suzuki, M. *Chem. Phys. Lett.* **1985**, *122*, 361.
- (74) Chu, J. O.; Beach, D. B.; Estes, R. D.; Jasinski, J. M. *Chem. Phys. Lett.* **1988**, *143*, 135.
- (75) Chu, J. O.; Beach, D. B.; Jasinski, J. M. *J. Phys. Chem.* **1987**, *91*, 5340.
- (76) Jasinski, J. M. *J. Phys. Chem.* **1986**, *90*, 555.
- (77) Jasinski, J. M.; Chu, J. O. *J. Chem. Phys.* **1988**, *88*, 1678.

- (78) Safarik, I.; Sandhu, V.; Lown, E. M.; Strausz, O. P.; Bell, T. N. *Res. Chem. Intermed.* **1990**, *14*, 105.
- (79) Baggott, J. E.; Blitz, M. A.; Frey, H. M.; Lightfoot, P. D.; Walsh, R. *Chem. Phys. Lett.* **1987**, *135*, 39.
- (80) Jasinski, J. M.; Becerra, R.; Walsh, R. *Chem. Rev.* **1995**, *95*, 1203.
- (81) Moiseev, A. G.; Leigh, W. J. *Organometallics* **2007**, *26*, 6277.
- (82) Leigh, W. J.; Kostina, S. S.; Bhattacharya, A.; Moiseev, A. G. *Organometallics* **2010**, *29*, 662.
- (83) Belzner, J.; Dehnert, U.; Ihmels, H. *Tetrahedron* **2001**, *57*, 511.
- (84) Tortorelli, V. J.; Jones, M., Jr.; Wu, S.; Li, Z. *Organometallics* **1983**, *2*, 759.
- (85) Tortorelli, V. J.; Jones, M., Jr. *J. Am. Chem. Soc.* **1980**, *102*, 1425.
- (86) Conlin, R. T.; Gaspar, P. P. *J. Am. Chem. Soc.* **1976**, *98*, 3715.
- (87) Ando, W.; Shiba, T.; Hidaka, T.; Morihashi, K.; Kikuchi, O. *J. Am. Chem. Soc.* **1997**, *119*, 3629.
- (88) Pae, D. H.; Xiao, M.; Chiang, M. Y.; Gaspar, P. P. *J. Am. Chem. Soc.* **1991**, *113*, 1281.
- (89) Zhang, S.; Conlin, R. T. *J. Am. Chem. Soc.* **1991**, *113*, 4272.
- (90) Zhang, S.; Wagenseller, P. E.; Conlin, R. T. *J. Am. Chem. Soc.* **1991**, *113*, 4278.
- (91) Hojo, F.; Sekigawa, S.; Nakayama, N.; Shimizu, T.; Ando, W. *Organometallics* **1993**, *12*, 803.
- (92) Ishikawa, M.; Nakagawa, K. I.; Kumada, M. *J. Organomet. Chem.* **1979**, *178*, 105.
- (93) Platz, M. S. *Tet. Lett.* **1983**, *24*, 4763.
- (94) Houk, K. N.; Rondan, N. G.; Mareda, J. *J. Am. Chem. Soc.* **1984**, *106*, 4291.
- (95) Houk, K. N.; Rondan, N. G.; Mareda, J. *Tetrahedron* **1985**, *41*, 1555.
- (96) Horner, D. A.; Grev, R. S.; Schaefer, H. F., III *J. Am. Chem. Soc.* **1992**, *114*, 2093.
- (97) Espenson, J. H. *Chemical kinetics and reaction mechanisms*; McGraw-Hill, Inc.: New York, 1995.
- (98) Atwell, W. H.; Weyenberg, D. R. *J. Am. Chem. Soc.* **1968**, *90*, 3438.
- (99) Lei, D.; Hwang, R. J.; Gaspar, P. P. *J. Organomet. Chem.* **1984**, *271*, 1.
- (100) Lei, D.; Gaspar, P. P. *Chem. Commun.* **1985**, *1985*, 1149.
- (101) Jenkins, R. L.; Kedrowski, R. A.; Elliot, L. E.; Tappen, D. C.; Schlyer, D. J.; Ring, M. A. *J. Organomet. Chem.* **1975**, *86*, 347.
- (102) Ishikawa, M.; Ohi, F.; Kumada, M. *J. Organomet. Chem.* **1975**, *86*, C23.
- (103) Takeda, N.; Tokitoh, N.; Okazaki, R. *Chem. Lett.* **2000**, *2000*, 622.
- (104) Kolesnikov, S. P.; Egorov, M. P.; Galminas, A. M.; Ezhova, M. B.; Nefedov, O. M.; Leshina, T. V.; Taraban, M. B.; Kruppa, A. I.; Maryasova, V. I. *J. Organomet. Chem.* **1990**, *391*, C1.



- (105) Nakao, R.; Oka, K.; Dohmaru, T.; Nagata, Y.; Fukumoto, T. *Chem. Commun.* **1985**, 1985, 766.
- (106) Lehnig, M.; Klaukien, H.; Reininghaus, F. *Ber. Bunsenges. Phys. Chem.* **1990**, *94*, 1411.
- (107) Ishikawa, M.; Nakagawa, K. I.; Katayama, S.; Kumada, M. *J. Organomet. Chem.* **1981**, *216*, C48.
- (108) Oka, K.; Nakao, R. *J. Organomet. Chem.* **1990**, *390*, 7.
- (109) Ishida, S.; Iwamoto, T.; Kabuto, C.; Kira, M. *Chem. Lett.* **2001**, 2001, 1102.
- (110) Kira, M.; Sakamoto, K.; Sakurai, H. *J. Am. Chem. Soc.* **1983**, *105*, 7469.
- (111) Taraban, M. B.; Volkova, O. S.; Plyusnin, V. F.; Kruppa, A. I.; Leshina, T. V.; Egorov, M. P.; Nefedov, O. M. *J. Phys. Chem. A* **2003**, *107*, 4096.
- (112) Appler, H.; Neumann, W. P. *J. Organomet. Chem.* **1986**, *314*, 247.
- (113) Becerra, R.; Cannady, J. P.; Walsh, R. *J. Phys. Chem. A* **2006**, *110*, 6680.
- (114) Leigh, W. J.; Harrington, C. R. *J. Am. Chem. Soc.* **2005**, *127*, 5084.
- (115) Leigh, W. J.; Lollmahomed, F.; Harrington, C. R. *Organometallics* **2006**, *25*, 2055.
- (116) Boganov, S. E.; Faustov, V. I.; Egorov, M. P.; Nefedov, O. M. *Russ. Chem. Bull. Int. Ed.* **2004**, *53*, 960.
- (117) Heaven, M. W.; Metha, G. F.; Buntine, M. A. *J. Phys. Chem. A* **2001**, *105*, 1185.
- (118) Heaven, M. W.; Metha, G. F.; Buntine, M. A. *Aust. J. Chem.* **2001**, *54*, 185.
- (119) Alexander, U. N.; King, K. D.; Lawrance, W. D. *Phys. Chem. Chem. Phys.* **2001**, *3*, 3085.
- (120) Baggott, J. E.; Blitz, M. A.; Frey, H. M.; Lightfoot, P. D.; Walsh, R. *Internat. J. Chem. Kinet.* **1992**, *24*, 127.
- (121) Becerra, R.; Cannady, J. P.; Walsh, R. *J. Phys. Chem. A* **1999**, *103*, 4457.
- (122) Becerra, R.; Cannady, J. P.; Walsh, R. *Phys. Chem. Chem. Phys.* **2001**, *3*, 2343.
- (123) Becerra, R.; Cannady, J. P.; Walsh, R. *J. Phys. Chem. A* **2003**, *107*, 11049.
- (124) Becerra, R.; Cannady, J. P.; Walsh, R. *Silicon Chem.* **2005**, *3*, 131.
- (125) Ando, W.; Sekiguchi, A.; Hagiwara, K.; Sakakibara, A.; Yoshida, H. *Organometallics* **1988**, *7*, 558.
- (126) Trinquier, G. *J. Chem. Soc., Far. Trans.* **1993**, *89*, 775.
- (127) Gu, T. Y. G.; Weber, W. P. *J. Am. Chem. Soc.* **1980**, *102*, 1641.
- (128) Steele, K. P.; Weber, W. P. *J. Am. Chem. Soc.* **1980**, *102*, 6095.
- (129) Steele, K. P.; Weber, W. P. *Inorg. Chem.* **1981**, *20*, 1302.
- (130) Kostina, S. S.; Leigh, W. J. *Unpublished work.*
- (131) Tokitoh, N.; Okazaki, R. *Coord. Chem. Rev.* **2000**, *210*, 251.
- (132) Gu, T. Y. G.; Weber, W. P. *J. Organomet. Chem.* **1980**, *195*, 29.
- (133) Raghavachari, K.; Chandrasekhar, J.; Gordon, M. S.; Dykema, K. J. *J. Am. Chem. Soc.* **1984**, *106*, 5853.

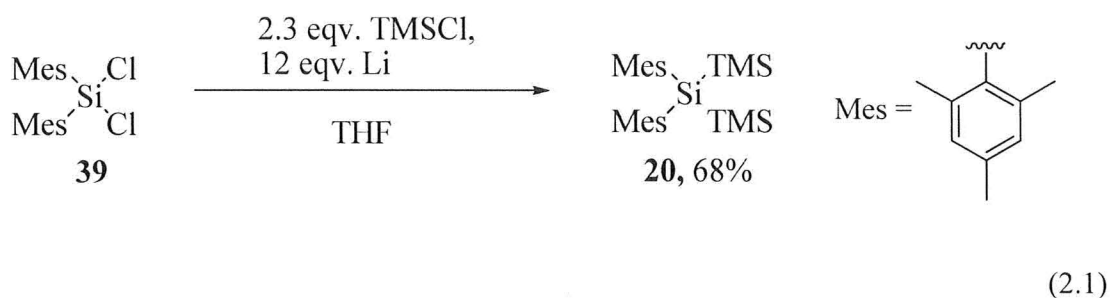
- (134) Su, S.; Gordon, M. S. *Chem. Phys. Lett.* **1993**, *204*, 306.
- (135) Lee, S. Y.; Boo, B. H. *J. Mol. Struct.: THEOCHEM* **1996**, *366*, 79.
- (136) Becerra, R.; Carpenter, I. W.; Gordon, M. S.; Roskop, L.; Walsh, R. *Phys. Chem. Chem. Phys.* **2007**, *9*, 2121.
- (137) Bobbitt, K. L.; Gaspar, P. P. *J. Organomet. Chem.* **1995**, *499*, 17.
- (138) Ando, W.; Ikeno, M. *Chem. Lett.* **1978**, *7*, 609.
- (139) Jasinski, J. M.; Meyerson, B. S.; Scott, B. A. *Annu. Rev. Phys. Chem.* **1987**, *38*, 109.
- (140) Driver, T. G.; Woerpel, K. A. *J. Am. Chem. Soc.* **2003**, *125*, 10659.
- (141) Calad, S. A.; Cirakovic, J.; Woerpel, K. A. *J. Org. Chem.* **2007**, *72*, 1027.
- (142) Driver, T. G.; Woerpel, K. A. *J. Am. Chem. Soc.* **2004**, *126*, 9993.
- (143) Clark, T. B.; Woerpel, K. A. *Org. Lett.* **2006**, *8*, 4109.
- (144) Calad, S. A.; Woerpel, K. A. *J. Am. Chem. Soc.* **2005**, *127*, 2046.
- (145) Clark, T. B.; Woerpel, K. A. *J. Am. Chem. Soc.* **2004**, *126*, 9522.
- (146) Cirakovic, J.; Driver, T. G.; Woerpel, K. A. *J. Org. Chem.* **2004**, *69*, 4007.
- (147) Ottosson, H.; Steel, P. G. *Chem. Eur. J.* **2006**, *12*, 1576.
- (148) Buchner, K. M.; Clark, T. B.; Loy, J. M. N.; Nguyen, T. X.; A., W. K. *Org. Lett.* **2009**, *11*, 2173.
- (149) Gately, S.; West, R. *Drug Dev. Res.* **2007**, *68*, 156.
- (150) West, R.; Moser, D. F.; Haaf, M. Silylene catalysis of olefin polymerization. US 6,576,729, 2003.
- (151) Furstner, A.; Krause, H.; Lehmann, C. W. *Chem. Commun.* **2001**, 2372.
- (152) Walker, R. H.; Miller, K. A.; Scott, S. L.; Cygan, Z. T.; Bartolin, J. M.; Kampf, J. W.; Banaszak Holl, M. M. *Organometallics* **2009**, *28*, 2744.
- (153) Becerra, R.; Frey, H. M.; Mason, B. P.; Walsh, R.; Gordon, M. S. *J. Chem. Soc., Faraday Trans.* **1995**, *91*, 2723.
- (154) Becerra, R.; Frey, H. M.; Mason, B. P.; Walsh, R. *J. Chem. Soc., Far. Trans.* **1993**, *89*, 411.
- (155) Blitz, M. A.; Frey, H. M.; Tabbutt, F. D.; Walsh, R. *J. Phys. Chem.* **1990**, *94*, 3294.
- (156) Becerra, R.; Boganov, S. E.; Egorov, M. P.; Krylova, I. V.; Nefedov, O. M.; Walsh, R. *Chem. Phys. Lett.* **2005**, *413*, 194.
- (157) Baggott, J. E.; Blitz, M. A.; Frey, H. M.; Walsh, R. *J. Am. Chem. Soc.* **1990**, *112*, 8337.
- (158) Ando, W.; Ikeno, M.; Sekiguchi, A. *J. Am. Chem. Soc.* **1978**, *100*, 3613.
- (159) Ishida, S.; Iwamoto, T.; Kira, M. *Organometallics* **2010**, *29*, 5526.
- (160) Scaiano, J. C.; Moss, R. A.; Platz, M. S.; Jones, M., Jr. In *Reactive Intermediate Chemistry*; John Wiley & Sons: New York, 2004, p 847.

- (161) Patyk, A.; Sander, W.; Gauss, J.; Cremer, D. *Angew. Chem. Int. Ed. Engl.* **1989**, 28, 898.
- (162) Anslyn, E. V.; Dougherty, D. A. *Modern Physical Organic Chemistry*; University Science Books: New York, 2005.

## Chapter 2 – Reactions of Dimesitylsilylene

### 2.1. Synthesis of 2,2 – dimesityl – 1,1,1,3,3,3 – hexamethyltrisilane (20)

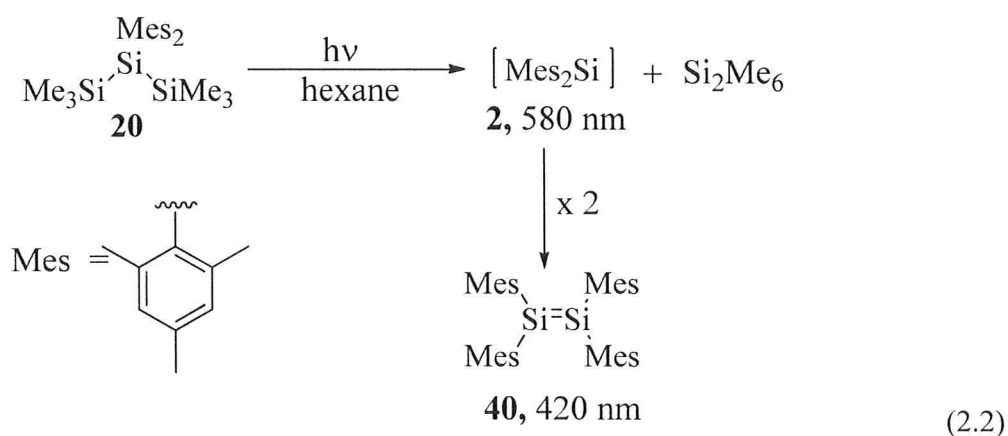
2,2 – Dimesityl – 1,1,1,3,3,3 – hexamethyltrisilane (**20**), the photochemical precursor to dimesitylsilylene (**2**), was synthesized by the previously reported route, as shown in equation 2.1.<sup>1</sup> Compound **20** was purified by repeated recrystallizations from hexanes.



### 2.2. Laser Flash Photolysis Experiments of 2,2 – dimesityl – 1,1,1,3,3,3 – hexamethyltrisilane (20)

Laser photolysis of **20** in deoxygenated hexanes solution afforded the characteristic absorptions due to free  $\text{SiMes}_2$  ( $\lambda_{\text{max}} = 290$  &  $580$  nm), which decayed over  $\sim 40$   $\mu\text{s}$  with second order kinetics with the concomitant growth of the long – lived absorption due to the dimerization product, tetramesityldisilene ( $\text{Si}_2\text{Mes}_4$ ; **40**,  $\lambda_{\text{max}} = 420$  nm), as reported previously (Eq 2.2, Fig. 2.1).<sup>2-4</sup> Addition of small quantities of silylene scavengers shortened the lifetimes of  $\text{SiMes}_2$  and quenched the formation of  $\text{Si}_2\text{Mes}_4$ .

The decay of the  $\text{SiMes}_2$  absorptions accelerated in direct proportion to the concentration of substrate added, in all but two cases ( $\text{AcOH}$  and  $\text{THF}^5$ ), affording linear plots of the pseudo-first-order rate constants ( $k_{\text{decay}}$ ) versus concentration of the substrate ( $[\text{Q}]$ ) in each case. The slopes of the plots, from linear least squares analysis according to equation 1.33, are assigned to the absolute second-order rate constants for reactions ( $k_{\text{Q}}$ ). The data obtained for the various scavengers studied are discussed in sequence below. The rate constants (except for alcohols) are collected in Table 2.1.



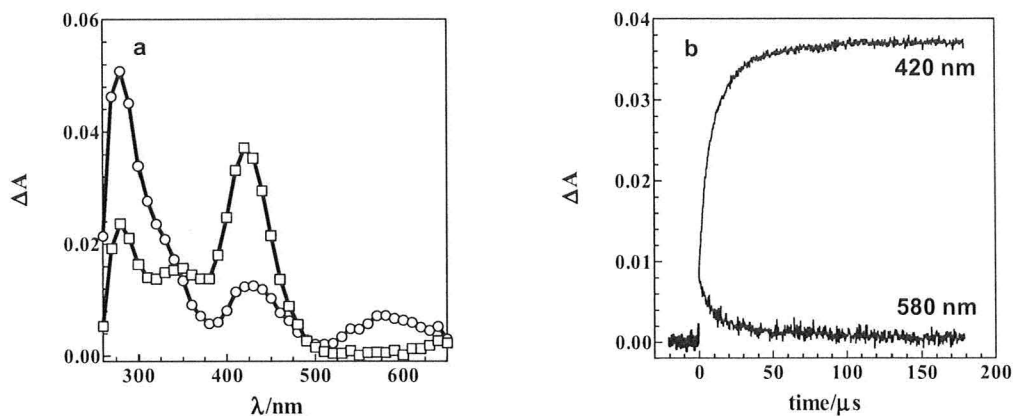


**Fig. 2.1.** (a) Transient absorption spectra recorded at 0.640–1.28  $\mu\text{s}$  (o), 155.20–157.44  $\mu\text{s}$  (□) after the laser pulse, by laser flash photolysis of a deoxygenated hexanes solution of **20** (ca.  $6 \times 10^{-5}$  M). (b) Transient growth/decay profiles recorded at 420 and 580 nm.

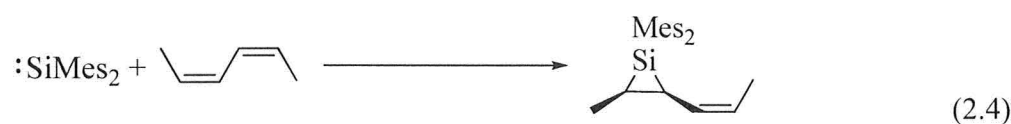
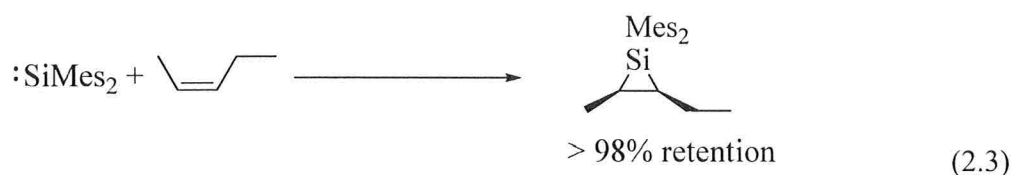
**Table 2.1.** Absolute rate constants for quenching of  $\text{SiMe}_2$  by various substrates studied in this work in hexanes solution at room temperature.

Substrate	$k_Q/10^8 \text{ M}^{-1} \text{ s}^{-1}$
Isoprene	$0.33 \pm 0.04$
BTMSE	$0.26 \pm 0.01$
$\text{CCl}_4$	$0.96 \pm 0.04$
AcOH	$35 \pm 3^a$

<sup>a</sup> Rate constant obtained from linear least-squares analysis of  $k_{\text{decay}}$  data at low concentrations (0.1 – 0.5 mM).

### 2.2.1. Reactions of SiMes<sub>2</sub> with alkenes and alkynes

Zhang and co-workers reported that SiMes<sub>2</sub> reacts with alkenes and dienes to form siliranes and 2-vinyl-1-siliranes respectively as the main primary products, in a stereospecific manner (Eqs 2.3 – 2.4).<sup>6-7</sup>



The kinetics of the reactions of SiMes<sub>2</sub> and the parent diarylsilylene SiPh<sub>2</sub> with alkenes and dienes have been examined in previous laser flash photolysis studies of these species in cyclohexane and hexanes, respectively.<sup>2,8</sup> The rate constants for the reactions of SiPh<sub>2</sub> with 4,4-dimethyl-1-pentene (DMP) and cyclohexene were reported to be within a factor of three, and those for reactions with 2,3-dimethyl-1,3-butadiene (DMB) and isoprene are within a factor of two of the diffusional rate constant ( $k_{\text{diff}} = 2.3 \times 10^{10} \text{ M}^{-1}\text{s}^{-1}$  in hexane at 25 °C).<sup>8-9</sup> On the other hand, a ca. 3000-fold slower rate constant was reported for the reaction of SiMes<sub>2</sub> with cyclohexene ( $k_{\text{Q}} = 2.8 \times 10^6 \text{ M}^{-1} \text{ s}^{-1}$ )<sup>2</sup> compared to that for SiPh<sub>2</sub> ( $k_{\text{Q}} = 7.9 \times 10^9 \text{ M}^{-1} \text{ s}^{-1}$ ), which can be attributed to the combined electronic and steric effects associated with the mesityl groups.<sup>8</sup> In this work, the rate constant for the reaction of SiMes<sub>2</sub> with isoprene was measured and was found

to be  $3.3 \times 10^7 \text{ M}^{-1} \text{ s}^{-1}$ , which is about 400-fold smaller than that obtained for  $\text{SiPh}_2$  (Table 2.1). Figure 2.2 shows the plot of  $k_{\text{decay}}$  vs. isoprene concentration from the experiment. Isoprene absorbs at the laser wavelength (248 nm) and at concentrations higher than that used in the experiment, screens the light to such an extent that  $\text{SiMes}_2$  is formed with very low signal strengths, compromising the precision of the kinetic analyses. Conlin *et al.* examined the kinetics of the reaction of  $\text{SiMes}_2$  with DMB in cyclohexane solution, using an Nd – YAG (266 nm) laser and reported  $8.8 \times 10^6 \text{ M}^{-1} \text{ s}^{-1}$  as the value of the rate constant.<sup>2</sup> DMB absorbs considerably more strongly at 248 nm than at 266 nm, and at substrate concentrations required for clean pseudo-first-order decay kinetics of the silylene the signal strengths were too low to work with. Thus, we were not able to determine the rate constant for the reaction with this diene in our experimental set up.

Zhang and Conlin reported that the photolysis of **20** in the presence of isoprene afforded the two vinylsiliranes **41a** and **41b** in a 3:2 ratio, which was measured after ca. 90% conversion of **20** to products (Eq 2.5).<sup>7</sup> Isoprene and DMB exists mainly in the *s-trans* conformer at room temperature.<sup>10-11</sup> If the dienes react in these conformers and if steric factors are responsible for the smaller rate constants observed in the reactions of alkenes and dienes with  $\text{SiMes}_2$  compared to those for the reactions with  $\text{SiPh}_2$ , then one might expect both **41a** and **41b** to form with higher rate constants than the vinylsilirane





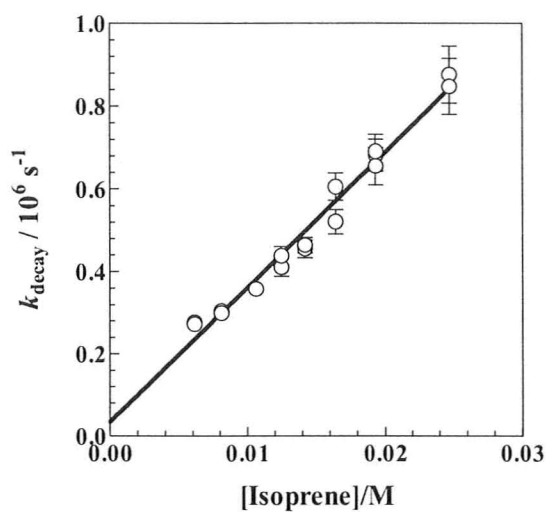


**Figure 2.2.** Plots of the pseudo-first-order rate constants ( $k_{\text{decay}}$ ) for the decay of  $\text{SiMes}_2$  vs.  $[\text{isoprene}]$  in hexanes solution at 25 °C.

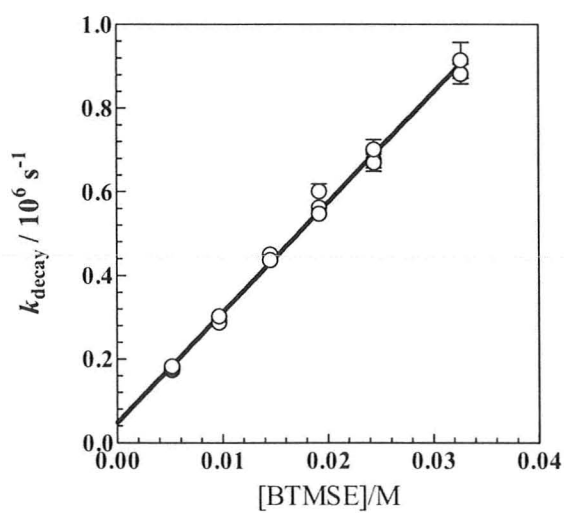


**Figure 2.3.** Plots of the pseudo-first-order rate constants ( $k_{\text{decay}}$ ) for the decay of  $\text{SiMes}_2$  vs.  $[\text{BTMSE}]$  in hexanes solution at 25 °C.

For the reactions of  $\text{SiPh}_2$  with substrates such as DMB, DMP and BTMSE, transient spectra recorded in the presence of sufficient substrate to reduce the lifetime of the silylene to  $\tau (= 1/k_{\text{decay}}) < 200$  ns, showed absorptions centered around 280 nm which did not decay within the maximum time window (0.9 s) that can be monitored by our system.<sup>8</sup> These species are assigned to the respective three-membered ring compounds on the basis of their extended lifetimes and the  $^1\text{H}$  NMR spectra of the photolyzed mixtures.<sup>8</sup> To achieve a 200 ns lifetime for the silylene,  $k_{\text{decay}}$  should be  $5 \times 10^6 \text{ s}^{-1}$ . For a second order reaction with rate constant  $1 \times 10^9 \text{ M}^{-1} \text{ s}^{-1}$ , this implies that the quencher concentration should be ca. 5mM, but if the rate of the reaction is  $1 \times 10^7 \text{ M}^{-1} \text{ s}^{-1}$ , it would now require ca. 0.5 M of the substrate. Thus, for the reactions of  $\text{SiMe}_2$  with isoprene and BTMSE ca. 0.5 M of the substrate concentrations are required to achieve a lifetime of the silylene as low as 200 ns, and this is when the screening comes into play in the case of isoprene leading to the formation of silylene in very low concentration. The situation is more an economic one in the case of BTMSE because of the quantities of the substrate that would be required. This limits our chances to use these substrates in such a concentration when the silylene lifetime is reduced to  $\tau < 200$  ns, where contributions of silylene decay is minimized allowing us to observe decays of other species having longer lifetimes. Nevertheless, decays at 280 nm for the highest concentration used in the case of isoprene and BTMSE showed absorptions that did not decay in 1 ms, the maximum time window which can be monitored at the present state of our system. These can be assigned to the silirane and silirene from isoprene and BTMSE

respectively; identical to the reported SiPh<sub>2</sub> derived siliranes and silirenes.<sup>8,15</sup> Figure 2.4 (a) shows the transient absorption spectra of the photolysis of ca. 0.05 mM **20** in the presence of ca. 23 mM BTMSE while Fig. 2.4 (b) shows a transient decay profile recorded at 280 nm for the photolysis of **20** in the presence of ca. 27 mM of BTMSE. The non-decaying absorption present at the end of the initial fast decay (due to SiMes<sub>2</sub>) at 280 nm is assigned to the silirene **42**.

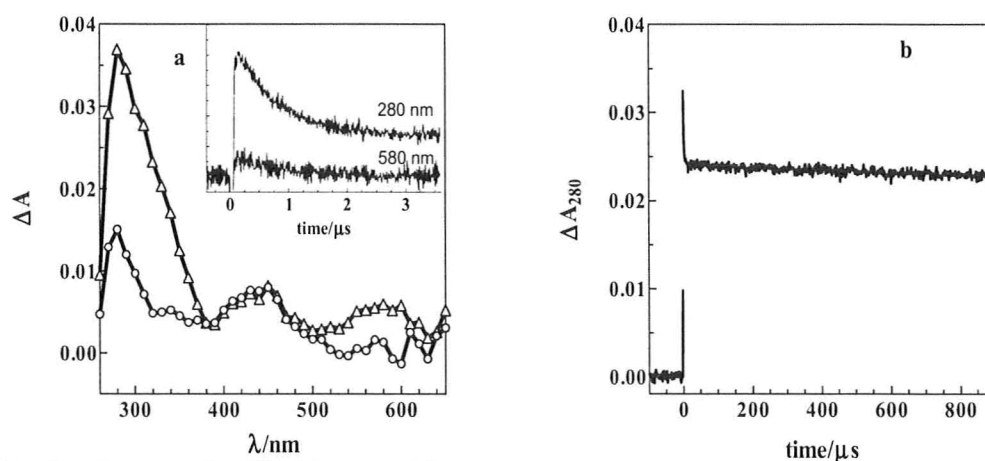
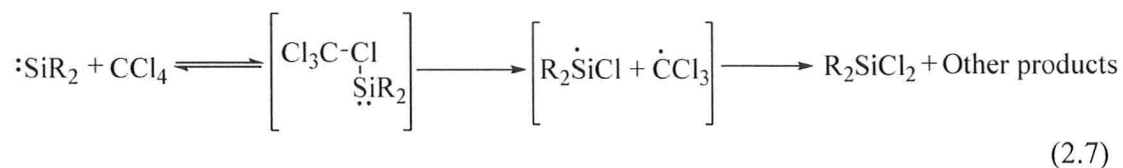


**Figure 2.4.** (a) Transient absorption spectra recorded at 0.096 - 0.122  $\mu\text{s}$  ( $-\Delta-$ ) and 2.144 - 2.170  $\mu\text{s}$  ( $-\circ-$ ) after laser pulse, by laser flash photolysis of a 0.05 mM solution of **20** in deoxygenated hexanes containing 23 mM of BTMSE; the inset shows transient decay profiles at 280 and 580 nm. (b) Transient decay profile recorded at 280 nm for the laser photolysis of ca. 0.05 mM of **20** in the presence of ca. 27 mM of BTMSE.

### 2.2.2. Reactions of SiMes<sub>2</sub> with CCl<sub>4</sub>

The reaction of silylenes with halocarbons is thought to proceed via a silylene-halocarbon Lewis acid-base complex.<sup>16-19</sup> SiMe<sub>2</sub><sup>18,20-21</sup> and SiPh<sub>2</sub><sup>8</sup> undergo chlorine atom abstraction with CCl<sub>4</sub> ultimately leading to the formation of respective dichlorosilanes. The overall reaction is thought to proceed through the pathway outlined in equation 2.7.



Analysis of  $k_{\text{decay}}$  vs. concentration data for SiMes<sub>2</sub> in the presence of CCl<sub>4</sub> in accordance with equation 1.33 afforded an absolute rate constant of  $k_{\text{CCl}_4} = 9.6 \times 10^7 \text{ M}^{-1} \text{ s}^{-1}$  for this reaction (Table 2.1). Transient absorption spectra recorded by laser flash photolysis of **20** in the presence of ca. 29 mM of CCl<sub>4</sub> revealed the characteristic absorption bands due to SiMes<sub>2</sub> at 290 nm and 580 nm, with the former band containing a more prominent shoulder at ca. 320 nm (Figure 2.5 (a)) than is exhibited in the spectrum of the silylene alone (Fig. 2.1 (a)). The signal at 330 nm exhibited somewhat longer lifetimes compared to that at 580 nm suggesting the presence of a different transient at that wavelength range. The lifetime of the species is less sensitive than SiMes<sub>2</sub> to CCl<sub>4</sub> concentration, affording a rate constant of  $k_{\text{CCl}_4} = (5.2 \pm 0.2) \times 10^7 \text{ M}^{-1} \text{ s}^{-1}$ , which is about 2 times lower than that for SiMes<sub>2</sub>. The value is about an order of two

smaller than those reported for the (Cl abstraction) reactions of  $\text{CCl}_4$  with  $\text{Et}_3\text{Si}\cdot$  or  $\text{Ph}_2(t\text{-Bu})\text{Si}\cdot$  but similar to that for  $(\text{Me}_3\text{Si})_3\text{Si}\cdot$ .<sup>22</sup> An analogous phenomenon was observed in the case of  $\text{SiPh}_2$ , where the species was tentatively assigned to be chlorodiphenylsilyl radical ( $\text{SiPh}_2\text{Cl}$ ) and its rate constant for the reaction with  $\text{CCl}_4$  was found to be  $k_{\text{Q}} = (8 \pm 1) \times 10^8 \text{ M}^{-1} \text{ s}^{-1}$ , also roughly 2 times smaller than the rate constant for the reaction of  $\text{SiPh}_2$  with  $\text{CCl}_4$ .<sup>8</sup> By analogy we assign this transient to the chlorodimesitylsilyl radical ( $\text{SiMes}_2\text{Cl}$ ). Figure 2.5(b) depicts the plots of  $k_{\text{decay}}$  vs. concentration of  $\text{CCl}_4$  for free  $\text{SiMes}_2$  and  $\text{SiMes}_2\text{Cl}$ .

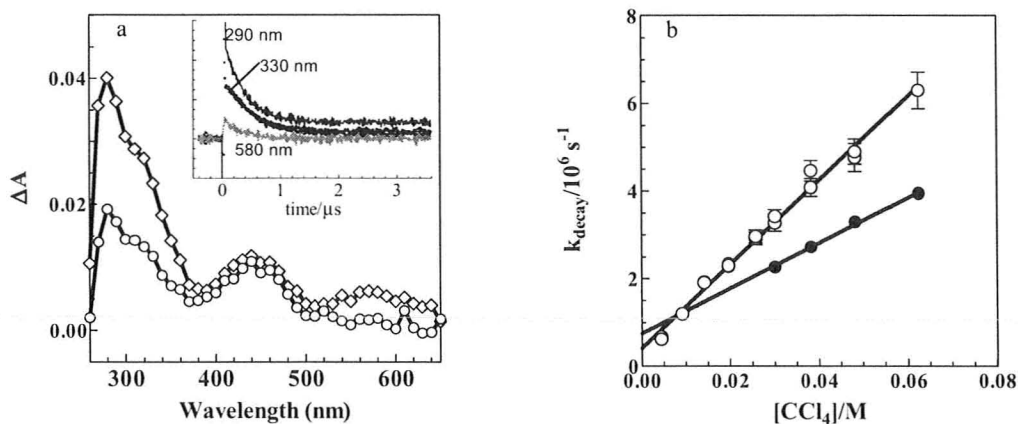
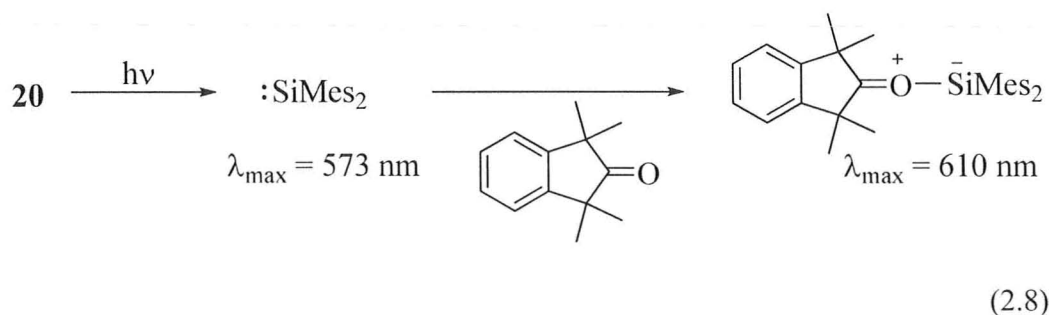


**Figure 2.5.** (a) Transient absorption spectra recorded at 0.16–0.19  $\mu\text{s}$  ( $\diamond$ ) and 0.54–0.59  $\mu\text{s}$  ( $\circ$ ) after laser pulse, by laser flash photolysis of a 0.05 mM solution of **20** in deoxygenated hexanes containing 29 mM of  $\text{CCl}_4$ ; the inset shows transient decay profiles at 290, 330 and 580 nm. (b) Plots of the pseudo – first – order decay rate coefficients ( $k_{\text{decay}}$ ) vs  $[\text{CCl}_4]$  of free  $\text{SiMes}_2$  (570 nm, ( $\circ$ )) and of  $\text{SiMes}_2\text{Cl}$  (330 nm, ( $\bullet$ )).

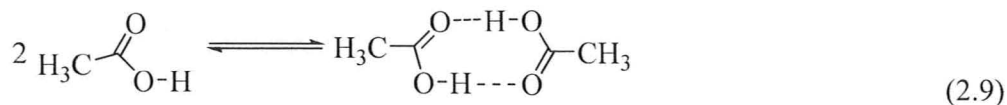
### 2.2.3. Reactions of SiMes<sub>2</sub> with AcOH

Silylenes react with acetic acid to give formal O-H insertion products, presumably *via* the mechanism outlined in equation 1.24.<sup>8,23</sup> Our group was unable to detect a complex between SiPh<sub>2</sub> and acetic acid, leading to the proposal that it is a steady state intermediate, never building up in high enough concentration to enable detection.<sup>8</sup> Similar to this observation, with SiMes<sub>2</sub> we were unable to detect any complex for its reaction with acetic acid. Ando and co-workers photolyzed **20** in the presence of 1,1,3,3 – tetramethylmethyl – 2 – indanone in isopentane (IP)/3 – methylpentane (3 – MP) and 3 – MP matrixes at 77K, which upon careful annealing led to the formation of new absorptions that were assigned to the corresponding silacarboxyl ylide, with an absorption maximum at 610 nm (Eq 2.8).<sup>24</sup> Assuming the assignment is correct, this suggests that the reactions of silylenes with carbonyl compounds proceeds *via* an initial complexation step.



For SiPh<sub>2</sub>, a plot of the pseudo – first – order decay rate coefficients ( $k_{\text{decay}}$ ) vs. concentration of acetic acid is linear over the 0 - 0.5 mM concentration range in AcOH

(in a re-examination, the plot was found to be linear up to 1 mM AcOH), affording a rate constant of  $k_{\text{AcOH}} = 1.0 \times 10^{10} \text{ M}^{-1} \text{ s}^{-1}$ .<sup>8</sup> However, with  $\text{SiMe}_2$  and AcOH, the quenching plot exhibits downward curvature at AcOH concentrations above 0.5 mM (Figure 2.6 (a)). This is presumably due to the self association of acetic acid in hydrocarbon solvents (Eq 2.9);<sup>25</sup> the dimer can be expected to be much less reactive than the monomer and the effect should be more pronounced in the case of bulkier silylene. At low concentrations of AcOH where it exists largely in monomeric form in hexanes (up to 0.5 mM), the pseudo-first-order decays followed a linear dependence on AcOH concentration, affording an apparent absolute rate constant  $k_{\text{AcOH}} = 3.5 \times 10^9 \text{ M}^{-1} \text{ s}^{-1}$  (Table 2.1).



Correction of the AcOH concentrations to account for the monomer – dimer equilibrium leads to the plot shown in Fig. 2.6.(b). The slope affords  $k_{\text{AcOH}} = 8.3 \times 10^9 \text{ M}^{-1} \text{ s}^{-1}$ , which we interpret as the true rate constant for reaction with AcOH in its monomeric form.



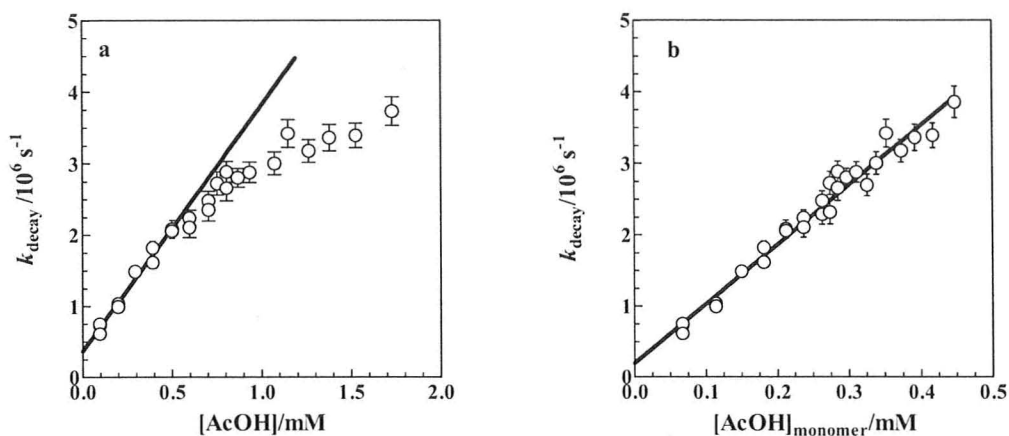


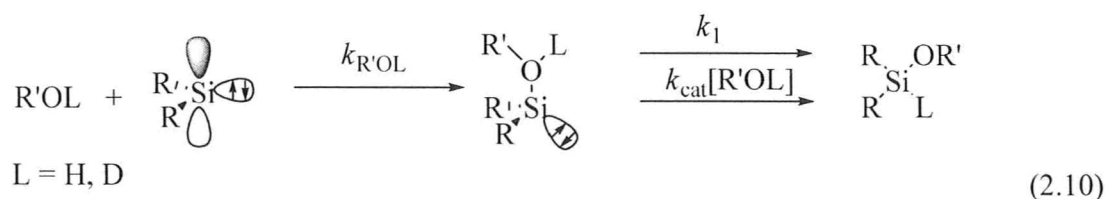
**Figure 2.6.** (a) Plots of the pseudo-first-order rate constants ( $k_{\text{decay}}$ ) for decay of  $\text{SiMes}_2$  vs. bulk  $\text{AcOH}$  concentrations in hexanes solution at 25 °C. (b) Plots of the pseudo-first-order rate constants ( $k_{\text{decay}}$ ) for decay of  $\text{SiMes}_2$  vs. monomeric  $\text{AcOH}$  concentrations in hexanes solution at 25 °C.

#### 2.2.4. Reactions of $\text{SiMes}_2$ with alcohols<sup>3</sup>

Silylenes and germylenes react with alcohols via the initial formation of the corresponding Lewis acid-base complex followed by proton transfer from oxygen to the Si/Ge center (Eq. 1.22).<sup>26-29</sup> In the case of silylenes, the mechanism of equation 1.22 is supported by theoretical calculations,<sup>30-37</sup> low temperature matrix spectroscopic studies,<sup>38</sup> as well as kinetic studies in both the gas phase<sup>29,36-37,39-40</sup> and in solution.<sup>4,41-43</sup> The intermediate complex of ethanol with  $\text{SiMe}_2$  was first observed at 300 – 320 nm as a “fleeting intermediate” by Levin *et al*, but was not characterized.<sup>43</sup> A similar observation was also made for the  $\text{SiPh}_2$  – methanol complex in hexanes solution in an

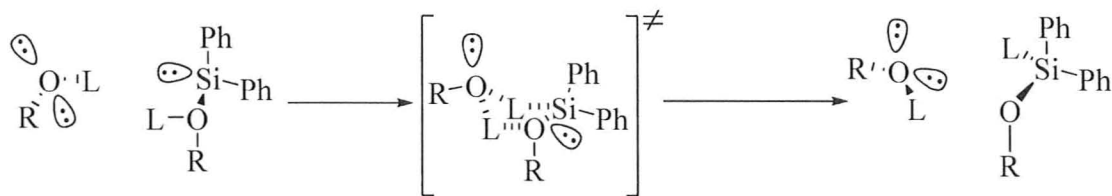
earlier study by our group.<sup>4</sup> Steele and Weber established through competition experiments that the reactions of SiMe<sub>2</sub> and SiMePh with various alcohols exhibit a primary kinetic isotope effect of  $k_{\text{H}}/k_{\text{D}} \approx 2$ .<sup>41</sup> Preliminary kinetic studies of the reaction of SiMes<sub>2</sub> with MeOH in hexanes afforded a linear plot for  $k_{\text{decay}}$  versus [MeOH] over the 1 – 8 mM alcohol concentration range, but the plot exhibited a negative intercept.<sup>4</sup> This is consistent with a higher order dependence on alcohol concentration at low concentrations of the alcohol.<sup>4</sup> All these results warranted a closer look at the reaction of silylenes with alcohols.

The results of more detailed kinetic studies of the reactions of SiMe<sub>2</sub>, SiMes<sub>2</sub> and SiPh<sub>2</sub> with MeOH/D and *t* – BuOH/D suggest the mechanism depicted in equation 2.10 for SiPh<sub>2</sub> and SiMe<sub>2</sub>.<sup>3</sup> The catalytic proton transfer by another molecule of alcohol was proposed to be the major pathway in converting the intermediate complexes to product in most of the cases (work done by Svetlana S. Kostina and Andrey Moiseev).<sup>3</sup>



The measured rate constants for the disappearance of SiPh<sub>2</sub> in its reactions with MeOH(D) and *t*-BuOH(D) are all within a factor of two of the diffusion controlled limit and do not vary appreciably with alcohol structure.<sup>3</sup> The primary products of these

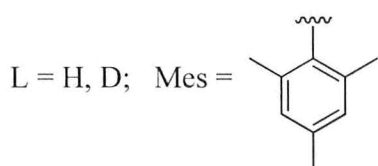
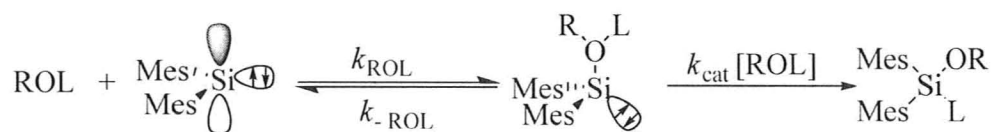
reactions were detected as transients with a distinct absorption band centered at  $\lambda_{\max} \sim 360 \text{ nm}$ ,<sup>3</sup> the wavelength characteristic of the complexes of  $\text{SiPh}_2$  with  $O$  – donors such as THF and methoxytrimethylsilane ( $\text{MeOTMS}$ ).<sup>8</sup> The maximum intensities of the signals due to these complexes, and the concentration range in which they can be detected, increase in the order  $\text{MeOH} < \text{MeOD} < t\text{-BuOH} < t\text{-BuOD}$ , indicating a significant dependence on alcohol structure and isotopic substitution. These transients exhibited a rapid growth, followed by a decay which accelerated with increasing alcohol concentration. Plots of the decay rate constants for the silylene – alcohol complexes vs. alcohol concentration were linear and linear least squares analysis afforded the absolute rate constants for each alcohol. These decreased in the order of  $\text{MeOH} > \text{MeOD} > t\text{-BuOH} > t\text{-BuOD}$ . The data affords a kinetic isotope effect of  $k_{\text{HH}}/k_{\text{DD}} \approx 2$  for the reaction of the  $\text{SiPh}_2\text{-MeOH(D)}$  complex with  $\text{MeOH(D)}$  and  $k_{\text{HH}}/k_{\text{DD}} = 10.8 \pm 2.4$  for the reaction of the  $\text{SiPh}_2\text{-}t\text{-BuOH(D)}$  complex with  $t\text{-BuOH(D)}$ .<sup>3</sup> Such a large kinetic isotope effect was explained by a proposed mechanism involving simultaneous *double* proton transfer (Eq 2.11); the net isotope effect in this case should be given by the product of the isotope effects associated with the individual protons in flight in the transition state (work done by Svetlana Kostina and Andrey Moiseev).



L = H, D

(2.11)

The simplest modification to the mechanism of equation 2.10 that could explain the negative intercept/higher order dependence on alcohol concentration for silylene decay is the introduction of reversibility in the first step of equation 2.10. A second modification that is justified by the results for  $\text{SiMe}_2$  and  $\text{SiPh}_2$  is to set  $k_1 = 0$ , *i. e.*, it is vanishingly small relative to  $k_{\text{cat}}[\text{ROH}]$ , even in the limit of  $[\text{ROH}] \rightarrow 0$ . Equation 2.12 shows the proposed mechanism for the reaction, while equation 2.13 depicts the dependence of the pseudo first-order rate constant for silylene decay, assuming the steady state approximation holds for the intermediate complex.



(2.12)

$$k_{\text{decay}} = k_0 + k_{\text{ROL}}k_{\text{cat}}[\text{ROL}]^2 / (k_{-\text{ROL}} + k_{\text{cat}}[\text{ROL}]) \quad (2.13)$$

Equation 2.13 predicts a linear dependence of  $k_{\text{decay}}$  on  $[\text{ROL}]$  at high concentrations of  $\text{ROL}$ , when  $k_{\text{cat}}[\text{ROL}] \gg k_{-\text{ROL}}$ , with proportionality factor  $k_{\text{ROL}}$ . The non-linear dependence on  $[\text{ROL}]$  is predicted to occur at low concentration of alcohols. Support for the steady state approximation comes from the fact that transient absorption spectra in the presence of  $\text{MeOH}$  or  $t\text{-BuOH}$ , did not show any evidence for a new transient in the 300 – 330 nm range that might be assigned to the  $\text{SiMe}_2 - \text{ROH}$  complexes. This contrasts the situation with  $\text{SiMe}_2$  and  $\text{SiPh}_2$ , where the silylene-alcohol complexes are observed at  $\lambda_{\text{max}} = 300$  and  $\lambda_{\text{max}} = 360$  nm, respectively.<sup>3</sup> The complexation reaction of THF with  $\text{SiMe}_2$  was also found to be reversible, with an equilibrium constant of  $K = 3 \text{ M}^{-1}$ .<sup>5</sup>

The actual plots of  $k_{\text{decay}}$  versus  $[\text{ROL}]$  do indeed show nonlinear dependences on alcohol concentration at low concentrations, for all the alcohols studied (Fig. 2.7). The results fit well to equation 2.14, which is the analytically tractable form of equation 2.13.<sup>3</sup>

$$k_{\text{decay}} = k_0 + k_{\text{ROL}}(k_{\text{cat}}/k_{-\text{ROL}})[\text{ROL}]^2 / (1 + (k_{\text{cat}}/k_{-\text{ROL}})[\text{ROL}]) \quad (2.14)$$

The combination of steric and electronic effects of the bulky mesityl substituents slow down the initial complexation step in the reaction with  $\text{MeOH}$  by more than an order of magnitude compared to that with  $\text{SiPh}_2$  (Table 1.3).<sup>3-4</sup> The complexation rate

constant is further reduced by about 7-fold in the case of *t*-BuOH relative to MeOH (Table 2.2).<sup>3</sup> No isotope effect is observed, consistent with the expectation that only small secondary effects should operate on the complexation step.

**Table 2.2.**<sup>3</sup> Kinetic data for the quenching of free SiMe<sub>2</sub> by alcohols in deoxygenated hexanes at 25 °C.<sup>a</sup>

ROL	$k_{\text{ROL}}/10^9 \text{ M}^{-1}\text{s}^{-1}$	$(k_{\text{cat}}/k_{\text{-ROL}})/\text{M}^{-1}$
MeOH	1.01 ± 0.09	550 ± 150
MeOD	1.26 ± 0.25	220 ± 100
<i>t</i> – BuOH	0.136 ± 0.005	36 ± 7
<i>t</i> – BuOD	0.136 ± 0.009	64 ± 5

<sup>a</sup> From analysis of  $k_{\text{decay}}$  vs. [ROL] data according to eq. 5; listed as the average ± standard deviation of three independent determinations in each case.

The data provide less detail on the catalytic proton transfer step than what is observable with SiPh<sub>2</sub> and SiMe<sub>2</sub>, where the silylene complexes can be detected. For SiMe<sub>2</sub> we could determine only the ratio of rate constants for reaction of the complex and reversion to free reactants. These indicate that the efficiency of the catalytic process for the MeOH complex is ca. ten times higher than that for the *t* – BuOH complex. The isotope effects on  $k_{\text{cat}}/k_{\text{-ROL}}$  are small and are found to be a small normal effect of  $2.5 \pm 1.8$  for MeOH/D and a small inverse effect  $0.56 \pm 0.2$  for *t* – BuOH/D.<sup>3</sup> Secondary

isotope effects on  $k_{\text{ROL}}$ , if any, are expected to be small as there is no change in hybridization of the atoms of the alcohols involved, and thus it was concluded that the isotope effects on  $k_{\text{cat}}$  must be quite small for both alcohols.<sup>3</sup> One of the reasonable mechanisms consistent with this observation is a sequential deprotonation/protonation process, which should be less sterically demanding than the concerted double proton transfer proposed for  $\text{SiPh}_2 - \text{ROL}$  complexes. It is also evident that product formation is ca. 10 times more efficient for the MeOH complex than  $t - \text{BuOH}$  complex, which means faster catalysis and(or) slower reversion to free reactants in the former compared to the latter.<sup>3</sup>

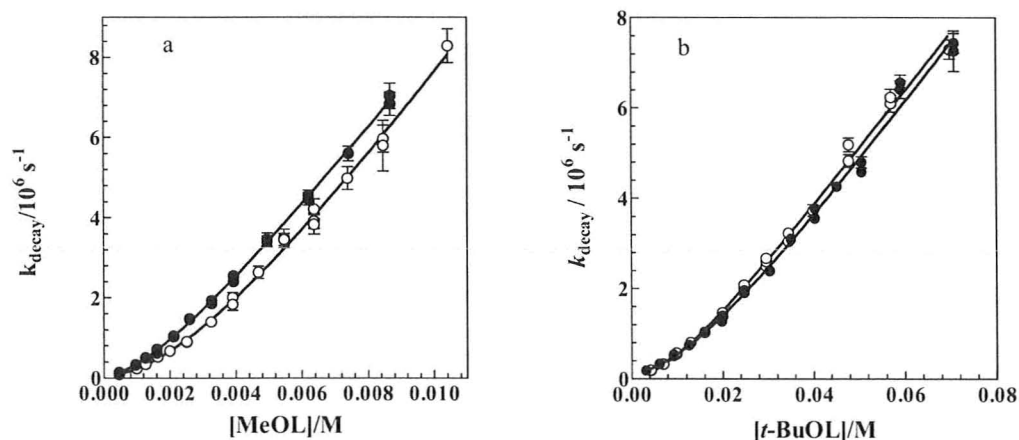


**Figure 2.7.**<sup>3</sup> (a) Plots of the pseudo-first order rate constants for decay of  $\text{SiMes}_2$  vs.  $[\text{MeOL}]$  ( $L = \text{H}$ , (●) or  $\text{D}$  (○)) in hexane at  $25^\circ \text{C}$ . (b) Plots of the pseudo-first order rate constants for decay of  $\text{SiMes}_2$  vs.  $[t\text{-BuOL}]$  ( $L = \text{H}$ , (●) or  $\text{D}$  (○)) in hexane at  $25^\circ \text{C}$ . The solid lines are the non-linear least squares fits of the data to equation 2.13.

## References

- (1) Tan, R. P.; Gillette, G. R.; Yokelson, H. B.; West, R. *Inorg. Synth.* **1992**, *29*, 19.
- (2) Conlin, R. T.; Netto-Ferreira, J. C.; Zhang, S.; Scaiano, J. C. *Organometallics* **1990**, *9*, 1332.
- (3) Leigh, W. J.; Kostina, S. S.; Bhattacharya, A.; Moiseev, A. G. *Organometallics* **2010**, *29*, 662.
- (4) Moiseev, A. G.; Leigh, W. J. *Organometallics* **2007**, *26*, 6268.
- (5) Kostina, S. S.; Leigh, W. J. *Unpublished work*.
- (6) Zhang, S.; Wagenseller, P. E.; Conlin, R. T. *J. Am. Chem. Soc.* **1991**, *113*, 4278.
- (7) Zhang, S.; Conlin, R. T. *J. Am. Chem. Soc.* **1991**, *113*, 4272.
- (8) Moiseev, A. G.; Leigh, W. J. *Organometallics* **2007**, *26*, 6277.
- (9) Espenson, J. H. *Chemical kinetics and reaction mechanisms*; McGraw-Hill, Inc.: New York, 1995.
- (10) Durig, J. R.; Compton, D. A. C. *J. Phys. Chem.* **1979**, *83*, 2879.
- (11) Mui, P. W.; Grunwald, E. *J. Phys. Chem.* **1984**, *88*, 6340.
- (12) Seyferth, D.; Annarelli, D. C.; Vick, S. C. *J. Am. Chem. Soc.* **1976**, *98*, 6382.
- (13) Ishikawa, M.; Nishimura, K.; Sugisawa, H.; Kumada, M. *J. Organomet. Chem.* **1980**, *194*, 147.
- (14) Atwell, W. H. *Organometallics* **2009**, *28*, 3573.
- (15) Leigh, W. J.; Huck, L. A.; Held, E.; Harrington, C. R. *Silicon Chem.* **2005**, *3*, 139.
- (16) Ishikawa, M.; Nakagawa, K. I.; Katayama, S.; Kumada, M. *J. Organomet. Chem.* **1981**, *216*, C48.
- (17) Oka, K.; Nakao, R. *J. Organomet. Chem.* **1990**, *390*, 7.
- (18) Taraban, M. B.; Volkova, O. S.; Plyusnin, V. F.; Kruppa, A. I.; Leshina, T. V.; Egorov, M. P.; Nefedov, O. M. *J. Phys. Chem. A* **2003**, *107*, 4096.
- (19) Becerra, R.; Cannady, J. P.; Walsh, R. *J. Phys. Chem. A* **2006**, *110*, 6680.
- (20) Kira, M.; Sakamoto, K.; Sakurai, H. *J. Am. Chem. Soc.* **1983**, *105*, 7469.
- (21) Nakao, R.; Oka, K.; Dohmaru, T.; Nagata, Y.; Fukumoto, T. *Chem. Commun.* **1985**, *1985*, 766.
- (22) Chatgililoglu, C. *Chem. Rev.* **1995**, *95*, 1229.
- (23) Bobbitt, K. L.; Gaspar, P. P. *J. Organomet. Chem.* **1995**, *499*, 17.
- (24) Ando, W.; Hagiwara, K.; Sekiguchi, A. *Organometallics* **1987**, *6*, 2270.
- (25) Fujii, Y.; Yamada, H.; Mizuta, M. *J. Phys. Chem.* **1988**, *92*, 6768.
- (26) Gaspar, P. P.; Jones, M., Jr.; Moss, R. A. In *Reactive Intermediates, Vol. 3*; John Wiley & Sons: New York, 1985, p 333.



- (27) Gaspar, P. P.; West, R. In *The chemistry of organic silicon compounds, Vol. 2*; Rappoport, Z., Apeloig, Y., Eds.; John Wiley and Sons: New York, 1998, p 2463.
- (28) Tokitoh, N.; Ando, W.; Moss, R. A.; Platz, M. S.; Jones, M., Jr. In *Reactive Intermediate Chemistry*; John Wiley & Sons: New York, 2004, p 651.
- (29) Becerra, R.; Walsh, R. *Phys. Chem. Chem. Phys.* **2007**, *9*, 2817.
- (30) Raghavachari, K.; Chandrasekhar, J.; Gordon, M. S.; Dykema, K. J. *J. Am. Chem. Soc.* **1984**, *106*, 5853.
- (31) Su, S.; Gordon, M. S. *Chem. Phys. Lett.* **1993**, *204*, 306.
- (32) Lee, S. Y.; Boo, B. H. *J. Mol. Struct.: THEOCHEM* **1996**, *366*, 79.
- (33) Schoeller, W. W.; Schneider, R. *Chem. Ber.* **1997**, *130*, 1013.
- (34) Heaven, M. W.; Metha, G. F.; Buntine, M. A. *J. Phys. Chem. A* **2001**, *105*, 1185.
- (35) Heaven, M. W.; Metha, G. F.; Buntine, M. A. *Aust. J. Chem.* **2001**, *54*, 185.
- (36) Alexander, U. N.; King, K. D.; Lawrance, W. D. *J. Phys. Chem. A* **2002**, *106*, 973.
- (37) Becerra, R.; Goldberg, N.; Cannady, J. P.; Almond, M. J.; Ogden, J. S.; Walsh, R. *J. Am. Chem. Soc.* **2004**, *126*, 6816.
- (38) Gillette, G. R.; Noren, G. H.; West, R. *Organometallics* **1989**, *8*, 487.
- (39) Baggott, J. E.; Blitz, M. A.; Frey, H. M.; Lightfoot, P. D.; Walsh, R. *Internat. J. Chem. Kinet.* **1992**, *24*, 127.
- (40) Becerra, R.; Cannady, J. P.; Walsh, R. *J. Phys. Chem. A* **2003**, *107*, 11049.
- (41) Steele, K. P.; Weber, W. P. *Inorg. Chem.* **1981**, *20*, 1302.
- (42) Steele, K. P.; Tzeng, D.; Weber, W. P. *J. Organomet. Chem.* **1982**, *231*, 291.
- (43) Levin, G.; Das, P. K.; Bilgrien, C.; Lee, C. L. *Organometallics* **1989**, *8*, 1206.

**Chapter 3 – Photochemistry of 1,1,1,3,3,3 – Hexamethyl - 2,2-bis(3,4,5-trimethylphenyl)trisilane and reactions of bis(3,4,5-trimethylphenyl)silylene (SiTmp<sub>2</sub>)**

### 3.1. Overview

This chapter introduces the need for a new diarylsilylene, in order to better separate the electronic and steric effects of ring substituents on the reactions of diarylsilylenes than is offered by comparisons of SiPh<sub>2</sub> and SiMes<sub>2</sub>.<sup>1-3</sup> The synthesis and the photochemical and laser flash photolysis studies of the precursor to the new silylene are presented in the following sections.

### 3.2. Choice of Aryl Substituents

A summary of the ratios of the absolute rate constants for corresponding reactions of SiPh<sub>2</sub> and SiMes<sub>2</sub> is listed in Table 3.1, which includes the ratios for CCl<sub>4</sub>, isoprene, BTMSE and AcOH in addition to the substrates listed in Table 1.6. The ratio of rate constants falls into the three main categories mentioned previously in section 1.8. Apparently it can be said that the steric interactions at the transition states of the rate determining step for the reactions with diarylsilylenes are low in the case of O<sub>2</sub>, AcOH and acetone, moderate for Et<sub>3</sub>SiH, MeOH, CCl<sub>4</sub> and high for the alkenes and alkynes. The change in steric effects from SiPh<sub>2</sub> to SiMes<sub>2</sub> is due to the two *ortho* methyl groups which can presumably interact strongly with substrates reacting at the silicon center.

The mesityl group is 2,4,6 – trimethylphenyl, having three methyl groups attached to the aryl ring, two at the *ortho* position and the remaining one on the *para* position. The simplest way to determine the electronic effects of the six methyl groups in SiMes<sub>2</sub>, is to move the *ortho* methyl groups to the *meta* positions. In doing this, although the methyl group is moved one carbon further (removing hyperconjugation effects of *ortho* methyl group, if any, which can result in partial negative charge on the carbon attached to the silicon), the polarity of the aryl moiety is enhanced in the direction of electron donation towards the silicon center. Thus, the aryl group of choice would be 3,4,5 – trimethylphenyl (Tmp), which should have similar electronic effects as the Mes group. Thus the ratios of the absolute rate constants for the reactions of this new silylene (**1**) relative to the corresponding ones for SiPh<sub>2</sub> should give the contribution of electronic effects on the reaction kinetics while the corresponding ratio  $k_{\text{Tmp}}/k_{\text{Mes}}$  should measure the contribution of steric effects on diarylsilylene reactivity (Fig. 3.1). The summation of Hammett  $\sigma$  – values ( $\Sigma\sigma$ ) for one of the aryl groups in **1** (- 0.31) is slightly greater than  $\sigma$  value of an OCH<sub>3</sub> group at the *para* position (- 0.27).<sup>4</sup>

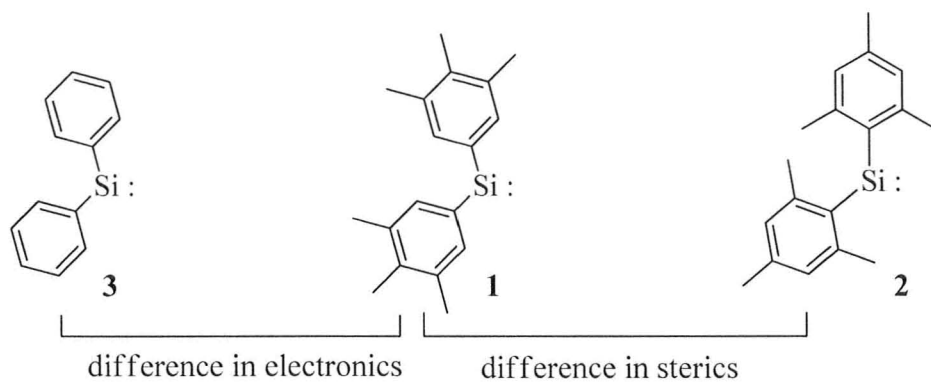


**Figure 3.1.** Diagram showing the new silylene  $\text{SiTmp}_2$  (1) in the middle, which is expected to allow separation of the steric and electronic effects in  $\text{SiMes}_2$ .

**Table 3.1.** Ratios of Absolute Rate Constants for the Reaction of Diphenyl – and Dimesitylsilylene with Various Silylene Scavengers in Hexanes or Cyclohexane solution at 25 °C (including present work).<sup>1-3,5</sup>

Scavenger	$k_{(\text{SiPh}_2)}/k_{(\text{SiMes}_2)}$
$\text{O}_2^a$	3.8
$\text{AcOH}^b$	2.9
Acetone <sup>c</sup>	1.7
$\text{Et}_3\text{SiH}^a$	41.8
$\text{MeOH}^d$	17.8
$\text{CCl}_4^b$	14.3
Cyclohexene <sup>a</sup>	2800
$\text{DMB}^a$	1600
Isoprene <sup>b</sup>	438.7
$\text{BTMSE}^b$	292.3

<sup>a</sup> Data from ref. 1 in cyclohexane and ref. 3 in hexanes. <sup>b</sup> Data from ref. 1 in cyclohexane and this work in hexanes. <sup>c</sup> Data from ref. 1 in cyclohexane and ref. 2 in hexanes. <sup>d</sup> Data from ref. 5 in hexanes.

### 3.3. Choice of Precursor to New Silylene (1)

The photochemical precursor for the new silylene could be 1,1,1,3,3,3 – hexamethyl – 2,2 – bis(3,4,5–trimethylphenyl)trisilane (**43**) or 1,1,3,3 – tetramethyl – 2,2 – bis(3,4,5–trimethylphenyl) – 1,2,3 – trisilacyclohexane (**44**, Fig. 3.2). Taking into consideration the likelihood of 1,3 – silyl migration as a competitive photochemical process with silylene extrusion (*e. g.* Eq. 1.16)<sup>3,6-10</sup> and the extent to which this competing reaction is suppressed in trisilacyclohexane derivatives (*e. g.* Eq. 1.14),<sup>2-3,8</sup> **44** is expected to be the better choice of precursor to SiTmp<sub>2</sub>, but we decided to begin with **43** due to the relative ease of its synthesis.

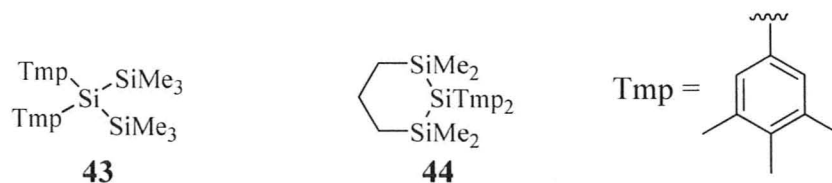
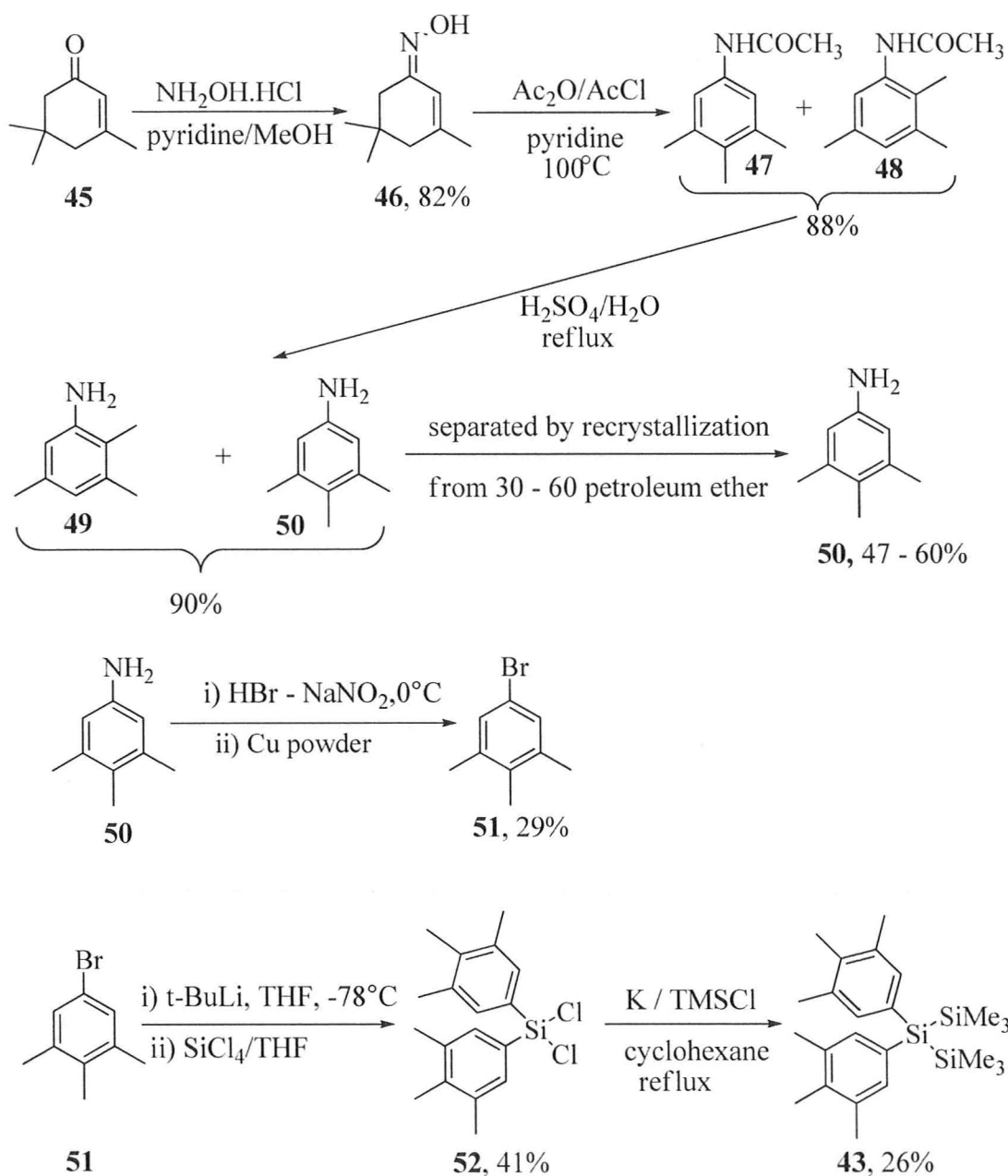


**Figure 3.2.** Plausible precursors to SiTmp<sub>2</sub>.

### 3.4. Synthesis of 1,1,1,3,3,3 – hexamethyl – 2,2 – bis(3,4,5–trimethylphenyl)trisilane (**43**)

The synthesis of 1,1,1,3,3,3 – hexamethyl – 2,2 – bis(3,4,5–trimethylphenyl)hexamethyltrisilane (**43**) was carried out as outlined in Scheme 3.1. 3,4,5 – Trimethylaniline (**50**) was synthesized and isolated following Beringer and Ugelow's previously reported method.<sup>11</sup> The amine was then converted to 1 – bromo –

3,4,5 – trimethylbenzene (**51**) following Gattermann conditions using hydrobromic acid, sodium nitrite and copper granules.<sup>12</sup> Compound **51** was treated with *t* – BuLi at – 78 °C to form the corresponding aryllithium derivative, which was then reacted with half an equivalent of silicon tetrachloride to obtain dichlorobis(3,4,5-trimethylphenyl)silane (**52**) as a white solid. The precursor **43** was obtained as white needles in 26% yield by reaction of **52** with trimethylsilylchloride and potassium metal, after purification by column chromatography followed by recrystallizations from hexanes and methanol. Trisilane **43** was identified on the basis of its <sup>1</sup>H, <sup>13</sup>C, and <sup>29</sup>Si NMR, infrared and mass spectra, and combustion analysis.

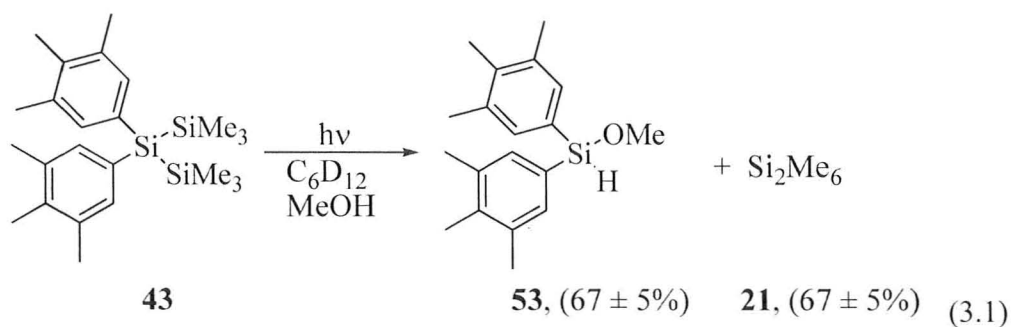


**Scheme 3.1** Synthesis of 1,1,1,3,3,3 - hexamethyl - 2,2 - bis(3,4,5-trimethylphenyl)trisilane (**43**).



### 3.5. Steady State Photolysis of **43**

To establish the course of the photochemistry of **43**, steady state photolysis of **43** (ca. 0.04 M) was carried out in cyclohexane- $d_{12}$  containing MeOH (0.10 M) and 1,4-dioxane (0.01 M) as internal integration standard. In the experiment, the solution of **43** in cyclohexane- $d_{12}$  was placed in a quartz NMR tube and was deoxygenated by purging with argon, and then the requisite amount of dry MeOH was added to it. The NMR tube was sealed with a cap and irradiated with two 254 nm low pressure Hg lamps in a merry-go-round apparatus. The progress of the reaction was monitored by  $^1\text{H}$  NMR spectroscopy. The major products detectable were the silylene – MeOH insertion product bis(3,4,5-trimethylphenyl)methoxysilane (**53**;  $67 \pm 5\%$ ) and hexamethyldisilane (**21**;  $67 \pm 5\%$ ), as shown in Eq. 3.1. The product yields were determined relative to consumed **43** from the slopes of concentration vs. time plots over the range of 0 – 8 % conversion in **43** (Fig. 3.3). The results indicate that the chemical yield of extrusion of silylene **1** from precursor **43** is higher than that for the extrusion of  $\text{SiPh}_2$  from the acyclic trisilane **26** (see Eq. 1.16), which upon photolysis yielded a ca. 50% of the corresponding silylene derived product.<sup>13</sup>



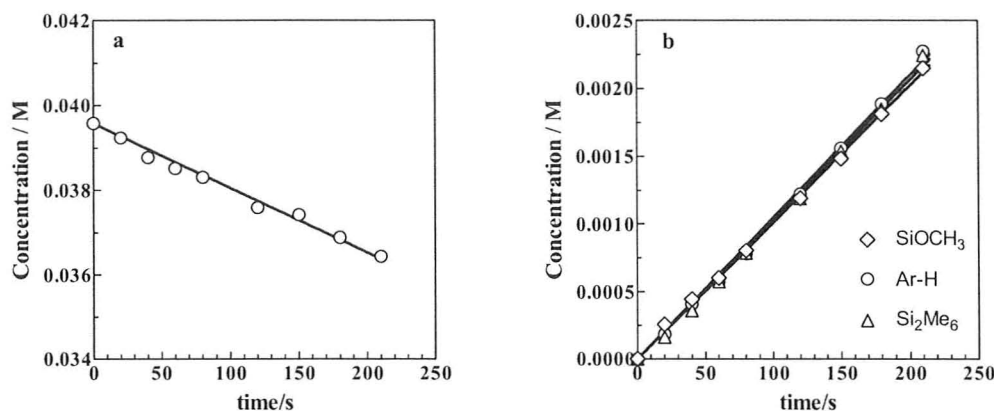


**Figure 3.3.** Concentration vs. time plots for (a) **43** (slope:  $-0.00001527 \pm 0.0000007$ ). (b) **53**, and Si<sub>2</sub>Me<sub>6</sub> (slopes: **53**,  $0.00001010 \pm 0.0000002$  from OMe,  $0.0001048 \pm 0.0000002$  from Ar-H; Si<sub>2</sub>Me<sub>6</sub>,  $0.00001030 \pm 0.0000003$ ) from photolysis of **43** (0.03956 M) in C<sub>6</sub>D<sub>12</sub> containing 0.10 M MeOH.

Preliminary identification of **53** was based on its <sup>1</sup>H NMR spectrum, which shows singlets at  $\delta$  5.233 ppm and 3.462 ppm in an area ratio of 1:3. These can be compared to the chemical shifts of the Si-H ( $\delta$  5.356 ppm) and OMe ( $\delta$  3.521 ppm) protons in the spectrum of diphenylmethoxysilane in the same solvent.<sup>2,6</sup> The <sup>1</sup>H NMR spectrum of the photolysate also showed several weak signals in the methoxy region and an array of resonances in the  $\delta$  3.5 – 6.5 and  $\delta$  0.8 – 1.8 ranges, which are tentatively assigned to the MeOH adducts of silene **54**, resulting from 1,3 – silyl migration into the aryl ring. No attempts were made to quantify their yields as they were difficult to detect at low conversion. Fig. 3.4 shows the <sup>1</sup>H NMR spectra of **43** in cyclohexane-*d*<sub>12</sub> containing MeOH, before and after photolysis for 15 min. (ca. 28% conversion of **43**).

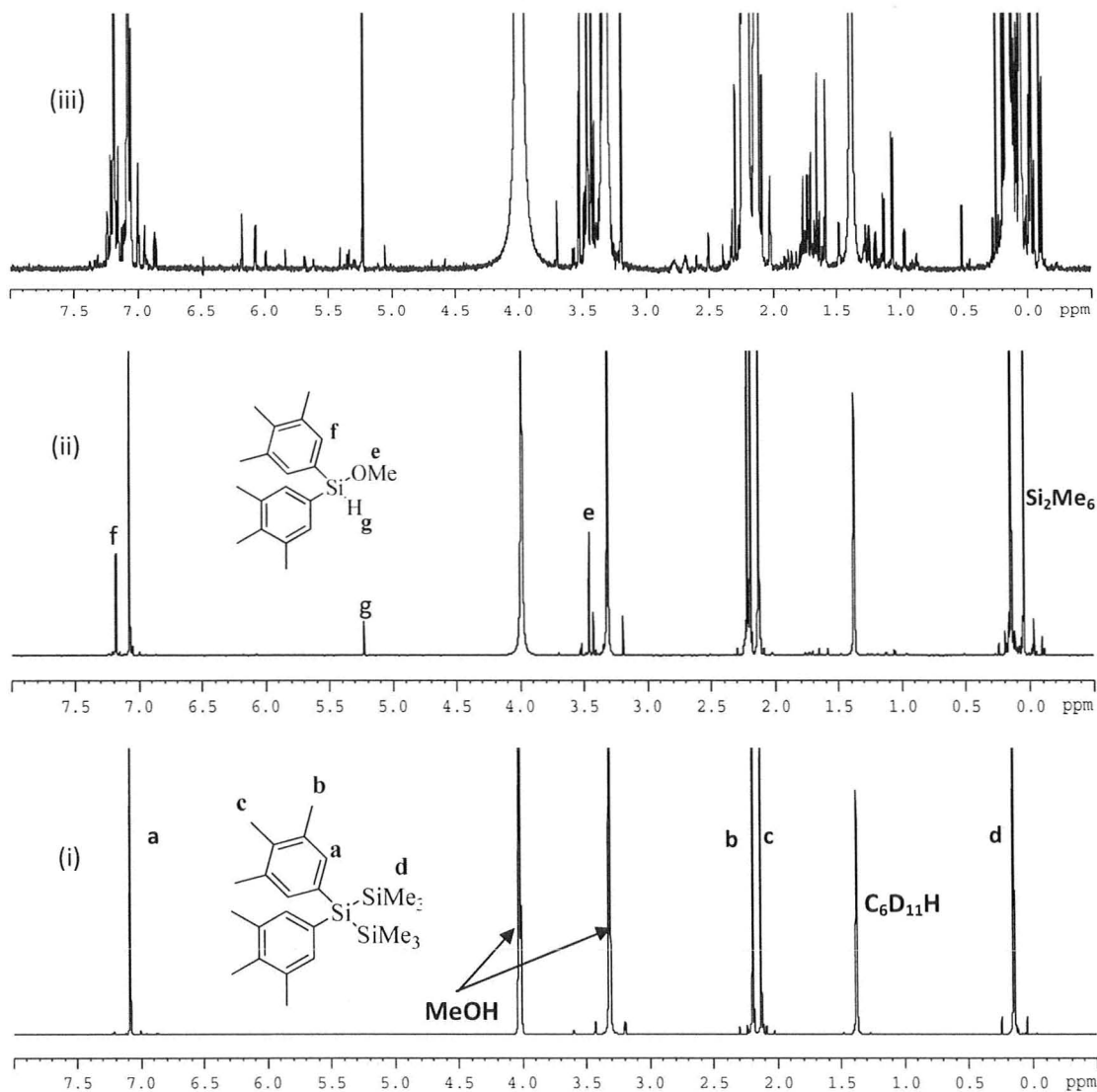
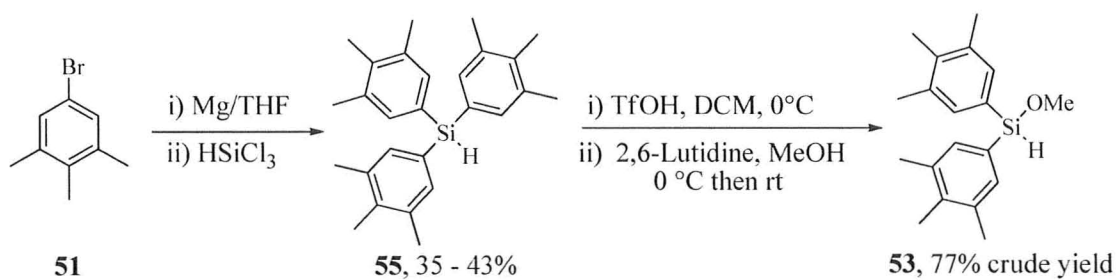


**Figure 3.4.** (i)  $^1\text{H}$  NMR spectrum **43** in  $\text{C}_6\text{D}_{12}$  in the presence of MeOH (0.4 M). (ii)  $^1\text{H}$  NMR spectra **43** after photolysis for 15 min in  $\text{C}_6\text{D}_{12}$  in the presence of 0.4 M MeOH. (iii) Expansion of  $^1\text{H}$  NMR spectra **43** after photolysis for 15 min in  $\text{C}_6\text{D}_{12}$  in the presence of 0.4 M MeOH showing array resonances in the  $\delta$  3.5 – 6.5 and  $\delta$  0.8 – 1.8 ranges.

The product identification was confirmed by  $^1\text{H}$  NMR analysis of the crude photolysis mixture after spiking it with independently prepared **53**. The independent synthesis of **53** was carried out in two steps from **51**, as outlined in Scheme 3.2.

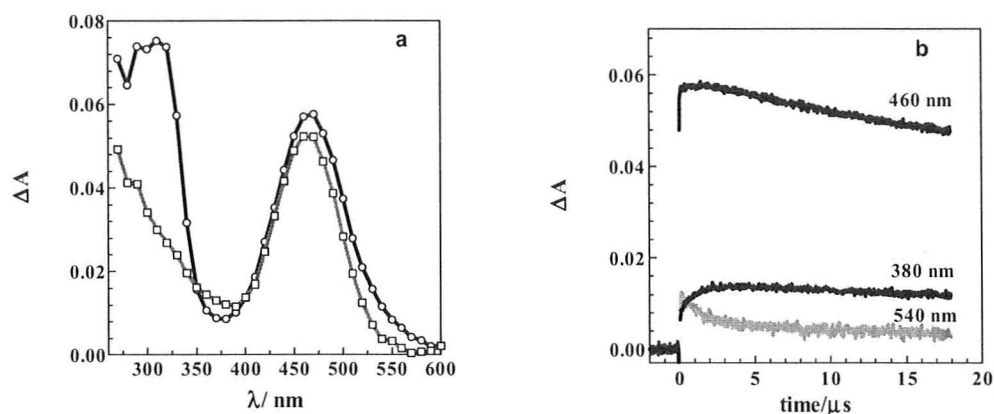


**Scheme 3.2.** Synthesis of methoxybis(3,4,5-trimethylphenyl)silane (**53**).

### 3.6. Laser Flash Photolysis of 1,1,1,3,3,3 – hexamethyl - 2,2 – bis(3,4,5–trimethylphenyl)trisilane (43)

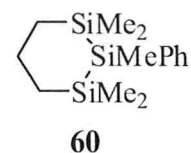
Laser flash photolysis of a flowing, deoxygenated solution of **43** (ca.  $6 \times 10^{-5}$  M) in anhydrous hexanes using a KrF excimer laser (248nm, ~20 ns, ~100 mJ), leads to strong transient absorptions in the 260-600 nm range. Transient UV/vis spectra revealed three distinct overlapping transient species: two long-lived species ( $\tau > 400 \mu\text{s}$ ) with  $\lambda_{\text{max}} = 460$  nm and 380 nm and a shorter-lived species ( $\tau 4 - 10 \mu\text{s}$ ) with absorption bands centered at 520 nm and 320 nm. The shorter-lived species and the long-lived species at 460 nm form with the laser pulse, while the transient at 380 nm was observed to grow in over the first 3 – 8  $\mu\text{s}$  after excitation (Fig.3.5). We assign the transient at 520 nm to the silylene bis(3,4,5–trimethylphenyl)silylene (SiTmp<sub>2</sub>) (**1**) and at 460 nm to the silene **53** generated from 1,3-silyl migration into the aryl ring, a reaction well known for phenylated trisilanes.<sup>10,13-14</sup> The transient at 380 nm is probably the water complex of the silylene arising from inadequate drying of the solvent or solvent handling system. In an early publication by our group, a similar weak growth profile centered at 360 nm in the transient spectra of the photolysis of **22** in hexanes was assigned to the corresponding disilene,<sup>2</sup> but was later found to be absent in the spectra for the photolysis of the compound when the hexanes were more scrupulously dried.<sup>5</sup> There is also a slight growth at 460 nm, occurring on a timescale similar to that at 380 nm. This growth is more likely due to disilene **56**, and this is also close to the absorption maximum of tetraphenyldisilene.<sup>2-3</sup> As expected the lifetime of the 520 nm transient and the peak

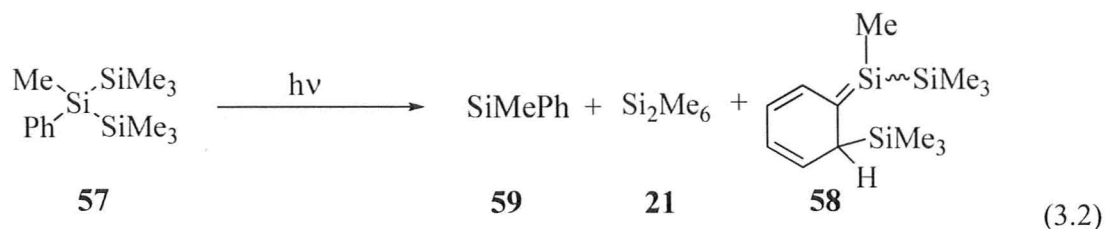




**Fig. 3.5.** (a) Transient absorption spectra recorded at 160-224 ns (o), 9.12-9.18  $\mu$ s ( $\square$ ) after the laser pulse, by laser flash photolysis of a deoxygenated hexanes solution of **42** (ca.  $6 \times 10^{-5}$  M). (b) Transient growth/decay profiles recorded at 380, 460 and 540 nm.

These assignments are analogous to those made earlier by our group in a laser flash photolysis study of the SiPh<sub>2</sub> and SiMePh precursors **26** and **57**, respectively, where long-lived silenes **27** and **58** were observed centered at 460 nm and 440 nm, respectively (Eq 1.16, 3.2).<sup>7</sup> At the long wavelength tail of the intense silene bands were found short-lived species which were assigned to the silylenes based on their lifetimes, absorption maxima ( $\sim 520$  nm), and absolute rate constants for quenching by substrates such as Et<sub>3</sub>SiH and MeOH; these correspond closely with those for SiMePh (**59**) and SiPh<sub>2</sub> determined by laser flash photolysis of cyclic trisilanes **60** and **22** respectively, from which silene formation is suppressed considerably.<sup>3,7-8</sup>





In the present case, the assignments are further supported by the transient behaviour observed upon addition of ca. 5 mM triethylsilane ( $\text{Et}_3\text{SiH}$ ) to the solution, which shortened the transient lifetimes at 520 nm to about 270 ns and quenched the growth portion at 380 nm, but had little effect on the lifetime of the long-lived absorption at 460 nm (Fig. 3.6). The difference spectrum that results from subtracting the second spectrum (1.76-1.82  $\mu\text{s}$ ) from the first (64-128 ns) exhibits absorption bands with  $\lambda_{\text{max}}$  at 520 nm and 315 nm, which are assigned to silylene **1**. Silylene **1** is best monitored at 540-550 nm where the signal is still reasonably strong and better separated from that due to silene **54**.



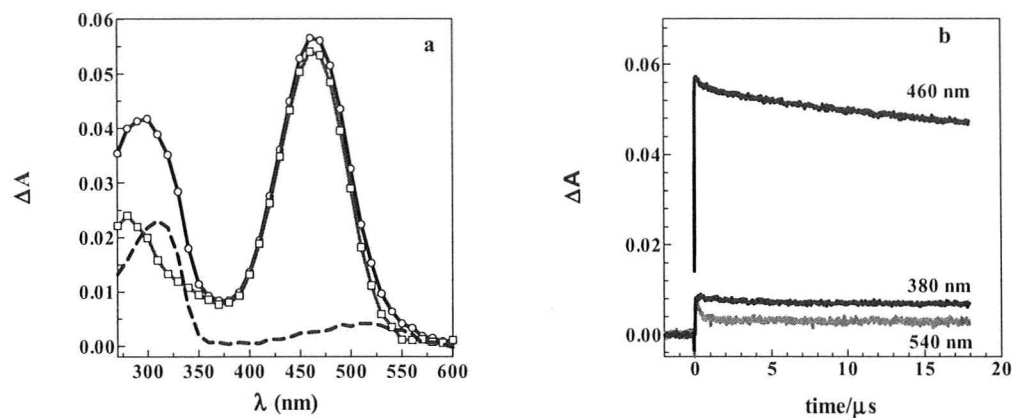


**Fig. 3.6.** (a) Transient absorption spectra recorded at 160 – 224 ns (o), 1.44 – 1.50  $\mu$ s ( $\square$ ) after the laser pulse, by laser flash photolysis of a deoxygenated hexanes solution of **43** (ca.  $6 \times 10^{-5}$  M) containing 5 mM  $\text{Et}_3\text{SiH}$ . The dashed line is the difference spectrum resulting from subtracting the 1.44 – 1.50  $\mu$ s spectrum from the 160 – 224 ns spectrum. (b) Transient decay profiles recorded at 380, 460 and 540 nm.

Addition of small quantities of the substrates listed in Table 3.2 enhanced the decay rate of the silylene in direct proportion to the concentration of the substrate added in all cases, affording linear plots of the pseudo-first-order rate constants ( $k_{\text{decay}}$ ) versus concentration ( $[Q]$ ). The slopes of the plots, from linear least squares analysis according to Equation 1.33, are assigned to the absolute second-order rate constants for the reaction ( $k_Q$ ), and are listed along with those for  $\text{SiPh}_2$  and  $\text{SiMes}_2$  in Table 3.2. The kinetics experiments summarized in Table 3.2 will be discussed individually in detail in the following several sections of this chapter.

**Table 3.2.** Absolute rate constants (in units of  $10^9 \text{ M}^{-1} \text{ s}^{-1}$ ) for quenching of  $\text{SiPh}_2$ ,  $\text{SiMes}_2$  and  $\text{SiTmp}_2$  by various substrates in hexanes or cyclohexane solution at  $25^\circ \text{C}$ 

Substrate	$\text{SiPh}_2^{a, b}$	$\text{SiMes}_2$	$\text{SiTmp}_2$
<b><math>\text{Et}_3\text{SiH}</math></b>	$3.3 \pm 0.2$	$0.079 \pm 0.004^c$	$0.65 \pm 0.06$
<b>MeOH</b>	$18 \pm 2.0^e$	$0.97 \pm 0.08^e$	$10.4 \pm 0.4$
<b>AcOH</b>	$10.1 \pm 1.0$	$3.5 \pm 0.3^d$	$5.6 \pm 0.1$
<b>Acetone</b>	$14.4 \pm 2.0$	$8.3 \pm 0.4^b$	$8.9 \pm 0.4$
<b>THF</b>	$15.2 \pm 1.0$	-	$8.3 \pm 0.8$
<b><math>\text{O}_2</math></b>	$0.12 \pm 0.02$	$0.032 \pm 0.004^c$	$0.081 \pm 0.005$
<b>DMB</b>	$14.5 \pm 1.0$	$0.0088 \pm 0.0007^c$	$6.3 \pm 0.20$
<b>Isoprene</b>	$13.6 \pm 1.0$	$0.031 \pm 0.004$	$6.1 \pm 0.30$
<b>Cyclohexene</b>	$7.9 \pm 0.7$	$0.0028 \pm 0.003^c$	$4.3 \pm 0.20$
<b>BTMSE</b>	$7.6 \pm 0.6$	$0.026 \pm 0.001$	$1.6 \pm 0.09$
<b><math>\text{CCl}_4</math></b>	$1.37 \pm 0.09$	$0.096 \pm 0.004$	$0.68 \pm 0.02$

<sup>a</sup> In hexanes, data from ref. 3. <sup>b</sup> In hexanes, data from ref. 2 <sup>c</sup> In cyclohexane at  $25^\circ \text{C}$ ; data from ref. 1. <sup>d</sup> Rate constant obtained at low concentration of AcOH (up to 0.5 mM). <sup>e</sup> In hexanes, data from ref 4.

### 3.6.1. Reactions of SiTmp<sub>2</sub> with Alkenes, Dienes and Alkynes

In the present study, the absolute rate constant for the reaction of SiTmp<sub>2</sub> with cyclohexene has been measured ( $k_{\text{cyclohexene}} = 4.3 \times 10^9 \text{ M}^{-1} \text{ s}^{-1}$ ) and was found to be almost a factor of two slower than that for SiPh<sub>2</sub> under similar conditions.<sup>3</sup> Thus, SiMes<sub>2</sub> reacts ca. 1500 times slower than SiTmp<sub>2</sub>, which can be attributed to the effects of non – bonded (steric) interaction between the substituents on the silylene and the alkene on the rate determining step. Figure 3.7 shows the plot of  $k_{\text{decay}}$  vs. concentration of cyclohexene, the linear least squares analysis of which gave the obtained rate constant.

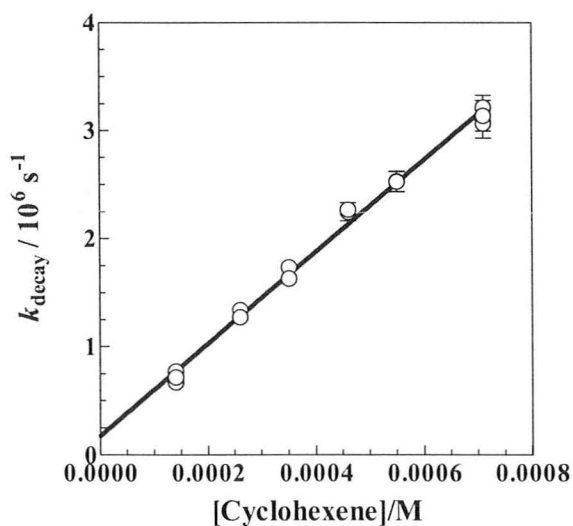


**Fig. 3.7.** Plots of the pseudo-first-order rate constants ( $k_{\text{decay}}$ ) for the decay of SiTmp<sub>2</sub> vs. [cyclohexene] in hexanes solution at 25 °C.

With dienes like 2,3-dimethyl-1,3-butadiene (DMB) and isoprene, the rate constants for the reactions of SiTmp<sub>2</sub> are  $k_{\text{DMB}} = 6.3 \times 10^9 \text{ M}^{-1} \text{ s}^{-1}$  and  $k_{\text{isoprene}} = 6.1 \times 10^9 \text{ M}^{-1} \text{ s}^{-1}$ , respectively. The values are larger than that for the reaction with cyclohexene but follow the same trend, decreasing in the order  $k_{\text{SiPh}_2} \sim 2k_{\text{SiTmp}_2} \sim 1600k_{\text{SiMes}_2}$  for DMB and  $k_{\text{SiPh}_2} \sim 2k_{\text{SiTmp}_2} \sim 440k_{\text{SiMes}_2}$  for isoprene. Figure 3.8 shows the plots of  $k_{\text{decay}}$  vs. concentration of the dienes, DMB and isoprene, the linear least squares analysis of which gave the obtained rate constants.

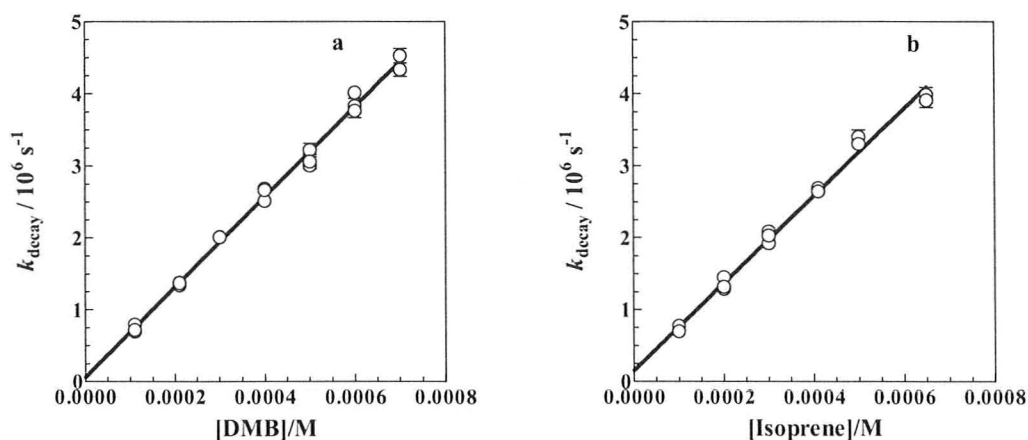


**Fig. 3.8.** Plots of the pseudo-first-order rate constants ( $k_{\text{decay}}$ ) for the decay of SiTmp<sub>2</sub> vs. (a) [DMB] and (b) [isoprene], in hexanes solution at 25 °C.

The absolute rate constant for the reaction of the alkyne BTMSE with SiTmp<sub>2</sub> was determined to be  $k_{\text{BTMSE}} = 6.3 \times 10^9 \text{ M}^{-1} \text{ s}^{-1}$  and follow a similar trend in reactivity as observed with the alkenes and 1,3 – dienes; the rate constant for the diarylsilylenes decreasing in the order  $k_{\text{SiPh}_2} \sim 5k_{\text{SiTmp}_2} \sim 300k_{\text{SiMes}_2}$ . Figure 3.9 shows the plot of  $k_{\text{decay}}$  vs. concentration of BTMSE.

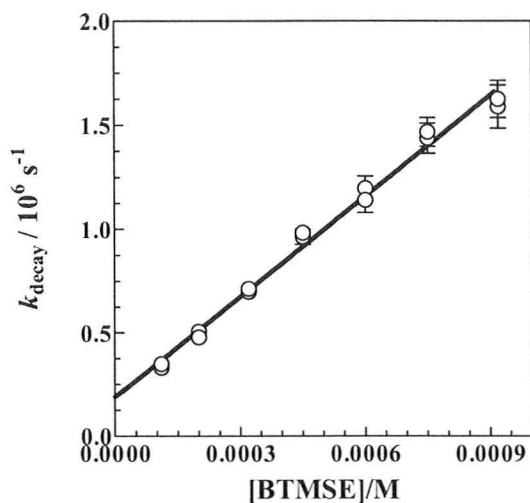


**Fig. 3.9.** Plots of the pseudo-first-order rate constants ( $k_{\text{decay}}$ ) for the decay of  $\text{SiTmp}_2$  vs.  $[\text{BTMSE}]$  in hexanes solution at 25 °C.

Transient absorption spectra recorded for hexanes solutions of **43** containing 0.7 – 0.9 mM DMB, isoprene, cyclohexene, or BTMSE showed long-lived absorptions centered at ca. 280 nm that showed no sign of decay over 2 ms after the laser pulse. These absorptions can be assigned to the corresponding three membered ring compounds – the siliranes or silirene, and are consistent with earlier reports by our group for  $\text{SiPh}_2^3$  and for  $\text{SiMes}_2$  (Section 2.2.1) in the presence of these substrates. Figure 3.10 (a – d) shows the transient spectra recorded over various time windows after the laser pulse in these experiments, along with decay profiles recorded at 280 nm.

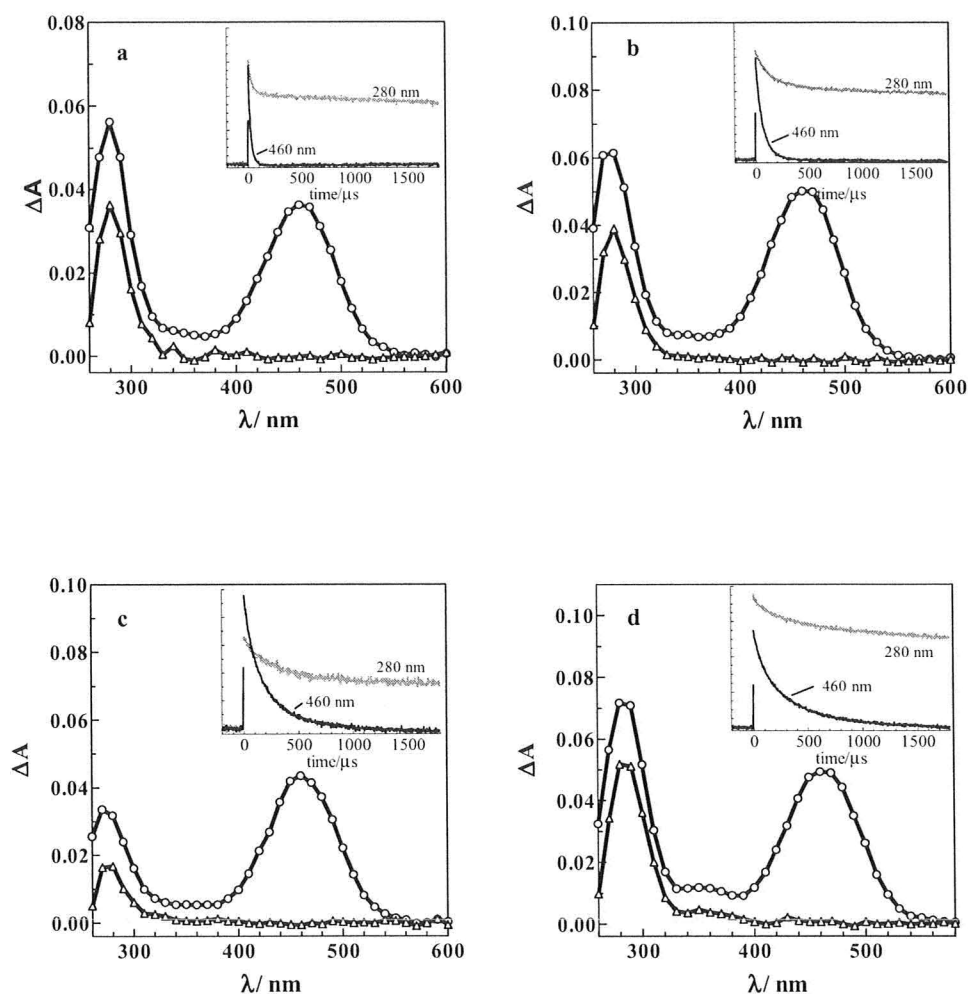
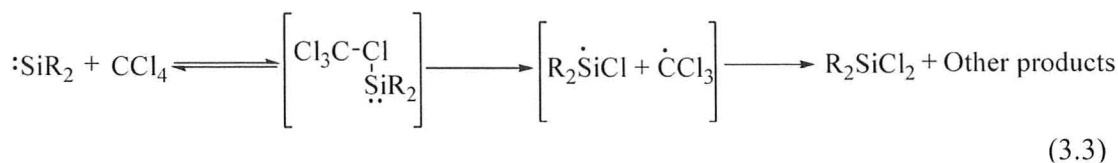


**Figure 3.10.** (a) Transient absorption spectra recorded by laser flash photolysis of deoxygenated hexanes solution of **43** (ca.  $6 \times 10^{-5}$  M) containing (a) 0.70 mM DMB, 3.20 – 9.60  $\mu$ s (○-) and 1552.00 – 1574.40  $\mu$ s (-Δ-) after the laser pulse, (b) 0.69 mM isoprene, 3.20 – 9.60  $\mu$ s (○-) and 1552.00 – 1574.40  $\mu$ s (-Δ-) after the laser pulse, (c) 0.71 mM cyclohexene, 6.40 – 19.20  $\mu$ s (○-) and 1552.00 – 1571.20  $\mu$ s (-Δ-) after the laser pulse, and (d) 0.92 mM BTMSE, 6.40 – 19.20  $\mu$ s (○-) and 1552.00 – 1574.40  $\mu$ s (-Δ-) after the laser pulse. The insets show transient decay recorded at 280 and 460 nm.

### 3.6.2. Reaction of SiTmp<sub>2</sub> with CCl<sub>4</sub>

The absolute rate constants for the reaction of SiTmp<sub>2</sub> and silene **54** with CCl<sub>4</sub> were found to be  $k_{\text{CCl}_4} = 6.8 \times 10^8 \text{ M}^{-1} \text{ s}^{-1}$  and  $k_{\text{CCl}_4} = 8.6 \times 10^7 \text{ M}^{-1} \text{ s}^{-1}$ , respectively (see Fig. 3.11). SiTmp<sub>2</sub> reacts ca. twice slower with CCl<sub>4</sub> than SiPh<sub>2</sub>, indicating that electron donating groups on the phenyl rings retard the reaction. This is consistent with the two step mechanism of Eq. 3.3, with the first step as rate determining. This is in contrast to what has been observed for the reactions of diarylgermylenes with CCl<sub>4</sub>, for which a Hammett reaction constant of  $\rho = -0.38 \pm 0.10$  was observed.<sup>15</sup> This was proposed to be the result of a fast reversible complexation, followed by rate determining dissociative inner sphere electron transfer from Ge to the substrate to yield the Ph<sub>2</sub>GeCl and CCl<sub>3</sub> radicals.<sup>15</sup>



The absolute rate constant obtained for the reaction of silene **54** with CCl<sub>4</sub> is about 4 times greater than that obtained from the silene **27**, generated due to 1,3 – silyl migration from the photolysis of 1,1,1,3,3,3-hexamethyl-2,2-diphenyltrisilane.<sup>7</sup> It has been suggested that the reaction of silenes of these types with CCl<sub>4</sub> proceeds *via* Cl atom abstraction to yield the corresponding cyclohexadienyl – type radical (**61**) and the trichloromethyl radical (Eq. 3.4).<sup>7,16</sup> The oxidation potential of the 1 – silahexatrienyl

moiety of silene **54** should be lower than that of silene **27** and this is expected to accelerate the initial electron transfer step.<sup>7,16</sup>

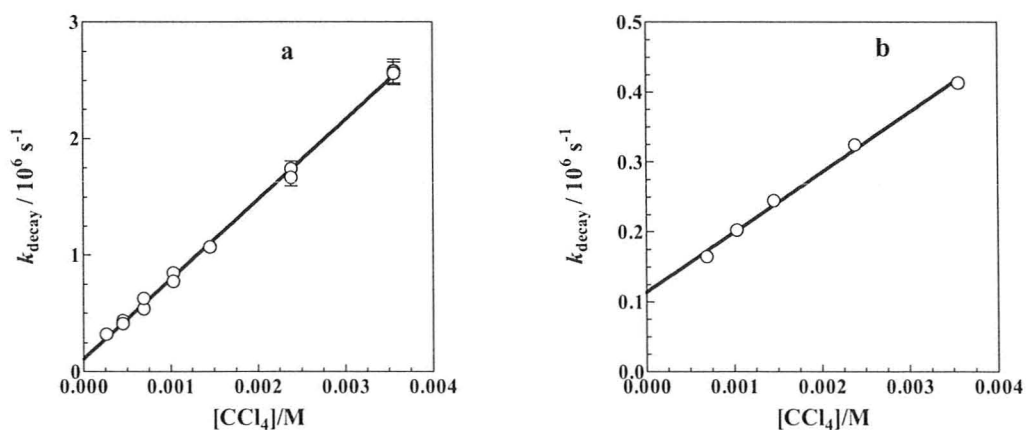
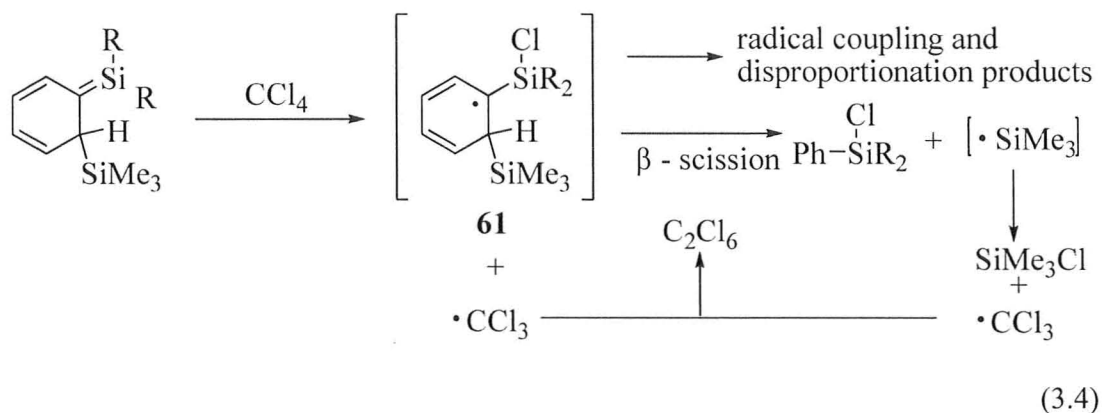


**Fig. 3.11.** Plots of the pseudo-first-order rate constants ( $k_{\text{decay}}$ ) for (a) the decay of SiTmP<sub>2</sub> vs. [CCl<sub>4</sub>] and (b) the decay of silene **54** vs. [CCl<sub>4</sub>], in hexanes solution at 25 °C.



### 3.6.3. Reactions of SiTmp<sub>2</sub> with Oxygenated Substrates

SiMe<sub>2</sub> and SiPh<sub>2</sub> undergo Lewis acid – base complexation reactions with THF at close to the diffusion controlled rate, the complexes exhibiting  $\lambda_{\text{max}} = 310$  nm for SiMe<sub>2</sub><sup>17-18</sup> in cyclohexane solvent and  $\lambda_{\text{max}} = 360$  nm for SiPh<sub>2</sub> in hexanes.<sup>3</sup> On the other hand, SiMes<sub>2</sub> reacts reversibly with THF, and exhibits the relatively small equilibrium constant of  $K_{\text{eq}} = 3 \text{ M}^{-1}$ .<sup>19</sup> In a situation like this,  $k_{\text{Q}}$  cannot be measured, because at concentrations high enough to cause a measurable reduction in the amount of free silylene remaining at equilibrium, the initial pseudo – first – order decay is too fast to be resolved from the laser pulse. Analogously, alcohols react with SiMe<sub>2</sub> and SiPh<sub>2</sub> via an effectively irreversible initial complexation step followed by catalyzed proton transfer from oxygen to the silicon center. Kinetic simulations (calculations done by W. J. Leigh) established an upper limit of  $k_{-\text{MeOH}} \approx 10^5 \text{ s}^{-1}$  for the rate constant for the reversion of the SiPh<sub>2</sub> – MeOH complex to the free reactants and this afforded a lower limit of  $K_{\text{eq}} \geq 2 \times 10^5 \text{ M}^{-1}$  for the equilibrium constant for complexation of SiPh<sub>2</sub> with MeOH.<sup>5</sup> In contrast, for SiMes<sub>2</sub> the complexation step has a substantially smaller equilibrium constant, leading to kinetics consistent with reversible complexation followed by alcohol – catalyzed proton transfer in the second step (see Section 1.6.4 and 2.2.4 for details).<sup>5</sup> The new silylene SiTmp<sub>2</sub> stands as an important candidate to check whether the reversibility is due to electronics or is solely a manifestation of steric effects. In both cases, with THF and MeOH, linear plots of  $k_{\text{decay}}$  vs. concentration of

the quencher were obtained (see Fig. 3.12) indicating irreversible quenching similar to that obtained in the case of SiPh<sub>2</sub>. For the transient spectrum of the reaction of SiTmp<sub>2</sub> with THF there is a band centered at ~ 375 nm, which appear to grow in over a similar time scale as the decay of the silylene and can be tentatively assigned to the SiTmp<sub>2</sub> – THF complex (Fig. 3.13 (a)). The intensity of the band however did not show any appreciable dependence on the THF concentration. Unfortunately though, we were unable to detect any complex of MeOH with SiTmp<sub>2</sub> (see Fig. 3.13 (b)). This is probably due to the intense silene bands which obscured the presence of any weakly absorbing complexes. For the reaction of SiTmp<sub>2</sub> with MeOH the plot for  $k_{\text{decay}}$  versus [MeOH] exhibited an almost zero intercept, the errors in this case not allowing choosing between negative and positive intercepts (Fig. 3.12 (b)). A negative intercept would mean a higher order dependence on alcohol concentration, consistent with a reversible complexation step (*cf.* Section 2.2.4). The absolute rate constants for the reaction of SiTmp<sub>2</sub> with MeOH and THF are  $k_{\text{MeOH}} = 1.04 \times 10^{10} \text{ M}^{-1} \text{ s}^{-1}$  and  $k_{\text{THF}} = 8.3 \times 10^9 \text{ M}^{-1} \text{ s}^{-1}$  respectively, each being approximately two times slower than that observed for SiPh<sub>2</sub> (see Table 3.2).<sup>3,5</sup>

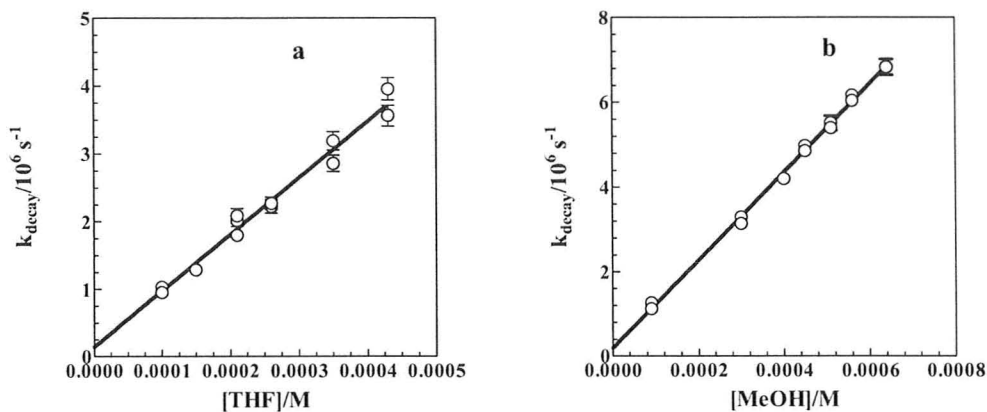


**Fig. 3.12.** Plots of the pseudo-first-order rate constants ( $k_{\text{decay}}$ ) for decay of SiTmp<sub>2</sub> vs. (a) [THF] and (b) [MeOH], in hexanes solution at 25 °C.

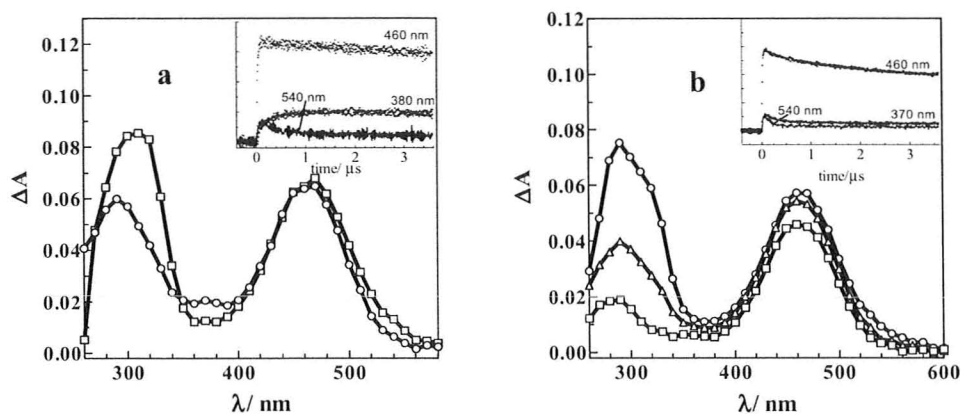


**Fig. 3.13.** (a) Transient absorption spectra recorded 128 – 141 ns (□-) and 864 – 877 ns (○-) after the laser pulse, from laser flash photolysis of **43** (ca.  $6 \times 10^{-5}$  M) in deoxygenated hexanes containing 0.26 mM THF; the inset shows transient growth/decay profiles recorded at 380 nm, 460 nm, and 540 nm. (b) Transient absorption spectra recorded 77 – 90 ns (○-), 224 – 250 ns (Δ-), and 1.50 – 1.53 μs (□-) after the pulse, from laser flash photolysis of **43** in deoxygenated hexanes containing 0.56 mM MeOH; the inset shows transient decay profiles recorded at 380 nm, 460 nm, and 540 nm.

The absolute rate constants obtained for the reactions of SiTmp<sub>2</sub> with acetone and acetic acid are  $k_{\text{acetone}} = 8.9 \times 10^9 \text{ M}^{-1} \text{ s}^{-1}$  and  $k_{\text{AcOH}} = 5.6 \times 10^9 \text{ M}^{-1} \text{ s}^{-1}$ . The rate constants are essentially same as those obtained for SiMes<sub>2</sub>, within the limits of error. This implies that there are minimal non-bonded interactions in the transition state of the rate determining step for the reaction of silylenes with acetone, and the small rate retardation from SiPh<sub>2</sub> to SiTmp<sub>2</sub> or SiMes<sub>2</sub> is due solely to the inductive effect of the three methyl groups attached to each aryl substituent which reduces the silylene Lewis acidity. Our group was unable to detect a complex of SiPh<sub>2</sub> with acetone or acetic acid, and thus the complexes were proposed to be formed as true steady state intermediates, never building up in high enough concentrations to enable detection (*cf.* Eq. 1.21).<sup>2-3</sup> Similar to this observation, and that observed for SiMes<sub>2</sub> in this work for acetic acid and acetone in earlier studies by our group,<sup>2</sup> we were unable to detect any complex for the reactions with acetone or acetic acid (see Fig. 3.14). The plots of  $k_{\text{decay}}$  vs. concentrations of acetic acid and acetone are shown in Fig. 3.15.

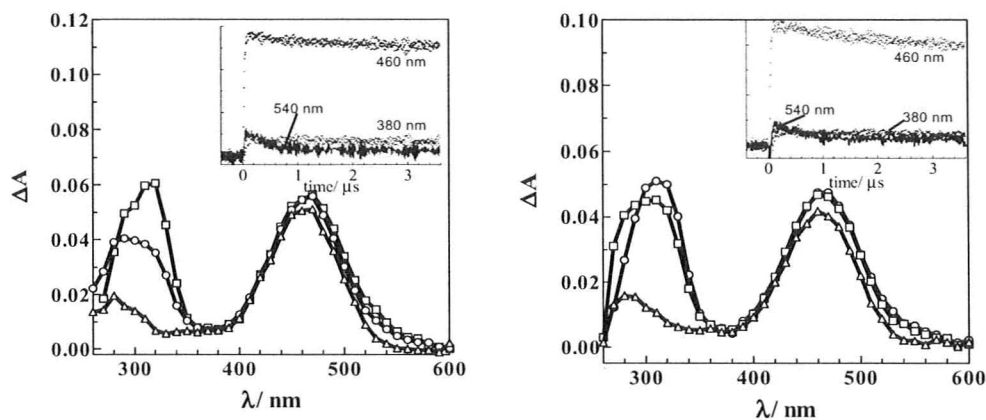


**Fig. 3.14.** (a) Transient absorption spectra recorded 96 – 109 ns ( $\square$ ), 352 – 378 ns ( $\circ$ ) and 2.78 – 2.81  $\mu$ s ( $\Delta$ ) after the laser pulse, from laser flash photolysis of **43** (ca.  $6 \times 10^{-5}$  M) in deoxygenated hexanes containing 0.30 mM acetone; the inset shows transient growth/decay profiles recorded at 380 nm, 460 nm, and 540 nm. (b) Transient absorption spectra recorded 205 – 218 ns ( $\circ$ ), 352 – 378 ns ( $\square$ ), and 2.16 – 2.20  $\mu$ s ( $\Delta$ ) after the pulse, from laser flash photolysis of **43** in deoxygenated hexanes containing 0.30 mM AcOH; the inset shows transient decay profiles recorded at 380 nm, 460 nm, and 540 nm.

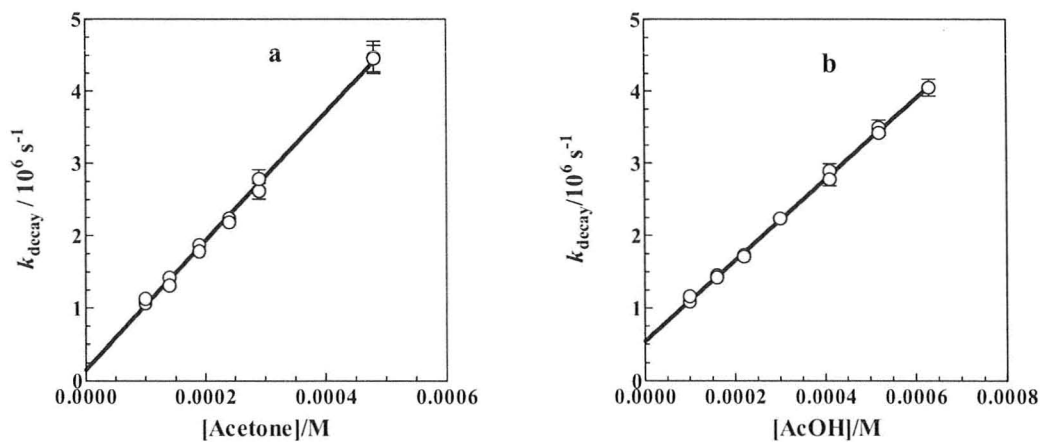
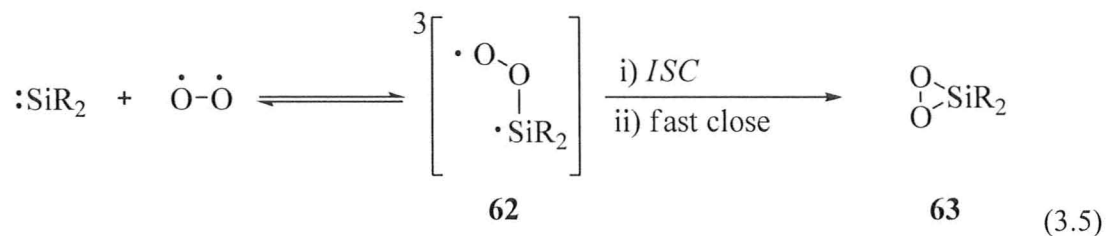


**Fig. 3.15.** Plots of the pseudo-first-order rate constants ( $k_{\text{decay}}$ ) for the decay of SiTmp<sub>2</sub> vs. (a) [acetone] and (b) [acetic acid], in hexanes solution at 25 °C.

The reactions of transient silylenes with molecular oxygen have been studied in the gas phase for the parent silylene ( $\text{SiH}_2$ ),<sup>20</sup> in low temperature matrices for  $\text{SiMe}_2$ ,<sup>21</sup>  $\text{SiMe}_2$ ,<sup>22</sup> and  $\text{SiMePh}$ ,<sup>23</sup> and in solution for  $\text{SiMe}_2$ ,<sup>3,17</sup>  $\text{SiMe}_2$ ,<sup>1</sup> and  $\text{SiPh}_2$ .<sup>3</sup> The reaction has also been studied theoretically.<sup>20-21,23-24</sup> Ando *et al.* observed a weak absorption at  $\lambda_{\text{max}} \approx 320$  nm for the reaction product of  $\text{SiMe}_2$  with  $\text{O}_2$  in an oxygen matrix at 16 K using UV/vis spectroscopy.<sup>21</sup> On the basis of IR spectra and RHF/6-31 (g) calculations, they ascribed it to the silanone oxide (**62**, Eq. 3.5). An analogous absorption centered at  $\lambda_{\text{max}} \approx 370$  nm was observed for the reaction of  $\text{SiPh}_2$  with  $\text{O}_2$  in hexanes solution at 25 °C in an earlier study by our group and the absorption was again assigned to the corresponding triplet silanone oxide.<sup>3</sup> No such intermediates were observed for  $\text{SiMe}_2$  in solution.<sup>3</sup> Sander and co-workers showed by IR spectroscopy that in 0.5 %  $\text{O}_2$ -doped matrices,  $\text{O}_2$  reacts with  $\text{SiMe}_2$ ,<sup>22</sup> and  $\text{SiMePh}$ <sup>23</sup> at 40 K to form the corresponding dioxasiliranes (**63**, Eq. 3.5) without the formation of any detectable intermediates. Thus the reaction mechanism is thought to be as shown in Eq. 3.5, where the first-formed species is a triplet silanone oxide which undergoes intersystem crossing to the singlet state followed by ring closure to form the corresponding dioxasilirane.<sup>3</sup> Theoretical calculations predict a very low activation barrier for the ring closure; ca. 5 kcal mol<sup>-1</sup> for  $\text{SiH}_2$ <sup>20</sup> at G3 level of theory, and about 0.8 kcal mol<sup>-1</sup> for  $\text{SiMePh}$ <sup>23</sup> at B3LYP/6-311++G(d,p) level of theory, which could explain the failure to observe the intermediate triplet silanone oxide **62** in some cases.



The absolute rate constant for the reaction of SiTmp<sub>2</sub> with O<sub>2</sub> was obtained from the slope of a three point plot of  $k_{\text{decay}}$  in argon -, air -, and O<sub>2</sub> saturated hexane vs. [O<sub>2</sub>] (Fig. 3.16 (a)) and found to be  $k_{\text{O}_2} = 8.1 \times 10^7 \text{ M}^{-1} \text{ s}^{-1}$ , which is just a factor of 2.5 larger than that obtained by Conlin and co-workers for SiMe<sub>2</sub> at room temperature in cyclohexane solution.<sup>1</sup> Silene **54** was also found to be sensitive O<sub>2</sub>, and the rate constant obtained from a two point plot of  $k_{\text{decay}}$  in air -, and O<sub>2</sub> saturated hexanes vs. [O<sub>2</sub>] (Fig. 3.16 (b)) was found to be  $k_{\text{O}_2} = 5 \times 10^7 \text{ M}^{-1} \text{ s}^{-1}$  which is similar to that reported for the corresponding silene from 2,2-diphenyl-1,1,1,3,3,3-hexamethyltrisilane.<sup>7</sup> The transient absorption spectra from laser photolysis of **43** in O<sub>2</sub> – saturated hexanes did not show any hint of a detectable intermediate (Fig.3.17).

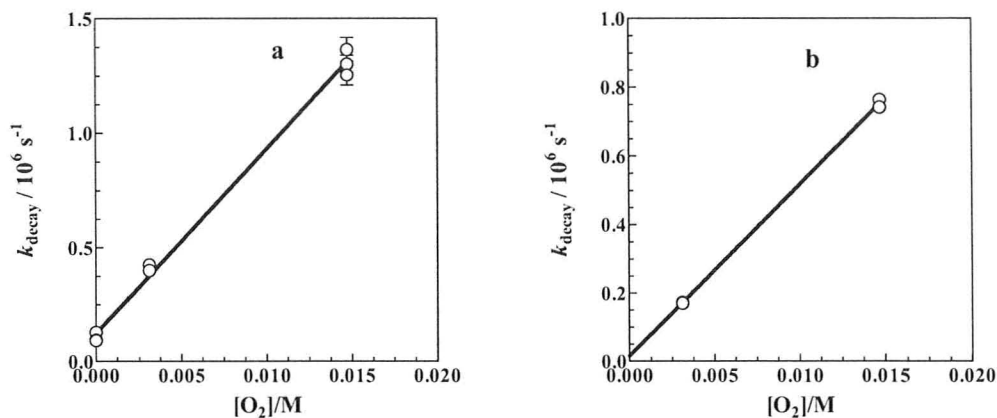


**Fig. 3.16.** Plots of the pseudo-first-order rate constants ( $k_{\text{decay}}$ ) for (a) the decay of SiTmp<sub>2</sub> vs. [O<sub>2</sub>] and (b) the decay of silene **54** vs. [O<sub>2</sub>], in hexanes solution at 25 °C.

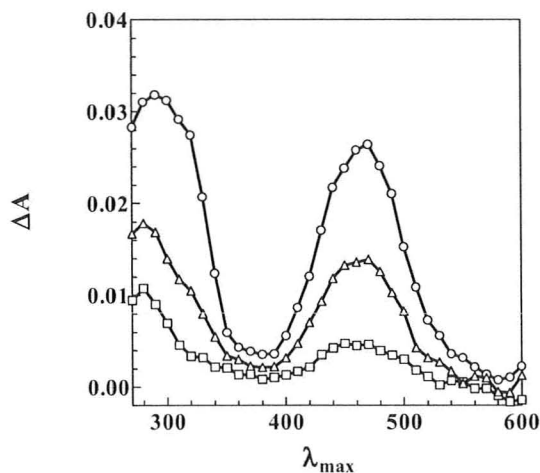


**Fig. 3.17.** Transient absorption spectra recorded at 480 – 554 ns (o), 1.28 – 1.36 μs (Δ), and 2.72 – 2.82 μs (□) after the laser pulse, by laser flash photolysis of a O<sub>2</sub> saturated hexanes solution of **43** (ca.  $6 \times 10^{-5}$  M).

### 3.7.4. Reaction of SiTmp<sub>2</sub> with Et<sub>3</sub>SiH

The absolute rate constant for the reaction of SiTmp<sub>2</sub> with triethylsilane (Et<sub>3</sub>SiH) was determined to be  $k_{\text{Et}_3\text{SiH}} = 6.5 \times 10^8 \text{ M}^{-1}\text{s}^{-1}$  which is a factor of five slower than that



for  $\text{SiPh}_2$  but an order of magnitude faster than that for  $\text{SiMes}_2$ ; thus  $k_{\text{SiPh}_2} \sim 5k_{\text{SiTmp}_2} \sim 42k_{\text{SiMes}_2}$ . This is consistent with the two – step mechanism of Eq. 3.6, with the first step as rate determining. Fig. 3.18 shows the plots for  $k_{\text{decay}}$  vs. concentrations of  $\text{Et}_3\text{SiH}$ .

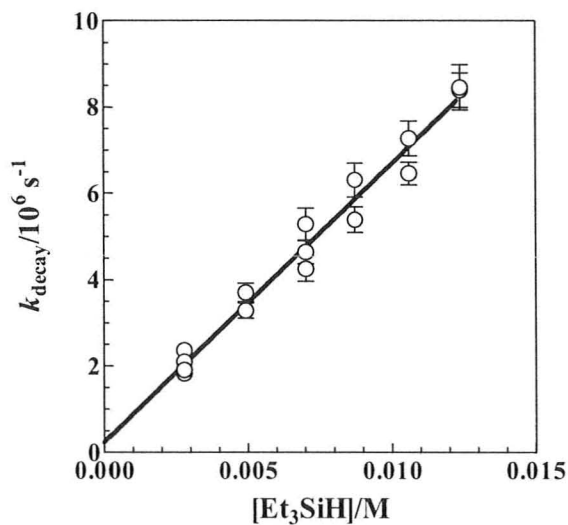
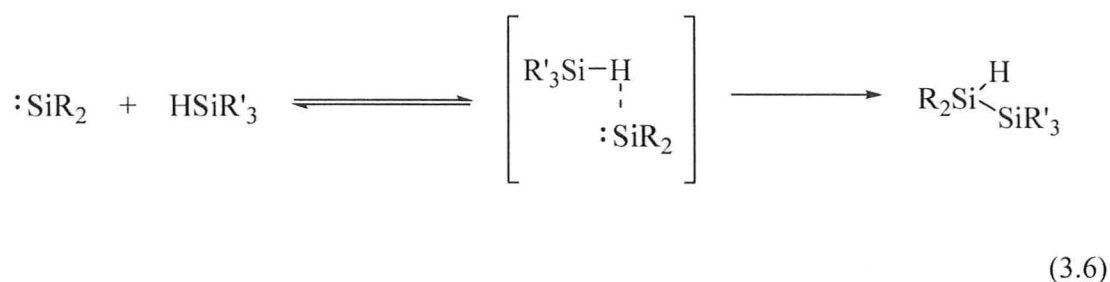


**Fig. 3.18.** Plots of the pseudo-first-order rate constants ( $k_{\text{decay}}$ ) for the decay of  $\text{SiTmp}_2$  vs.  $[\text{Et}_3\text{SiH}]$  in hexanes solution at  $25^\circ\text{C}$ .

## References

- (1) Conlin, R. T.; Netto-Ferreira, J. C.; Zhang, S.; Scaiano, J. C. *Organometallics* **1990**, *9*, 1332.
- (2) Moiseev, A. G.; Leigh, W. J. *Organometallics* **2007**, *26*, 6268.
- (3) Moiseev, A. G.; Leigh, W. J. *Organometallics* **2007**, *26*, 6277.
- (4) Hansch, C.; Leo, A.; Taft, R. W. *Chem. Rev.* **1991**, *91*, 165.
- (5) Leigh, W. J.; Kostina, S. S.; Bhattacharya, A.; Moiseev, A. G. *Organometallics* **2010**, *29*, 662.
- (6) Moiseev, A. G.; Leigh, W. J. *J. Am. Chem. Soc.* **2006**, *128*, 14442.
- (7) Leigh, W. J.; Moiseev, A. G.; Coulais, E.; Lollmahomed, F.; Askari, M. S. *Can. J. Chem.* **2008**, *86*, 1105.
- (8) Moiseev, A. G.; Coulais, E.; Leigh, W. J. *Chem. Eur. J.* **2009**, *15*, 8485.
- (9) Ishikawa, M.; Nakagawa, K. I.; Ishiguro, M.; Ohi, F.; Kumada, M. *J. Organomet. Chem.* **1978**, *152*, 155.
- (10) Ishikawa, M.; Nakagawa, K. I.; Enokida, R.; Kumada, M. *J. Organomet. Chem.* **1980**, *201*, 151.
- (11) Beringer, F. M.; Ugelow, I. *J. Am. Chem. Soc.* **1953**, *75*, 2635.
- (12) Baciocchi, E.; Dalla Cort, A.; Ebersson, L.; Mandolini, L.; Rol, C. *J. Org. Chem.* **1986**, *51*, 4544.
- (13) Miyazawa, T.; Koshihara, S. Y.; Liu, C.; Sakurai, H.; Kira, M. *J. Am. Chem. Soc.* **1999**, *121*, 3651.
- (14) Ishikawa, M.; Kumada, M. *Adv. Organomet. Chem.* **1981**, *19*, 51.
- (15) Huck, L. A.; Leigh, W. J. *Can. J. Chem.* **in press**.
- (16) Leigh, W. J.; Sluggett, G. W. *Organometallics* **1994**, *13*, 269.
- (17) Levin, G.; Das, P. K.; Bilgrien, C.; Lee, C. L. *Organometallics* **1989**, *8*, 1206.
- (18) Yamaji, M.; Hamanishi, K.; Takahashi, T.; Shizuka, H. *J. Photochem. Photobiol. A: Chem.* **1994**, *81*, 1.
- (19) Kostina, S. S.; Leigh, W. J. *Unpublished work*.
- (20) Becerra, R.; Bowes, S. J.; Ogden, J. S.; Cannady, J. P.; Adamovic, I.; Gordon, M. S.; Almond, M. J.; Walsh, R. *Phys. Chem. Chem. Phys.* **2005**, *7*, 2900.
- (21) Akasaka, T.; Nagase, S.; Yabe, A.; Ando, W. *J. Am. Chem. Soc.* **1988**, *110*, 6270.

- (22) Patyk, A.; Sander, W.; Gauss, J.; Cremer, D. *Angew. Chem. Int. Ed. Engl.* **1989**, *28*, 898.
- (23) Bornemann, H.; Sander, W. *J. Am. Chem. Soc.* **2000**, *122*, 6727.
- (24) Nagase, S.; Kudo, T.; Akasaka, T.; Ando, W. *Chem. Phys. Lett.* **1989**, *163*, 23.

## Chapter 4 – Summary and Conclusion

### 4.1. Contributions of the study

1,1,1,3,3,3 – Hexamethyl – 2,2 – bis(3,4,5–trimethylphenyl)trisilane (**43**) was synthesized and photolyzed successfully to yield a new diarylsilylene, SiTmp<sub>2</sub>, which was detected directly in solution by time-resolved UV/vis spectroscopy. Although the photolysis of **43** afforded both the silylene and the strongly absorbing silene resulting from the 1,3 – silyl migration, we were able to separate their signals and study the reactivity of SiTmp<sub>2</sub> in a quantitative manner. Absolute rate constants have been determined for the reactions of SiTmp<sub>2</sub> with a wide variety of substrates for which rate constants were already reported for the parent diarylsilylene, SiPh<sub>2</sub>.<sup>1-2</sup> The reactivities of SiMes<sub>2</sub> with some substrates such as AcOH, isoprene, CCl<sub>4</sub>, BTMSE, MeOH/D and *t* – BuOH/D were also studied for the first time. A comparison of the rate constants for SiPh<sub>2</sub> and SiTmp<sub>2</sub> for each substrate provides a quantitative assessment of electronic effects on diarylsilylene reactivity, the first such study to be carried out. In almost all cases it was found that electronic factors reduce the absolute rate constants by a factor of 2, except for the reactions with triethylsilane and BTMSE where a factor of ca. 5 rate retardation were observed. This indicates that in general the inductive electron-donating effect associated with six methyl groups on the aromatic rings plays only a small role in the modification of diarylsilylene reactivity. A measure of the sensitivity of diarylsilylene reactivity to steric effects of the *ortho* – methyl groups in the mesityl

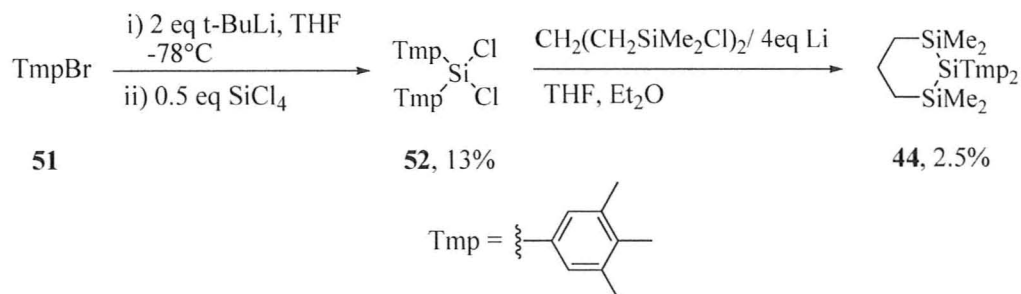
substituent, is the relative rate constants for the reactions of SiTmp<sub>2</sub> and SiMes<sub>2</sub>. It has been observed that for substrates like acetone, acetic acid and O<sub>2</sub> there is almost no sensitivity to steric effects. In these reactions the complexation steps are believed to be the rate determining steps, and the complex in each case can form and/or orient itself in a fashion that minimises interactions with the *ortho* – methyl groups (Eqs 1.23, 3.5). For substrates such as CCl<sub>4</sub> and Et<sub>3</sub>SiH there is modest sensitivity towards steric effect, rate constants for SiTmp<sub>2</sub> being ca. 7 – 8 times higher than that for SiMes<sub>2</sub>. A similar steric effect was also observed on the rate constants for the initial complexation step in the reactions with MeOH, which is about an order of magnitude smaller for SiMes<sub>2</sub> than for SiTmp<sub>2</sub>.<sup>3</sup> A moderate to high sensitivity towards steric interactions have been observed for the reactions with alkenes, alkynes and dienes. The sensitivity is dependent on the structure of these unsaturated substrates; it increases from the alkyne BTMSE ( $k_{\text{SiTmp}_2}/k_{\text{SiMes}_2} \approx 60$ ) to the dienes isoprene ( $k_{\text{SiTmp}_2}/k_{\text{SiMes}_2} \approx 200$ ) and DMB ( $k_{\text{SiTmp}_2}/k_{\text{SiMes}_2} \approx 700$ ), cyclohexene ( $k_{\text{SiTmp}_2}/k_{\text{SiMes}_2} \approx 1500$ ) being the most sensitive substrate. This gives us an idea about the steric congestion in the transition states of the rate determining step for the reaction of diarylsilylenes with various substrates.

Though we were successful in measuring the rate constants for the reactions of SiTmp<sub>2</sub> with several substrates, we were unable to detect important intermediates such as the complex of SiTmp<sub>2</sub> with MeOH with this precursor (**43**) because of the intense silene band. In accordance with earlier reports<sup>1,4</sup> it can be speculated that 1,3 – silyl

migration can be suppressed by using the six – membered cyclotrisilane precursor (**43**) to SiTmp<sub>2</sub>.

#### 4.2. Future directions

The reactivities of SiTmp<sub>2</sub> towards various substrates in solution have been studied in this thesis using precursor **43**. Unfortunately, we were unable to detect important expected intermediates, such as the MeOH – silylene complex using **43** as the source of SiTmp<sub>2</sub>, and this restricts us from getting a better understanding of the reaction mechanisms. The most probable reason for this phenomenon is the intense bands of silene **54** which interfered in the detection of these intermediates. To prevail over such a situation, efforts in the synthesis of trisilacyclohexane precursor **44** are in progress in our group as the 1,3 – silyl migration is expected to be suppressed in this case. Recently, Derek R. Morim, a summer student in our group synthesized a small batch (ca. 3 mg) of this compound following the route shown in Scheme 4.1. Attempts are underway in our laboratory to optimize the yields of **44**.



**Scheme 4.1.** Synthesis of **44**

Laser flash photolysis of **44** in hexanes led to the formation of two distinct transient absorptions: one formed with the laser pulse ( $\lambda_{\text{max}} \approx 500 \text{ nm}$ ;  $\tau \approx 9 \text{ } \mu\text{s}$ ) and a longer lived band ( $\lambda_{\text{max}} \approx 460 \text{ nm}$ ;  $\tau \gg 100 \text{ } \mu\text{s}$ ), the bulk of which grew in after the laser pulse in timescale similar to the decay of the first species (Fig. 4.1). Based on the lifetimes and the absorbing region (*cf.* Section 3.6) the 500 nm band can be assigned to SiTmp<sub>2</sub> and 460 nm could be due to due to the presence of 1,3 – silyl migration product and the disilene. These assignments are similar to those for the laser flash photolysis **22** in hexanes solution in which the band for SiPh<sub>2</sub> was observed at 515 nm and the tetraphenyldisilene and silene **24** at 460 nm.<sup>1</sup> No mechanistic significance can be attributed to the non – detection of intermediates using **43** as the precursor to SiTmp<sub>2</sub>. Using **44** as the precursor to SiTmp<sub>2</sub>, the intensity of the silene band at 460 nm is reduced by at least a factor of 3 (Fig. 4.1(a)). This reduction in intensity of the silene band in the laser flash photolysis spectrum of **44** indicates the possibility of detection of these intermediates in future flash photolysis studies and this will help in ascertaining mechanisms for the reactions involved.

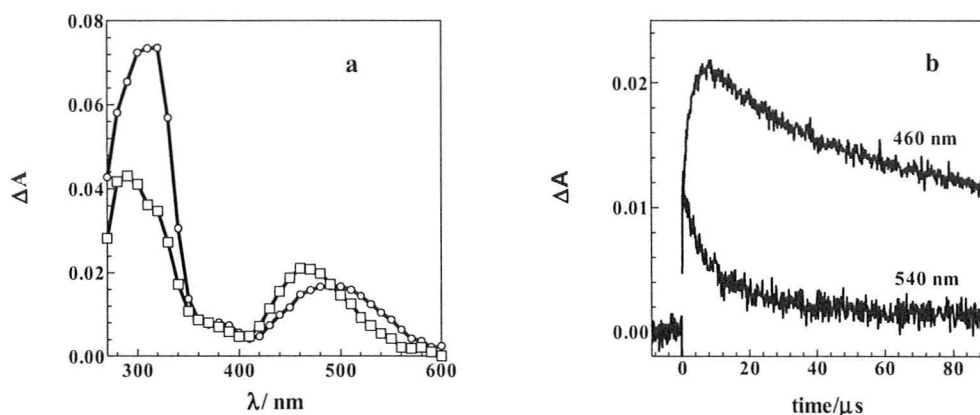


**Fig. 4.1.** (a) Transient absorption spectra recorded at 1.44 – 1.76  $\mu\text{s}$  (o), 9.12 – 9.76  $\mu\text{s}$  ( $\square$ ) after the laser pulse, by laser flash photolysis of a deoxygenated hexanes solution of **44**. (b) Transient growth/decay profiles at 460 and 540 nm.

The elucidation of mechanisms for the reactions of silylenes with different substrates remains one of the primary goals for the group. Recent variable temperature studies with  $\text{SiPh}_2$  by Margaret Reid in our group showed that the activation energies are all close to zero for the reactions of the silylene with different alkenes. This infers a two step mechanism for the reaction, with a slow second step, the first step being a reversible complex formation. Measurement of activation parameters for the reactions of  $\text{SiPh}_2$  with substrates other than alkenes and of  $\text{SiMe}_2$  and  $\text{SiTm}_2$  with all the substrates studied in this thesis would be an extension to the present work. These values along with the present data will lead to a more complete picture of the mechanisms of the reactions of diarylsilylenes.



### References

- (1) Moiseev, A. G.; Leigh, W. J. *Organometallics* **2007**, *26*, 6268.
- (2) Moiseev, A. G.; Leigh, W. J. *Organometallics* **2007**, *26*, 6277.
- (3) Leigh, W. J.; Kostina, S. S.; Bhattacharya, A.; Moiseev, A. G. *Organometallics* **2010**, *29*, 662.
- (4) Moiseev, A. G.; Coulais, E.; Leigh, W. J. *Chem. Eur. J.* **2009**, *15*, 8485.

## Chapter 5 – Experimental

### 5.1. General

$^1\text{H}$  and  $^{13}\text{C}$  NMR spectra were recorded on a Bruker AV200 or a Bruker AV600 spectrometer in deuterated chloroform ( $\text{CDCl}_3$ ) or deuterated benzene ( $\text{C}_6\text{D}_6$ ) and were referenced to the residual proton of the solvent and  $^{13}\text{C}$  respectively, while  $^{29}\text{Si}$  spectra were recorded on AV600 using HMBC pulse sequence and were referenced to an external solution of tetramethylsilane. GC/MS analyses were done on a Varian Saturn 2200 GC/MS/MS system equipped with a VF-5ms capillary column (30 m  $\times$  0.25 mm; 0.25  $\mu\text{m}$ ; Varian, Inc.). High resolution mass spectra and exact masses were determined on a Micromass GCT (GC-EI/CI Time of Flight Mass Spectrometer) using electron impact ionization (70 eV) or on a Micromass Quattro Ultima (LC-ESI/APCI Triple Quadrupole Mass Spectrometer) using electrospray ionization. Infrared spectra were recorded as KBr pellets using a Nicolet 510 FTIR spectrometer, with a DTGS detector, and are baseline corrected. Static UV/vis absorption spectra were recorded on a Varian Cary 50 UV/vis spectrophotometer. Elemental analyses were performed on a Thermo FlashEA 1112 elemental analyzer. Melting points were recorded using Fisher Johns Melting Point apparatus or on a Mettler FP82 hot stage mounted on a polarising microscope. Column chromatography was carried out using 230-400 mesh silica gel (Silicycle).

## 5.2. Solvents

Hexanes (EMD OmniSolv) were dried by passage through activated alumina under nitrogen using a Solv – Tek solvent purification system (Solv – Tek Inc.) while tetrahydrofuran (Caledon) was refluxed over sodium metal for several days and then distilled. Cyclohexane (Caledon) and dichloromethane (Caledon) were refluxed over  $P_2O_5$  and distilled. Hexanes (Caledon) for chromatographic purposes, methanol (Caledon), pyridine (Caledon) and petroleum ether (Caledon) were used as received. Chloroform –  $d$ , cyclohexane –  $d_{12}$  and benzene –  $d_6$  were used as received.

## 5.3. Commercial Reagents

For synthetic applications, the following reagents were purchased from Sigma-Aldrich and used as received: isophorone,  $NH_2OH.HCl$ , acetic anhydride, acetyl chloride,  $SiCl_4$ ,  $HSiCl_3$ . *Tert*-butyl lithium (Sigma-Aldrich) was titrated according to previously reported<sup>1</sup> method before use and 2,6-lutidine (Sigma-Aldrich) was refluxed over  $P_2O_5$  and distilled. Other reagents used as received:  $H_2SO_4$  (Caledon),  $HBr$  (Fisher Scientific), copper granules (Fisher Scientific), trifluoromethanesulfonic acid (Fluka),  $Me_3SiCl$  (Gelest), magnesium (EMD), sodium nitrite (Anachemia Canada).

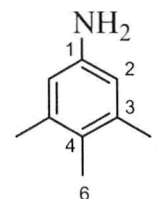
For photolysis experiments (steady state, laser flash): All the substrates investigated in this work were obtained from commercial source at the highest purity level available. Isoprene (Sigma-Aldrich), 2,3-dimethyl-1,3-butadiene (Sigma-Aldrich),

bis(trimethylsilyl)acetylene (Gelest) and cyclohexene (Sigma-Aldrich) were passed as neat liquids through short silica gel columns for purification. Glacial acetic acid (Caledon) was used as received. Acetone (Caledon) was stirred for 48 h over anhydrous calcium sulphate and distilled before use. Methanol (Caledon) was refluxed over magnesium methoxide and distilled, while  $\text{CCl}_4$  (Sigma-Aldrich) was distilled over phosphorus pentoxide and distilled. Triethylsilane (Gelest) was distilled before use. *Tert* – butanol (anhydrous), methanol – *Od* (99 atom %D), and *tert* – butanol – *Od* (99 atom%D) were used as received from Sigma-Aldrich.

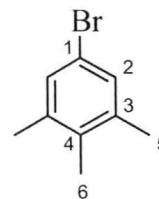
#### 5.4. Synthesis

**2,2 – Dimesityl – 1,1,1,3,3,3 – hexamethyltrisilane (20, mp 169.2 – 170.8 °C):**  $^1\text{H}$  NMR (200 MHz,  $\text{CDCl}_3$ )  $\delta = -0.14$  (s, 18H), 2.17 (s, 6H), 2.23 (br, 12H), 6.75 (s, 4H). The compound was synthesized by previously reported method and the  $^1\text{H}$  NMR spectrum and the melting point agrees with data reported.<sup>2</sup>

**3,4,5 – Trimethylaniline (50, mp 77.5 – 79.5 °C):**  $^1\text{H}$  NMR (600 MHz,  $\text{CDCl}_3$ )  $\delta = 2.09$  (s, 3H,  $\text{C}^6\text{H}$ ), 2.23 (s, 6H,  $\text{C}^5\text{H}$ ), 3.44 (br, 2H,  $\text{NH}$ ), 6.42 (s, 2H,  $\text{C}^2\text{H}$ );  $^{13}\text{C}$  NMR (150 MHz,  $\text{CDCl}_3$ )  $\delta = 14.54$  ( $\text{C}^6$ ), 20.74 ( $\text{C}^5$ ), 114.85 ( $\text{C}^2$ ), 125.17 ( $\text{C}^3$  or  $4$ ), 137.42 ( $\text{C}^3$  or  $4$ ), 143.67 ( $\text{C}^1$ ). The HSQC or HMBC experiments did not allow us to assign C3 or C4 unambiguously. The compound was synthesized in three steps from isophorone as described previously and identified on the basis of reported melting point value of 78 – 79.5 °C.<sup>3</sup>



**3,4,5-trimethyl-1-bromobenzene (51):** In a 100 mL two neck round-bottom flask fitted with a stir bar were placed 3,4,5-trimethylaniline (8.68 g, 0.06 mol) and water (15 mL). To this mixture was added concentrated HBr (48% by weight, 45 mL, 0.39 mol) to form a slurry. The round-bottom flask was then stoppered and cooled to 0° C in an ice-bath. Next, NaNO<sub>2</sub> (5.8 g, 0.08 mol) was added to the flask in small portions over a period of 1.5 h; after each addition the flask was quickly stoppered and vigorously stirred. Once the addition of NaNO<sub>2</sub> was completed, Cu granules (1.75 g, 0.03 mol) were added to the reaction mixture and the round-bottom flask was fitted with a condenser. The temperature was then increased using an oil bath to initiate the reaction. At 60° C, the solution started bubbling and the heat source was quickly removed. The reaction mixture boiled vigorously, unaided, for 30 min and then it was stirred for 2 more days at room temperature. At the end of the second day, the mixture was made alkaline with a saturated sodium hydroxide solution and extracted with ether (3×50 mL), the ether extracts were combined and washed with brine, dried over anhydrous sodium sulfate and evaporated on a rotary evaporator to yield an orange-yellow oil (10.00 g). Column chromatography on silica gel with hexanes as eluant afforded a colorless oil (3.74 g, 29%) which was identified to be 3,4,5-trimethyl-1-bromobenzene on the basis of the following data: <sup>1</sup>H NMR (600 MHz, CDCl<sub>3</sub>) δ = 2.11 (s, 3H, C<sup>6</sup>H), 2.25 (s, 6H, C<sup>5</sup>H), 7.15 (s, 2H, C<sup>2</sup>H); <sup>13</sup>C NMR (150 MHz, CDCl<sub>3</sub>) δ = 15.18 (C<sup>6</sup>), 20.50 (C<sup>5</sup>), 118.62 (C<sup>1</sup>), 130.27 (C<sup>2</sup>), 134.11 (C<sup>3</sup> or 4),



138.65 (C<sup>3</sup> or <sup>4</sup>). The HSQC or HMBC experiments did not allow us to assign C3 or C4 unambiguously. The <sup>1</sup>H NMR spectrum agrees with data reported elsewhere.<sup>4</sup>

**Dichlorobis(3,4,5-trimethylphenyl)silane (52)** (*Synthesis in cooperation with Derek R. Morim*): To a flame-dried 50 mL three-necked round-bottom flask under argon were added dry THF (11 mL) followed by 3,4,5-trimethyl-1-bromobenzene (0.8006 g, 4.02 mmol), and stirred to mix. The reaction flask was then cooled to -78°C using an isopropanol/dry-ice bath and *tert*-BuLi (5.6 mL of a 1.43 M solution in pentane, 8.01 mmol) was added drop-wise over 15 m. The reaction mixture was further stirred at -78°C for 30 min. In another 100 mL two-necked flame-dried round-bottom flask were added SiCl<sub>4</sub> (0.23 mL, 2.00 mmol) and dry THF (8 mL) solution, and stirred to mix. The solution was then cooled to -78°C using an isopropanol/dry-ice bath and to it were cannulated drop-wise, the reaction mixture from the other flask, over 8 min. After the addition was complete, the flask was allowed to come to room temperature and the reaction mixture was stirred for 18 h. The solvent was then evaporated using a high vacuum pump and the residue was digested with dry hexanes (40 mL) to precipitate salts. The clear supernatant liquid was then cannulated into a pre-weighed flask and the solvent was evaporated using a high vacuum pump to obtain the crude product as white solid (0.6969 g). The material was dissolved in dry hexanes, transferred to a flame-dried Kugelrohr distillation apparatus, and distilled under vacuum (130 °C, 1 mm Hg). Dichlorobis(3,4,5-trimethylphenyl)silane was obtained (0.3464 g, 41%) as a white

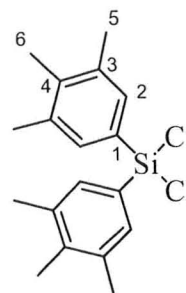
crystalline product and identified on the basis of the following data:  $^1\text{H}$  NMR (600MHz,  $\text{C}_6\text{D}_6$ )  $\delta = 1.80$  (s, 6H,  $\text{C}^6\text{H}$ ), 1.95 (s, 12H,  $\text{C}^5\text{H}$ ), 7.62 (s, 4H,  $\text{C}^2\text{H}$ );

$^{13}\text{C}$  NMR (150 MHz,  $\text{C}_6\text{D}_6$ )  $\delta = 15.75$  ( $\text{C}^6$ ), 20.69 ( $\text{C}^5$ ), 129.68 ( $\text{C}^1$ ),

134.09 ( $\text{C}^2$ ), 137.09 ( $\text{C}^3$  or  $4$ ), 139.89 ( $\text{C}^3$  or  $4$ );  $^{29}\text{Si}$  NMR (119.2 MHz,

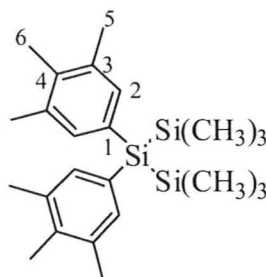
$\text{C}_6\text{D}_6$ )  $\delta = 7.25$ ; HRMS calculated for  $\text{C}_{18}\text{H}_{22}\text{SiCl}_2$ , 336.0868; found

336.0870. The HSQC or HMBC experiments did not allow us to assign C3 or C4 unambiguously.



**1,1,1,3,3,3 – Hexamethyl – 2,2 – bis(3,4,5–trimethylphenyl)trisilane (43):** A flame dried 50 mL two-neck round-bottom flask fitted with a condenser and a pressure-equalized addition funnel was charged with potassium metal (0.2007 g, 0.0051 g-atom) followed by dry cyclohexane (10 mL). The mixture was then heated to reflux to obtain a blue-grey solution, to which was added a solution of dichlorobis(3,4,5-trimethylphenyl)silane (0.3464 g, 1.03 mmol) and trimethylchlorosilane (0.55 mL, 4.33 mmol) in cyclohexane (10 mL), through the addition funnel drop-wise, over a period of 30 min.. The reaction mixture was refluxed for an additional 2 h, cooled to room temperature, and filtered under argon through a sintered glass frit. The precipitate was washed with dry cyclohexane (30 mL). The filtrate and washings were then combined and the solvent was evaporated on the rotary evaporator to obtain an off-white solid (0.2966 g). Column chromatography on silica gel with hexanes as eluant afforded a white solid (0.1144 g, 26%), which was recrystallized from methanol to yield white

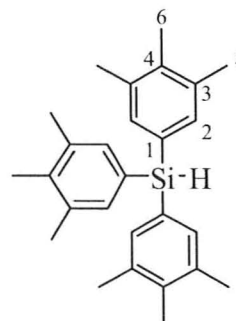
needles (mp 147.1-150.6 °C). The compound was identified as 1,1,1,3,3,3-hexamethyl-2,2-bis(3,4,5-trimethylphenyl)trisilane (**43**) on the basis of the following data:  $^1\text{H}$  NMR (600 MHz,  $\text{CDCl}_3$ )  $\delta$  = 0.17 (s, 18H,  $\text{SiCH}_3$ ), 2.17 (s, 6H,  $\text{C}^6\text{H}$ ), 2.25 (s, 12H,  $\text{C}^5\text{H}$ ), 7.10 (s, 4H,  $\text{C}^2\text{H}$ );  $^{13}\text{C}$  NMR (150 MHz,  $\text{CDCl}_3$ )  $\delta$  = - 0.16 ( $\text{SiC}$ ), 15.54 ( $\text{C}^6$ ), 20.74 ( $\text{C}^5$ ), 132.49( $\text{C}^1$ ), 135.23 ( $\text{C}^3$ ), 135.48 ( $\text{C}^2$ ), 135.72 ( $\text{C}^4$ );  $^{29}\text{Si}$  NMR (119.2 MHz,  $\text{CDCl}_3$ )  $\delta$  = - 16.60 ( $\text{SiSiC}$ ), -40.70 ( $\text{TmpSiSi}$ ); GC/MS (EI),  $m/z$  412 (20,  $\text{M}^+$ ), 397 (20), 339 (100), 281 (9), 265 (1), 251 (1), 235 (1), 219 (7), 205 (9), 177 (4), 159 (2), 145 (1), 119 (1), 73 (14); HRMS calculated for  $\text{C}_{24}\text{H}_{40}\text{Si}_3$  412.2438, found 412.2422; IR ( $\text{cm}^{-1}$ ) 3000 (m), 2947 (m), 1557 (m), 1475 (s), 1373 (s), 1260 (s), 1240 (s), 1113 (s), 862 (s), 831 (s), 744 (s), 711 (s), 688 (s). Anal. Calcd. for  $\text{C}_{24}\text{H}_{40}\text{Si}_3$ : C, 69.82; H, 9.77. Found: C, 69.51; H, 9.51. UV:  $\lambda_{\text{max}}$  = 247 nm,  $\epsilon$  = 25, 863  $\text{M}^{-1} \text{cm}^{-1}$ .



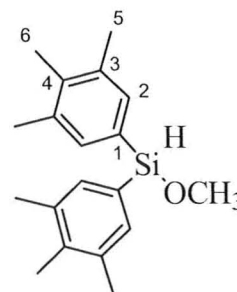
**Tris(3,4,5-trimethylphenyl)silane (55):** A 100 mL three neck round-bottom flask fitted with a condenser, pressure equalized addition funnel, and magnetic stir-bar was charged with freshly ground magnesium turnings (0.48 g, 0.0197 g-atom). The entire flask was then flame-dried and allowed to cool under dry  $\text{N}_2$  gas. A solution of 3,4,5-trimethyl-1-bromobenzene (2.58 g, 12.96 mmol) in dry THF (20 mL) was added to the addition funnel. Approximately 2 mL of this solution was added at once to the reaction flask followed by 2 drops of 1,2 – dibromoethane. Within minutes a vigorous exothermic reaction took place and the color of the solution turned deep green. The remaining



solution of the 3,4,5-trimethyl-1-bromobenzene in THF was then added drop-wise to the reaction flask over a period of 45 min. and then stirred at room temperature for 20h. Another 50 mL two-neck round-bottom flask, fitted with an addition funnel and a condenser, was charged with trichlorosilane (0.48 g, 3.56 mmol) and dry THF (5 mL). The Grignard reagent was then cannulated into the addition funnel and added drop-wise at 0 °C over a period of 75 min. The reaction mixture was stirred at 0 °C for 2 h, allowed to warm to room temperature, and then stirred for 2 days. The reaction mixture was quenched by drop-wise addition of water (50 mL) and was extracted with hexanes (3 × 50 mL). The combined organic fractions were dried over anhydrous sodium sulfate, filtered, and the solvent was evaporated on a rotary evaporator to yield a sticky white solid (1.40 g). Column chromatography on silica gel with hexanes as eluant afforded a white solid (0.80 g, 58 %), which was recrystallized from hexanes to yield a white powder (mp 162 – 163 °C). The compound was identified as tris(3,4,5-trimethylphenyl)silane (**55**) on the basis of the following data:  $^1\text{H}$  NMR (600 MHz,  $\text{CDCl}_3$ )  $\delta$  = 2.19 (s, 9H,  $\text{C}^6\text{H}$ ), 2.26 (s, 18H,  $\text{C}^5\text{H}$ ), 5.29 (s, 1H,  $\text{SiH}$ ), 7.23 (s, 6H,  $\text{C}^2\text{H}$ );  $^{13}\text{C}$  NMR (150 MHz,  $\text{CDCl}_3$ )  $\delta$  = 15.63 ( $\text{C}^6$ ), 20.66 ( $\text{C}^5$ ), 130.52 ( $\text{C}^1$ ), 135.14 ( $\text{C}^2$ ), 136.07 ( $\text{C}^3$  or  $4$ ), 136.97 ( $\text{C}^3$  or  $4$ );  $^{29}\text{Si}$  NMR (119.2 MHz,  $\text{CDCl}_3$ )  $\delta$  = -18.20; HRMS calculated for  $\text{C}_{27}\text{H}_{34}\text{Si}$ , 386.2430, found 386.2436. The HSQC or HMBC experiments did not allow us to assign C3 or C4 unambiguously.



**Methoxybis(3,4,5-trimethylphenyl)silane (53):** A two-neck 15 mL flask fitted with an argon inlet and a magnetic stirrer was flame-dried and then cooled under argon. The flask was charged with tris(3,4,5-trimethylphenyl)silane (**55**) (150 mg, 0.388 mmol) followed by dry dichloromethane (1.5 mL) and stirred to make a solution. The flask was cooled to 0 °C with an ice bath and then trifluoromethanesulfonic acid (34  $\mu$ L, 0.388 mmol) was added drop-wise to the reaction mixture using a gas tight syringe over a period of 3 min. The reaction mixture was stirred for a further 20 min and then 2,6-lutidine (115  $\mu$ L, 0.987 mmol) was added to it and the mixture stirred for another 5 min. Dry methanol (17.3  $\mu$ L, 0.427 mmol) was added and the reaction flask was allowed to come to room temperature, after which it was stirred for a further 3 h. The solvent was removed under vacuum to yield a white solid, which was extracted with dry hexanes (15 mL), by removal of the supernatant with a cannula. The hexanes were evaporated under vacuum to yield a white solid (0.091 mg) which appeared to be roughly 80 % pure **53** based on following data:  $^1\text{H}$  NMR (600 MHz,  $\text{C}_6\text{D}_6$ )  $\delta$  = 1.90 (s, 6H,  $\text{C}^6\text{H}$ ), 2.07 (s, 12H,  $\text{C}^5\text{H}$ ), 3.57 (s, 3H, OCH), 5.79 (s, 1H, SiH), 7.54 (s, 4H,  $\text{C}^2\text{H}$ );  $^{13}\text{C}$  NMR (150 MHz,  $\text{C}_6\text{D}_6$ )  $\delta$  = 15.74 ( $\text{C}^6$ ), 20.79 ( $\text{C}^5$ ), 52.47 (OC), 129.69 ( $\text{C}^1$ ), 134.88 ( $\text{C}^2$ ), 136.29 ( $\text{C}^3$  or  $4$ ), 136.47 ( $\text{C}^3$  or  $4$ );  $^{29}\text{Si}$  NMR (119.2 MHz,  $\text{C}_6\text{D}_6$ )  $\delta$  = -8.26; exact mass calculated for  $\text{C}_{19}\text{H}_{27}\text{OSi}$  (M+H) 299.1831, found (ESI) 299.1817.



### 5.5. Steady-State Photolysis Experiments

A solution of **43** (ca. 0.04 M) in cyclohexane-*d*<sub>12</sub> (~0.7 mL) was placed in a quartz NMR tube and then deoxygenated with dry Argon for 10 min. Methanol (5  $\mu$ L) was then added and the NMR tube was tightly capped. The solution was then photolyzed for 3.5 min using a Rayonet Photochemical Reactor (Southern New England Ultraviolet Co.) equipped with a merry-go-round and two RPR-2537 lamps (254 nm), monitoring by <sup>1</sup>H NMR spectroscopy every 20 – 30 s throughout the experiment. Product yields were calculated relative to consumed **43** from the slopes of concentration vs. time plots constructed from the <sup>1</sup>H NMR integrals. Errors are quoted as  $\pm 2\sigma$  from linear least square analysis of the data.

### 5.6. Laser Flash Photolysis Experiments

Nanosecond laser flash photolysis were carried out using the pulses from a Lambda-Physik Compex 120 excimer laser filled with Kr/F<sub>2</sub>/Ne (248 nm; ca. 20 ns; 95-110 mJ), coupled with a Luzchem Research mLFP-111 laser flash photolysis system, modified as described previously.<sup>5</sup> Solutions of **20** and **43** were prepared in anhydrous solutions of hexanes in a graduated 250 mL reservoir, fitted with a glass frit at the bottom to allow bubbling of Argon for at least 45 min. prior to and then throughout the experiment. Concentrations of these solutions were such (0.05 – 0.06 mM of **20** or **43**) that the absorbance at the excitation wavelength was between 0.70 – 0.85. The solutions were pumped from the reservoir through Teflon tubing connected to a 7 $\times$ 7 mm Suprasil

flow cell using a Masterflex 77390 peristaltic pump. The sample cell and transfer lines were dried in a vacuum oven (65-85 °C) before use. Reagents, as aliquots of standard solution, were directly added to the reservoir using microliter syringes. Transient decay rate constants were calculated by non-linear least-squares analysis of the absorbance-time profiles using the Prism 5.0 software packages (GraphPad Software Inc.) and the appropriate user-defined fitting equations, after importing the raw data from the Luzchem mLFP software. Rate constants were calculated by linear least-squares analysis of the decay rate – concentration data (2-17 points). Errors in absolute second-order rate constants are quoted as twice the standard deviation obtained from the least-squares analyses.

#### References

- (1) Suffert, J. *J. Org. Chem.* **1989**, *54*, 509.
- (2) Tan, R. P.; Gillette, G. R.; Yokelson, H. B.; West, R. *Inorg. Synth.* **1992**, *29*, 19.
- (3) Beringer, F. M.; Ugelow, I. *J. Am. Chem. Soc.* **1953**, *75*, 2635.
- (4) Baciocchi, E.; Dalla Cort, A.; Ebersson, L.; Mandolini, L.; Rol, C. *J. Org. Chem.* **1986**, *51*, 4544.
- (5) Shizuka, H.; Tanaka, H.; Tonokura, K.; Murata, K.; Hiratsuka, H.; Ohshita, J.; Ishikawa, M. *Chem. Phys. Lett.* **1988**, *143*, 225.